04-A (2-54)

[redacted] [redacted]

UNCLASSIFIED

1093

[redacted]

SANDIA SYSTEMATIC DECLASSIFICATION REVIEW
DOWNGRADING OR DECLASSIFICATION STAMP
CLASSIFICATION CHANGED TO: U
AUTHORITY: W. C. Layne
PERSON CHANGING MARKING AND DATE
RECORD ID: 97SN322
DATED: 1-28-97

[redacted]

SANDIA SYSTEMATIC DECLASSIFICATION REVIEW
1st Review Date: 2-13-80
Authority: ADC
Name: CCRP RA
2nd Review Date: 1-28-97
Authority: ADD
Name: INV Layne
Reason, Item (Optional Numbers):
1. Classification Retained
2. Classification Changed to: U
3. Contains No DOE Classified Information
4. Contains UCNI
5. Contains UCNI
6. Comments:

INVENTORIED
DATE FEB 1 1960

INVENTORIED

MAR 1 1960

SCTM-83-55-51

SEP 17 1957

BY ORG. 2743

INVENTORIED
DATE MAY 15 1961

3426-3

TRANSIENT HEATING AND STRESSING OF PLATES CAUSED BY THERMAL RADIATION FROM ATOMIC EXPLOSIONS

INVENTORIED

INVENTORIED

INVENTORIED

MAR 8 1965

DEC 1 1958

E. T. Clark

INVENTORIED

OCT 11 '55

3427-1

243

AUG 1 1963

4161

INVENTORIED

AUG 6

ABSTRACT 3427-1

The transient heating of plates caused by the thermal radiation from atomic explosions is investigated. Results are presented as graphs allowing rapid determination of the position-temperature-time relations for the irradiated plates.

Stresses arising from the nonuniform aspect of the plate heating are estimated; and the combinations of yield, range, and burst altitude are specified which result in large stresses due to nonuniform heating.

[redacted]

~~49546~~

Case No. 409.07

May 24 1955

INVENTORIED

INVENTORIED
DATE FEB 6 1961

INVENTORIED
DATE 3-8-64

[redacted]

UNCLASSIFIED

[redacted]

UNCLASSIFIED

DISTRIBUTION:

1/21A - Commanding General, AFSWP, Dev. Division. Attn: Major L. A. Barnes
2/21A - Commander AFSWC, KAFB. Attn: Major R. C. Mack (Thru FC/AFSWP)
3/21A - L. A. Gore, Rand Corporation, Santa Monica (Thru D. J. Leehey, mgr, SFOO)
4/21A - R. J. Vicars, APL/JHU, Silver Spring, Maryland
5/21A - M. V. Barton, Ramo-Wooldridge Corp., Los Angeles
6/21A - E. A. Witmer, Aero Elastic & Structures Res. Lab, MIT
7/21A - J. L. Kelley, Allied Rese ch Associates, Boston (Thru D. J. Leehey, mgr, SFOO)
8/21A - F. J. Janik, WCLSS-1 WADC, Dayton (Thru FC/AFSWP)
9/21A - S. C. Hight, 5100
10/21A - E. F. Cox, 5110 [redacted]
11/21A - R. W. Shephard, 5120
12/21A - W. M. Wells, 1332
13/21A - L. E. Bothell, 1215
14/21A - R. F. Brodsky, 5141
15/21A - R. K. Smeltzer, 1922-2
16-21/21A - M. K. Linn, 1923

UNCLASSIFIED

TABLE OF CONTENTS

		Page
	LIST OF ILLUSTRATIONS	4-5
	INTRODUCTION	6
	SUMMARY	7
	RECOMMENDATIONS	9
I.	TRANSIENT HEATING OF PLATES	10
II.	STRESSES IN PLATES CAUSED BY NONUNIFORM TRANSIENT HEATING	14
III.	SPECIFICATION OF YIELDS AND RANGES AT WHICH LARGE STRESSES WILL BE CAUSED BY NONUNIFORM HEATING	21
	REFERENCES	25

LIST OF ILLUSTRATIONS

Figure		Page
1	Shape function, q*, and its integral, $\int_0^{\tau^*} q^* d\tau^*$ versus time	26
2	Dimensionless temperature increase (t* - 1) versus time	27
3	Dimensionless temperature increase (t* - 1) versus time	28
4	Dimensionless temperature increase (t* - 1) versus time	29
5	Dimensionless temperature increase (t* - 1) versus time	30
6	Dimensionless temperature increase (t* - 1) versus time	31
7	Dimensionless temperature increase (t* - 1) versus time	32
7a	Temperature ratio profiles at various dimensionless times	33
8	Dimensionless temperature increase (t* - 1) versus time	34
8a	Temperature ratio profiles at various dimensionless times	35
9	Dimensionless temperature increase (t* - 1) versus time	36
9a	Temperature ratio profiles at various dimensionless times	37
10	Dimensionless temperature increase (t* - 1) versus time	38
10a	Temperature ratio profiles at various dimensionless times	39
11	Dimensionless temperature increase (t* - 1) versus time	40
11a	Temperature ratio profiles at various dimensionless times	41
12	Dimensionless temperature increase (t* - 1) versus time	42
12a	Temperature ratio profiles at various dimensionless times	43
13	Dimensionless temperature increase (t* - 1) versus time	44
13a	Temperature ratio profiles at various dimensionless times	45
14	Dimensionless temperature increase (t* - 1) versus time	46
14a	Temperature ratio profiles at various dimensionless times	47
15	Dimensionless temperature increase (t* - 1) versus time	48
15a	Temperature ratio profiles at various dimensionless times	49
16	Dimensionless temperature increase (t* - 1) versus time	50
16a	Temperature ratio profiles at various dimensionless times	51
17	Dimensionless temperature increase (t* - 1) versus time	52

[redacted]

UNCLASSIFIED

LIST OF ILLUSTRATIONS (Cont)

Figure		Page
17a	Temperature ratio profiles at various dimensionless times	53
18	Dimensionless temperature increase (t* - 1) versus time	54
18a	Temperature ratio profiles at various dimensionless times	55
19	Dimensionless temperature increase (t* - 1) versus time	56
19a	Temperature ratio profiles at various dimensionless times	57
20	Exponent of the temperature profile equation versus dimensionless time with β as a parameter	58
21	Ratio of the maximum front surface temperature increase to the final uniform temperature increase versus thermal pulse duration	59
22	Thermal stresses in a free plate	60
23	Ratio of the tension stress at the rear surface of the plate and near the plate support to the static ultimate stress for various plate thicknesses and thermal pulse duration	61
24	Maximum tension stresses on the rear surface near the edge of a nonuniformly heated 75ST aluminum plate fixed at its edges	62
25	Maximum tension stresses on the rear surface near the edge of a nonuniformly heated JS-1H magnesium plate fixed at its edges	63
26	Maximum tension stresses on the rear surface near the edge of a nonuniformly heated 18-8 stainless steel plate fixed at its edges	64
27	Time variations of front and rear surface temperature and stress for a typical case of nonuniform heating which produces large stresses in an aluminum plate	65
28	Yield and range combinations which produce a maximum stress ratio of 2-1/4 in 75ST aluminum plates having fixed edges and oriented normal to a radius from the burst point	66
29	Yield and range combinations which produce a maximum stress ratio of 2-3/4 in JS-1H magnesium plates having fixed edges and oriented normal to a radius from the burst point	67
30	Yield and range combinations which produce a maximum stress ratio of 4 in 18-8 stainless steel plates having fixed edges and oriented normal to a radius from the burst point	68
31	Yield and range combinations which produce a maximum stress ratio of 2-1/4 in 75ST aluminum plates having fixed edges and oriented normal to a radius from the burst point	69

UNCLASSIFIED

[redacted]

UNCLASSIFIED

INTRODUCTION

This report deals with (1) the transient heating of bare plates, such as unpainted panels of aircraft skin, caused by a thermal pulse shaped as that from an atomic explosion, (2) the stresses produced by the nonuniform portion of this transient heating, and (3) the conditions which lead to thermal inputs causing significant stresses due to nonuniform heating.

The one-dimensional transient heating of plates subjected to a typical atomic explosion thermal pulse is studied in Section I. The results obtained are relatively accurate empirical expressions for profiles of temperature at various times in plates of various thickness and material which are subjected to various magnitude and duration thermal pulses. From these data those heat input conditions resulting in particular degrees of nonuniform heating are defined.

In Section II the temperature profiles in aircraft skin panels caused by various thermal pulse inputs are approximately related to the stresses which arise from nonuniform heating in these panels.

In Section III the situations are discussed for which thermal inputs encountered cause large stresses due to nonuniform heating.

The work outlined above was carried out to determine if the phenomenon studied was a significant factor in solving the aircraft or missile lethality problem.

UNCLASSIFIED

UNCLASSIFIED

SUMMARY

Results obtained indicate that little damage to aircraft and missile skins will arise from the stresses associated with the nonuniform aspect of the transient heating* of the skin which can be produced by the thermal radiation from atomic explosions. Skins of very brittle materials are excepted from this statement.

More detailed results from the three sections of the report are presented below.

I. The one-dimensional heat transfer through bare plates is studied for an input pulse shaped as that from an atomic explosion. Cooling at either surface of the plates is not considered. The results obtained become less applicable as the maximum plate temperature approaches the melting temperature. The following inequality, valid for amounts of heat absorbed which are between 20% and 80% of the amount of heat required to bring a plate uniformly to its melting temperature, must be satisfied if the plate surface temperature is not to exceed the melting temperature.

$$\frac{Da}{L^2} \geq \left(\frac{\Delta t_f/t_M + 3}{3.8}\right)^{12.3}$$

In this relation D is the thermal pulse duration, a is the diffusivity of the plate material, L is the plate thickness, Δt_f is the final temperature increase, and t_M is the melting temperature.

The time-dependent temperature profiles through the plate are specified in a general manner. From these profiles the conditions producing any degree of nonuniform heating may be determined. In particular, the maximum surface temperature increase will not exceed 110% of the final temperature increase if the following inequality is satisfied.

$$D \geq 1.2\ L^2/a$$

For aluminum, durations of .58 second or greater will satisfy this expression for thicknesses of .02 foot or less.

The results obtained in this section are directly applicable to studies involving surface thermal damage, such as charring or bubbling, of irradiated materials whose conductivity is low.

II. An approximate relation is developed between the temperature profiles in a fixed-edge plate and the stress associated with the nonuniform aspect of these temperature profiles. These results are not valid if any part of the plate is heated to the plastic state. In addition, the validity of the stress relations depends on the following assumptions:

* Work on the uniform heating aspects of the lethality problem is in progress.

UNCLASSIFIED

[redacted] [redacted]

UNCLASSIFIED

1. The stresses near the center of a plate having fixed edges, such as a panel of aircraft skin, are reasonably well presented by the theory for the stresses in a nonuniformly heated free plate.
2. Neglected inertia effects will not greatly invalidate the results obtained using steady-state stress-temperature relations.
3. The curvature of the plate near its fixed edges is at least as large as the curvature of the plate near its center, but of opposite sense.

The calculations indicate that combinations of thermal pulse duration, heat absorbed, and plate thickness do exist for which tension stresses on the rear side of the plates considered near their fixed edges would, if the strain-stress relation were linear, exceed the static ultimate stress for 75 ST aluminum, JS-1H magnesium, and 18-8 stainless steel by factors as large as 2-1/4, 2-3/4, and 4, respectively. Maximum temperatures produced by these inputs are less than the melting temperature.

These calculations indicate that some permanent set will be caused by the inputs corresponding to the conditions stated above. However, since considerable plastic strain will occur prior to failure of 75 ST and 18-8, it is not expected that cracks will be caused in these materials. In the more brittle JS-1H magnesium, cracks might result from these input conditions.

III. Using approximate values of the energy contained in and the durations of the first and second thermal pulses produced by atomic explosions at different altitudes, the combinations of yield and range which produce large stresses in plates oriented normal to a radius from the burst point are specified. Typical results indicate that the inputs causing large stresses will be produced by the first thermal pulse at about 1000 feet from 29 KT near sea level and at about 4000 feet from 29 KT at an altitude of 100,000 feet.

For all yields greater than a few hundredths KT, the first thermal pulse at a given range causes greater stresses due to nonuniform heating than does the second thermal pulse. / ?

UNCLASSIFIED

[redacted]

UNCLASSIFIED

RECOMMENDATIONS

Although the obtained results do not indicate that the phenomenon studied plays an important role in aircraft lethality estimates, it is believed that some experimentation is warranted to establish the validity of the approximations made in this analysis.

It is recommended that the twenty-eight measurements suggested below be made during some appropriate full-scale test to check the assumptions made in relating the stress to the nonuniform temperature profiles.

1. At the range determined from Figure 29 for the chosen test yield, mount two 1-ft x 3-ft magnesium plates by weak springs to supporting frames high enough to be above the dust layer (essentially free plates). Plate thicknesses should be about .004 ft and .04 ft. At the center of the rear of each plate, measure strain along both axes. Also measure the rear surface temperature at these points, such that the rear surface stress can be evaluated. Time recordings should provide time resolution sufficient for a detailed picture of events during the first thermal pulse.

2. At the same range mount two 3-ft x 9-ft panels riveted on a frame of supporting members set on 1-ft x 3-ft centers, thus dividing the larger panel into nine similar 1-ft x 3-ft subpanels. Thicknesses of these panels should be the same as used above. The center 1-ft x 3-ft subpanel should fairly well represent a plate with fixed edges. Measurements of strain and temperature should be made on this subpanel at the center, 1/4 point, and near the edge of the rear surface along both of the panel axes. Time recordings of these quantities should be made during the first thermal pulse.

3. Two thermal input measurements should be made at the same range. Time recordings of thermal radiation per unit area per unit time are desired.

UNCLASSIFIED

UNCLASSIFIED

SECTION I

TRANSIENT HEATING OF PLATES

A. Definition of Symbols

t = temperature (^{o}Rankine)

τ = time (seconds)

x = distance (feet), $x = 0$ on the front surface of the plate

t_o = initial temperature (taken as 460°R in the problem solved)

τ_{40} = characteristic time, taken as the time from zero for q to decrease to 40% of q_{max}. In a time 2.5 τ_{40} about 90% to 95% of the total thermal radiation contained in a pulse has been emitted. Thus 2.5 τ_{40} is taken as the thermal pulse duration in this report.

q = thermal flux (B/ft^2 sec)

q_{max} = maximum thermal flux (B/ft^2 sec)

B = British Thermal Unit

L = plate thickness (feet)

A = area (square feet)

Q = total normally incident thermal radiation (B/ft^2)

$$= \int_0^{2.5\,\tau_{40}} q\,d\tau = .938\, q_{max}\, \tau_{40} \qquad \text{(See Fig. 1)}$$

$t^* = t/t_o$, dimensionless temperature

$\tau^* = \tau/\tau_{40}$, dimensionless time

$x^* = x/L$, dimensionless distance normal to the plate surface

$q^* = q/q_{max}$, the dimensionless thermal flux. q^* represents the shape of the thermal flux curve (q versus τ) as a function of τ^* (see Fig. 1). The shape chosen for q^* and plotted in Figure 1 closely approximates the measured thermal flux curves for the second thermal pulse of Tumbler Tests 3 and 4.

k = thermal conductivity (B/sec ft^{o}F)

γ = weight per unit volume (lbs/ft^3)

c = specific heat (B/lb ^{o}F)

a = thermal diffusivity (ft^2/sec) = $k/\gamma c$

α = thermal absorptivity - dimensionless

$\beta = a\,\tau_{40}/L^2$

$$K = \frac{\alpha L\, q_{max}}{t_o\, k} = \frac{\alpha L\, Q}{.938\, \tau_{40}\, t_o\, k}$$

UNCLASSIFIED

B. Problem Statement

From Reference 1 we write the one-dimensional heat transfer equation as

$$\partial(t^* - 1)/\partial\tau^* = \beta \frac{\partial^2(t^* - 1)}{\partial x^{*2}}$$

with boundary conditions

$$(t^* - 1)\Big|_{\tau^* = 0} = 0$$

$$\partial(t^* - 1)/\partial x^*\Big|_{x^* = 0} = -K q^* \quad ?$$

$$\partial(t^* - 1)/\partial x^*\Big|_{x^* = 1} = 0 \quad ?$$

As evident from the second and third boundary conditions heat is added with time at the front surface as specified by the pulse shape function, q^*, and no heat is transported across the rear surface. It is also evident that altering the temperature increase scale, i.e., the scale of $t^* - 1$, by the factor $1/K$ makes the stated problem independent of K. Therefore, the the resulting temperature distribution for a particular set of values of q^*, τ^*, β, and K may be used to represent the temperature distribution corresponding to the same values of q^*, τ^*, and β, but a different value of K, say K_1, by applying the factor K_1/K to the $t^* - 1$ scale. This independence of the character of the solution on the magnitude of K has further significance, since for a fixed input shape (i.e., for fixed q^* versus τ^*) it indicates that β is the primary parameter of the character of the solution.

Below are tabulated the values of the physical constants used in computing typical values of β and K for REAC solutions, and which have been used throughout this report.

TABLE I

Physical Constants Used In The Transient Heating Problem

Quantity	Aluminum	Magnesium	Stainless Steel
$k\ \left(\frac{B}{ft\ sec\ {}^\circ F}\right)$	330×10^{-4}	256×10^{-4}	112×10^{-4}
γ (lbs/ft^3)	172.8	110.5	491
c (B/lbs $^\circ$F)	.230	.248	.11
a (ft^2/sec)	830×10^{-6}	933×10^{-6}	207×10^{-6}
α	.5	.7	.5

Table II below lists the values of β and K which were used in the REAC solutions. The figures in which these solutions are graphed are also referenced in Table II.

[redacted]

UNCLASSIFIED

TABLE II

Values Of β And K Used For Each REAC Solution

β	374	249	93.4	62.3	41.5	27.7	23.3	15.6	3.74
K	.0142	.0213	.0284	.0426	.0426	.064	.0568	.0852	.0284
Reference Figure	2	3	4	5	6	7	8	9	10
β	2.44	.934	.622	.415	.277	2.77	.277	1.56	.156
K	.0426	.284	.426	.426	.64	.64	6.4	.852	8.52
Reference Figure	11	12	13	14	15	16	17	18	19

Figure 1 gives the function $q^*(\tau^*)$ and its integral which were used in solution of the problem.

C. Presentation of Results

The solutions for the various values of β and K are plotted in Figures 2 through 19 as the increase in temperature ratio versus dimensionless time (i.e., as $t^* - 1$ vs τ^*). On each figure is a table of factors which must be applied to the $t^* - 1$ scale to make the results apply to various aluminum plate thicknesses and thermal pulse durations. For a fixed thermal pulse duration the solutions can be applied to magnesium or stainless steel plates by redefining the terms indicated below:

$$L_{Mag.} = 1.06\ L_{Al.}$$

$$(\alpha Q)_{Mag.} = .73\ (\alpha Q)_{Al.}$$

$$L_{S.S.} = .50\ L_{Al.}$$

$$(\alpha Q)_{S.S.} = .68\ (\alpha Q)_{Al.}$$

In setting up the REAC problem, the plate was considered to consist of ten equally thick laminae. Accordingly the plot of each solution consists of ten temperature-ratio-versus-dimensionless-time graphs, one corresponding to the temperature variation at the mid-point of each of the ten laminae.

Inspection of Figures 2 through 19 show that in some of the problems solved the temperature variations in all laminae are practically the same, indicating uniform heating. For those solutions where nonuniform heating was evident, temperature profiles at various times were plotted (see Figures 7a through 19a). The information on each of Figures 7a through 19a may be applied to aluminum plates of different thicknesses heated by thermal pulses of various durations by multiplying the $(t^* - 1)$ values by the factors listed on the corresponding figure of

UNCLASSIFIED

[redacted]

[redacted] [redacted]

UNCLASSIFIED

Figures 7 through 19. These temperature profiles, plots of t^* versus x/L, could all be represented within a few per cent by curves of the type

$$(t^* - 1) = (t^*_R - 1) + (t^*_F - t^*_R)\left(\frac{x + L/2}{L}\right)^n .$$

In this equation subscripts F and R denote the front and rear surfaces of the heated plate. Note that the origin of x in this relation is now taken at the center of the plate and positive x is toward the front of the plate.

The values of n used to fit the temperature profiles are indicated on each graph of Figures 7a through 19a, and are plotted versus τ^* with β as a parameter in Figure 20. Note that n is independent of K.

The maximum temperature increase of the plate occurs at the front surface. In Figure 21 this temperature increase divided by the final uniform temperature increase has been plotted versus thermal pulse duration with plate thickness as a parameter. If a particular temperature increase is chosen as the maximum allowable temperature increase, this chart allows rapid determination of the conditions which produce the chosen surface temperature. As an example, one might decide that the maximum temperature increase should not exceed the final temperature increase by more than 10%. For this requirement the minimum thermal pulse duration for aluminum is given by

$$2.5\ \tau_{40} = .145\ (L/.01)^2 .$$

Thus, a .02-thick aluminum plate will not experience temperature increases greater than 110% of the final temperature increase unless the thermal pulse duration is less than .58 second.

Introducing the diffusivity, a, into this relation it becomes valid for all materials, since in this form the relation simply specifies a particular value of β, that parameter which controls the character of the transient heating:

$$2.5\ \tau_{40} = 1.20\ L^2/a .$$

Reference 2 investigates the heating of plates for square pulse inputs. There it is noted that a duration less than 1/16 L^2/a will permit the entire thermal pulse to be received before any heating of the rear surface occurs, thus certainly producing extensive nonuniform heating.

Taking account of the difference in pulse shape in a crude fashion the present results indicate that this duration should produce maximum temperature increases of from 2-1/2 to 4-1/2 times the final temperature increase. Therefore, the present work is in agreement with the above-stated conclusion of Reference 2.

UNCLASSIFIED

[redacted]

[redacted]

UNCLASSIFIED

SECTION II

STRESSES IN PLATES CAUSED BY NONUNIFORM TRANSIENT HEATING

General Discussion

The sketches below qualitatively depict during the period of nonuniform heating the deformation of fixed plates, such as panels of aircraft skin, subjected to thermal radiation on one surface.

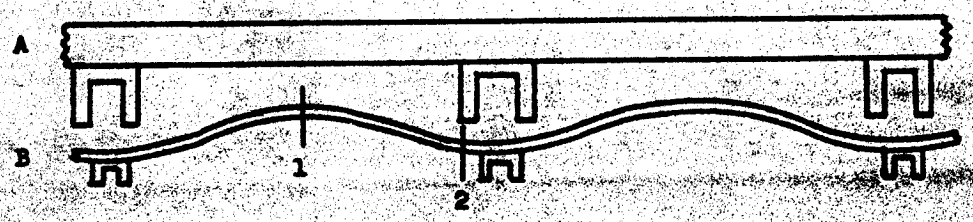

The incident thermal radiation, q , varies with time in such a manner that the most pronounced nonuniform heating occurs in the first half of the heating phase. The maximum stresses caused by the nonuniform heating* will also occur in this same period. Sketch A represents the case where stresses due to bending are not important for either of two reasons. The first of these reasons is that the unsupported plate width-to-thickness ratio is small enough that the edge fixity strongly affects the deformation and little bending occurs. The second reason is that the inertia of the plate is such that little bending of the plate has taken place during the time the heating is nonuniform. For the case where bending stresses are not important, one expects compression stresses through the plate having the same profile as that of the temperature increases. If adjacent plate edge supports can separate readily, then the compressive stresses may be reduced throughout the plate and tension stresses may occur near the rear surface.

In Sketch B bending stresses are important while the plate is nonuniformly heated. Such will be the case if the plate inertia does not greatly restrict bending, and if the plate width-to-thickness ratio is large. Aircraft skin panels generally have large width-to-thickness ratios. In fact, these ratios are generally so large that only a few degrees uniform temperature rise produces sufficient stress to cause buckling. In the analysis to follow we will apply steady-state temperature-stress relations for a free plate to predict the stresses associated with the transient nonuniform heating at station (1) on the restrained plate depicted in Sketch B. This assumes that the edge restraints have little effect on the stresses near the center of the plate, an assumption that should be satisfactory for plates that buckle readily. It also assumes that the inertia of the plate will not greatly retard its bending. Justification of

* It is emphasized that the stresses here considered do not include those which would arise from uniform heating of a restrained plate.

[redacted]

UNCLASSIFIED

this assumption is not undertaken in this report, however, some measurements could be made during a full-scale test to check this assumption. These measurements are described under Recommendations.

By assuming opposite plate curvatures near stations (1) and (2) of the plate shown in Sketch B, we will infer the stresses at station (2) from those estimated at station (1).

We will see that high tension stresses, possibly producing cracks in brittle materials, will exist under certain conditions at the rear side of the plate near station (2).

Prediction of Stresses

In Reference 3 the steady-state stresses existing in a nonuniformly heated free plate are given as

$$\sigma_z(x) = \sigma_y(x) = -\frac{\delta\, T(x)\, E}{1 - \nu} + \frac{1}{L(1 - \nu)} \int_{-L/2}^{L/2} \delta\, T(x)\, E\, dx$$

$$+ \frac{12x}{L^3(1 - \nu)} \int_{-L/2}^{L/2} \delta\, T(x)\, E\, x\, dx.$$

In this expression $\sigma_z(x)$ and $\sigma_y(x)$ are the steady-state stresses in two perpendicular directions parallel to the plate surface on an element of the material x units from the center of the plate; δ is the thermal expansion coefficient, E is Young's modulus, and ν is Poisson's ratio for the material being considered. As before, x is distance normal to the surface of the plate, and $x = 0$ is again taken at one-half of the plate thickness, L. Positive x is toward the front surface of the plate. $T(x)$ represents the temperature increase distribution in the x direction.

The first term on the right-hand side is the compression stress existing if the plate is completely fixed at its edges against translation and rotation. Since the free plate edge can translate, these compression stresses must be modified by tension stresses which would be produced by a tension force applied at the edge of the plate whose magnitude is just equal to the magnitude of the fictitious compression force implied in the first term to prevent edge translation. The second term represents these tension stresses. Similarly, the third term represents bending stresses which had to be added to correct the first term, since the edges of our free plate can rotate.

In Section I it was noted that the temperature ratio profiles at particular times could be well represented by equations of the following form:

$$t^* - 1 = t^*_R - 1 + (t^*_F - t^*_R) \left[\frac{x + L/2}{L}\right]^n.$$

[redacted]

UNCLASSIFIED

In this equation t_F^* and t_R^* are the values of the temperature ratio, t^*, on the front and rear faces of the plate where $x = L/2$ and $-L/2$, respectively.

Multiplying this equation by the reference temperature, t_o, we obtain the following equation for the distribution of temperature increases through the plate.

$$T(x) = (t^* - 1)\, t_o = \left\{ t_R^* + (t_F^* - t_R^*) \left[\frac{x + L/2}{L} \right]^n - 1 \right\} t_o$$

Substituting this relation into the integral equation for the thermal stresses and carrying out the integration yields the following:

$$\sigma_z(x) = \sigma_y(x) = -\frac{\delta E\, t_o\, (t_F^* - t_R^*)}{1 - \nu} \left\{ \left[\frac{x + L/2}{L} \right]^n - \frac{1}{n+1} - \frac{6nx/L}{(n+1)\cdot(n+2)} \right\}.$$

The characteristics of these stress distributions are discussed below. Extreme interior stresses will occur at points x_m obtained from $d\sigma/dx = 0$. This value of x is:

$$x_m = L \left\{ \left[\frac{6}{(n+1)\,(n+2)} \right]^{\frac{1}{n-1}} - \frac{1}{2} \right\}, \; n \neq 1.$$

Substituting this value of x_m we see the maximum interior stress is given by

$$\sigma_{z_m} = \sigma_{y_m} = -\frac{\delta E\, t_o\, (t_F^* - t_R^*)}{1 - \nu} \left\{ (1 - n) \left[\frac{6}{(n+1)\,(n+2)} \right]^{\frac{n}{n-1}} + \frac{2n - 2}{(n+1)\,(n+2)} \right\}$$

The maximum interior stress, its position, and the stress at the front and rear surfaces of the plate are plotted against the exponent n in Figure 22. It is seen for each n that the stress distribution consists of compression stresses at both the front and rear surface and a region of internal tension stresses. In magnitude the front surface stresses are always greatest. For $n = 0$ the temperature is constant throughout the plate, and the stresses here discussed are zero. For $n = 1$ the equation for $\sigma_z(x)$ or $\sigma_y(x)$ shows that the stress also is zero. This situation exists for a linear temperature profile, since the free plate studied can rotate and maintain a linear strain distribution as thermal strain occurs, thus remaining unstressed. As n becomes infinite the temperature profile becomes discontinuous at the front surface and the stress at the front surface tends toward

$$\sigma_z(L/2) = -\frac{\delta E\, t_o\, (t_F^* - t_R^*)}{1 - \nu},$$

while the rear surface stress passes through a maximum value and then tends toward zero. The maximum stress <u>within</u> the plate will occur for the same value of n between 1 and ∞. The graphs in Figure 22 indicate that $n = 5$ yields the maximum interior stress. This maximum interior stress occurs at a depth of about 0.38 of the plate thickness from the front surface.

UNCLASSIFIED

[redacted]

[redacted] [redacted]

UNCLASSIFIED

It should be noted that the stresses discussed above are all directly proportional to the amount of heat absorbed, since the term $(t_F^* - t_R^*)$ varies directly with the amount of heat absorbed.

The preceding equations and their graphs in Figure 22 completely define the stress near station 1 of the plates of Sketch B. Since complete failure is most easily caused by tension rather than compression stress (i.e., cracks lead to more severe damage than spalling or local compression failure), we will focus our attention on the most severe tension stresses in the plate. At station (1) the tension stresses are much less than the maximum compression stresses. We will see below that at station (2) the compression stresses are still greatest in magnitude, but the tension stresses are relatively much higher. We approximate the stresses at station (2) from those at station (1) by changing the sign of the term representing those stresses arising from bending of the plate. This assumes that the plate curvature near station 2 is opposite in sense to the curvature at station 1, but equal in magnitude. Thus at station (2), near the edge of the skin panel, the stress distribution is given by

$$\bar{\sigma}_z(x) = -\frac{\delta E\, t_o\, (t_F^* - t_R^*)}{1 - \nu} \left\{ \left[\frac{x + L/2}{L}\right]^n - \frac{1}{n+1} + \frac{6\, x/L\, n}{(n+1)\,(n+2)} \right\}$$

This stress distribution for station (2) shows compression at the front surface, no extreme interior stress, and tensile stresses at the rear surface. All stresses are zero for $n = 0$, however, $n = 1$ gives stresses at both surfaces, since the plate curvature is opposite to that which the plate would have if it were free. As n tends from 1 to ∞ the front surface stress departs from and returns to the same value, namely

$$\bar{\sigma}_z(L/2) = -\frac{\delta E\, t_o\, (t_F^* - t_R^*)}{1 - \nu}.$$

For all n between 1 and ∞ the front surface stress exceeds this value.

The rear surface stress tends from

$$\sigma_z(-L/2) = \frac{\delta E\, t_o\, (t_F^* - t_R^*)}{1 - \nu}$$

at $n = 1$ to zero at $n = \infty$.

In assessing the importance of these thermal stresses due to transient nonuniform heating we will specify those conditions for which the tension stress on the rear surface of the plate near station (2) would significantly exceed the static ultimate stress if the stress-strain relation were linear. Actually a stress equal to the static ultimate stress will produce plastic strain. Inputs leading to calculated stresses fictitiously exceeding the static ultimate stress will produce an amount of plastic strain which increases as the calculated fictitious stress increases.

UNCLASSIFIED

[redacted]

For convenience we define a stress ratio, S, as the ratio of the tension stress at the rear of the plate near station (2) to the static ultimate stress of the plate material. As indicated above, the calculated stress is a fictitious stress for values of S near or exceeding unity.

$$S = \frac{\sigma_z(-L/2)}{\sigma_{ult}} = \frac{\delta E\, t_o\, (t_F^* - t_R^*)}{\sigma_{ult}\,(1 - \nu)} \left(\frac{1}{n + 1} + \frac{3n}{(n + 1)\,(n + 2)} \right).$$

The transient heating solutions of Section I were used with this expression to obtain the time variations of S for various thermal pulse durations and plate thicknesses. These variations showed maximum stress ratios occurring at dimensionless times from .50 to .85. These maximum stress ratios, S_M, are plotted versus duration of the thermal pulse with plate thickness as a parameter in Figure 23. The data of Figure 23 are for aluminum plates absorbing enough heat to eventually cause a uniform 1000°F temperature increase throughout the plate.

For maximum stress ratios between 1 and 4 the following equation represents the data of Figure 23 to about 5%. (See the dashed line in Figure 23.)

$$2.5\,\tau_{40} = 3.32\,\frac{L^2}{a}\,S_M^{-1.6}$$

or

$$S_M = 2.12 \left[\frac{2.5\,\tau_{40}\,a}{L^2} \right]^{-.625}.$$

This relation can be generalized to apply to any amount of absorbed heat, since the stress is directly proportional to the amount of heat absorbed. Thus the stress ratio in the above equation can be modified by the ratio of Δt_f, the final uniform temperature increase, to 1000°F, the value for which Figure 23 was prepared.

$$S_M = 2.12 \left[\frac{2.5\,\tau_{40}\,a}{L^2} \right]^{-.625} \frac{\Delta t_f}{1000}$$

We can further generalize this stress ratio relation to apply to any material by multiplying the stress ratio by the following quantity:

$$\left[\frac{\sigma_{ult}\,(1 - \nu)}{\delta E} \right]_{75\ ST\ Al.} \times \left[\frac{\delta E}{\sigma_{ult}\,(1 - \nu)} \right]_{\text{any material.}}$$

Table III below lists the quantities needed to evaluate this term for the materials considered in this report.

TABLE III

Physical Constants Used In The Transient Stress Problem

Material	σ_{ult}	ν	δ	E	$\frac{\sigma_{ult}(1-\nu)}{\delta E}$
Al. Alloy 75 ST	75,000 psi	.33	$13.3 \times 10^{-6}/^{\circ}F$	10.3×10^{6} psi	367
Mag. Alloy JS-1H	42,000 psi	.28	$14 \times 10^{-6}/^{\circ}F$	6.5×10^{6} psi	332
Stainless Steel 18-8	125,000 psi	.305	$6.5 \times 10^{-6}/^{\circ}F$	27.6×10^{6} psi	485

Using the tabulated values for 75 ST aluminum, the final stress ratio equation becomes the following:

$$S_M = 777 \left[\frac{L^2/a}{2.5\,\tau_{40}}\right]^{.625} \frac{\Delta t_f}{1000} \left[\frac{\delta E}{\sigma_{ult}(1-\nu)}\right] \quad \text{any material.}$$

In applying this relation we must restrict ourselves to applications where temperatures high enough to invalidate our stress calculations are not encountered. We will assume that this limiting temperature is one near the melting temperature, an assumption which is certainly open to question. However, the use of this assumption is not out of line with some of the other approximations involved. Moreover, the direct dependence of stress on temperature increase allows each reader to adjust these results to any particular temperature increase with a minimum of effort.

In applying these results in this report we will neglect any thermal degradation of material strength. Motivations for this are twofold, namely: (1) extremely short duration elevated temperature effects on material properties are not well known, and (2) heating of the rear surface for those inputs which produce large stresses at the rear surface will not be excessive. The stresses which can be produced in 75 ST aluminum alloy, JS-1H magnesium alloy, and 18-8 stainless steel are shown in Figures 24, 25, and 26, respectively. Each of these graphs is a plot, with maximum stress ratio as a parameter, of thermal pulse duration multiplied by diffusivity divided by thickness squared versus amount of heat absorbed. The heat absorbed is expressed as a part of the heat absorption required to uniformly heat the plate to its melting temperature. On each graph is indicated the least value of the ordinate for which our stress calculations apply, as discussed above. To prepare these figures a 1200°F melting temperature was used for aluminum and magnesium, while 2800°F was used for the melting temperature of stainless steel. These figures show that combinations of heat absorbed, plate thickness, and thermal pulse duration exist for which the maximum stress ratio is between 2 and 3 for 75 ST aluminum and JS-1H magnesium and is greater than 4 for 18-8 stainless steel. It is believed that the plastic strains related to these calculated stress ratios are less than the rupture strains of the ductile materials typified by 18-8 and 75 ST. However in the more brittle materials, such as

UNCLASSIFIED

JS-1H, cracks may be caused. Figure 27 presents for 75 SF aluminum plates the front and rear surface temperature and stress variations with time for a typical combination of heat absorbed, plate thickness, and thermal pulse duration which causes large stresses. It is seen from this graph that the rear surface tension stress exceeds 3/4 of its maximum value for about 40% of the thermal pulse duration. It is also noted that the magnitude of the maximum front surface compression stresses is about 160% of the magnitude of the maximum rear surface tension stresses.

UNCLASSIFIED

UNCLASSIFIED

SECTION III

SPECIFICATION OF YIELDS AND RANGES AT WHICH LARGE STRESSES WILL BE CAUSED BY NONUNIFORM HEATING

In this section we will see if those combinations of heat absorbed, plate thickness, and thermal pulse duration which produce high stresses represent practical cases. To do this we will consider the response of different plates to thermal inputs associated with both the first and second thermal pulses of various yield weapons between sea level and 100,000 feet. Reference 4 shows that the shape of the first thermal pulse is not much different from the shape of the second thermal pulse. Thus we may assume that no large errors are introduced by neglecting this change in input pulse shape.

References 4 and 5 discuss the duration of and the energy contained in the thermal pulses at different altitudes. At sea level it is assumed that 1% of the total yield is contained in the first pulse and 33% of the yield in the second pulse. At 100,000 feet these figures become 50% and 17%, respectively. For all yields the energy contained in either pulse is assumed proportional to the total yield.* The relations below represent these data within 5% - 10% for altitudes between 20,000 and 100,000 feet. Zero attenuation is assumed, thus negating these results when cloud coverage cannot be neglected.

Duration of the First Thermal Pulse

$$D_1 = .92 \times 10^{-3} W^{1/3} \left[\frac{A + 200}{205}\right]^{4.1} \text{ seconds}$$

Energy Contained in the First Thermal Pulse

$$Q_1 = .157 \times 10^9 \frac{W}{R^2} \left[\frac{A + 200}{300}\right]^{11} \text{ B/ft}^2$$

Duration of the Second Thermal Pulse

$$D_2 = .192 \left[\frac{A + 200}{205}\right]^{4.1} W^{1/2} \text{ seconds}$$

Energy Contained in the Second Thermal Pulse

$$Q_2 = .105 \times 10^9 \frac{W}{R^2} \left\{1 - .5 \left[\frac{A + 200}{300}\right]^{11}\right\} \text{ B/ft}^2$$

In these relations W is total yield in kilotons, R is radial distance from the burst point in feet, and A is burst altitude in thousands of feet. In accordance with the work of

* More accurate prediction of the thermal yield as $.44\ W^{.94}$ is not deemed necessary in the yield range of interest. At a yield of 10,000 KT the method used predicts only 33% more thermal than that given by $.44\ W^{.94}$.

UNCLASSIFIED

[redacted]

Section I, the duration, D coincides with radiation of about 95% of the total energy in each pulse.

We now rewrite the general stress equation presented in Section II substituting

$$\Delta t_f = \frac{\alpha Q}{\gamma c L}, \text{ and } 2.5\ \tau_{40} = D.$$

$$S_M = 777 \left[\frac{L^2/\alpha}{D}\right]^{.625} \frac{\alpha Q}{1000\ \gamma c L} \left[\frac{\delta\ E}{\sigma_{ult}\ (1 - \nu)}\right] \quad \text{any material.}$$

Below this equation is specialized for 75 ST aluminum, JS-1H magnesium, and 18-8 stainless steel.

To remain in the region of valid stress calculations the following inequality, taken from the data of Figure 21, should be satisfied. For heats absorbed which are between 20% and 80% of that required to uniformly heat the plate to its melting temperature, this relation specifies that range of β's (i.e. pulse duration, plate thickness, and diffussivity) for which the maximum temperature is less than the melting temperature.

$$\frac{D\alpha}{L^2} \geq \left[\frac{\Delta t_f/\tau_M + 3}{3.8}\right]^{12.3}$$

Since this relation is somewhat unwieldy the following input restrictions, taken directly from Figures 24 through 26, will be used.

TABLE IV

Input Restrictions For Certain Stress Ratios

75 ST Aluminum	JS-1H Magnesium	18-8 Stainless Steel
$S_M = 2.25,\ \frac{Q}{L} \leq .8\ \frac{1200\ \gamma c}{\alpha}$	$S_M = 2.75,\ \frac{Q}{L} \leq .7\ \frac{1200\ \gamma c}{\alpha}$	$S_M = 4.0,\ \frac{Q}{L} \leq .8\ \frac{2800\ \gamma c}{\alpha}$
$= 76.1 \times 10^3$	$= 32.9 \times 10^3$	$= 242 \times 10^3$

For 75 ST aluminum the maximum stress ratio expression reduces to

$$S_M = .00223\ \frac{L^{.25}\ Q}{D^{.625}}$$

Substituting Q and D for the first thermal pulse this becomes

$$S_{M_1} = 975 \times 10^{-16.88}\ \frac{L^{.25}\ W^{.792}\ (A + 200)^{8.44}}{R^2}$$

UNCLASSIFIED

[redacted]

[redacted] [redacted]

$$Q_{1/L} = .157 \times 10^9 \frac{W}{LR^2}\left[\frac{A + 200}{300}\right]^{11} \quad \text{(The value tabulated above)}$$

For the second thermal pulse the equation is:

$$S_{M_2} = 6.58 \times 10^5 \left\{ 1 - .5 \left[\frac{A + 200}{300}\right]^{11} \right\} \left[\frac{205}{A + 200}\right]^{2.56} \frac{L^{.25}\, W^{.688}}{R^2}$$

$$Q_2/L = .105 \times 10^9 \frac{W}{LR^2}\left\{ 1 - .5 \left[\frac{A + 200}{300}\right]^{11} \right\} \leq \quad \text{(The value tabulated above)}$$

For JS-1H magnesium and 18-8 stainless steel these maximum stress ratio equations multiplied by the proper constant also apply. These multiplying constants are:

$$(S_M)_{\text{JS-1H mag}} = 2.07\ (S_M)_{\text{75 ST Aluminum}}$$

$$(S_M)_{\text{18-8 Stainless Steel}} = 1.32\ (S_M)_{\text{75 ST Aluminum}}$$

Figures 28 through 30 are plots of these maximum stress ratio equations for 75 ST aluminum, JS-1H magnesium, and 18-8 stainless steel heated by the first thermal pulse. The following table presents some interesting aspects of these figures.

TABLE V

Typical Yields And Ranges Resulting In Large Stresses During The First Thermal Pulse

Material	Maximum Stress Ratio	Alt.	Plate Thickness	Yield	Range
75 ST Aluminum	2 1/4	20,000	.004	29	1100
	2 1/4	100,000	.004	1	1100
	2 1/4	100,000	.004	29	4100
	1 1/2	20,000	.004	29	1350
	1 1/2	100,000	.004	1	1350
	1 1/2	100,000	.004	29	5000
JS-1H Magnesium	2 3/4	20,000	.004	29	1400
	2 3/4	100,000	.004	1	1400
	2 3/4	100,000	.004	29	5300
	1 1/2	20,000	.004	29	1900
	1 1/2	100,000	.004	1	1900
	1 1/2	100,000	.004	29	7200

UNCLASSIFIED

[redacted]

TABLE V (Cont)

Material	Maximum Stress Ratio	Alt.	Plate Thickness	Yield	Range
18-8 Stainless Steel	4	20,000	.004	29	950
	4	100,000	.004	1	950
	4	100,000	.004	29	3600
	1 1/2	20,000	.004	29	1550
	1 1/2	100,000	.004	1	1550
	1 1/2	100,000	.004	29	5800

It is seen that thermal inputs which cause high stress (and possibly cracks in JS-1H) will exist at about a 1000-foot range from 29 KT near sea level and at a similar range from 1 KT at 100,000 feet. At some 4000-5000 feet from 29 KT at 100,000 feet thermal inputs producing the same effects will be encountered.

Figure 31 presents similar data for the second thermal pulse. Comparing these data with those for the first thermal pulse it is seen that for yields greater than a few hundredths KT the first thermal pulse causes higher stresses due to nonuniform heating at a given distance than those stresses caused by the second thermal pulse.

E. T. CLARK - 5141

Case No. 409.07
May 24, 1955

UNCLASSIFIED

[redacted] [redacted]

REFERENCES

1. Jakob and Hawkins, "Elements of Heat Transfer".

2. Mack, R. C., "Damage to Metal Plates from High Intensity Short Duration Heat Pulses", SC-3459(TR), August 25, 1954, (Unclassified).

3. Timoshenko and Goodier, "Theory of Elasticity".

4. Shelton, F. H., "Phenomenology of a High Altitude Atomic Explosion", SC-3363(TR), April 28, 1954, (SRD).

5. Shelton, F. H., "High-Altitude Effects on Blast-Thermal Partition of Energy from Nuclear Explosions and Associated Scaling Laws", SC-2969(TR), September 1953, (SRD).

UNCLASSIFIED

UNCLASSIFIED

[redacted]

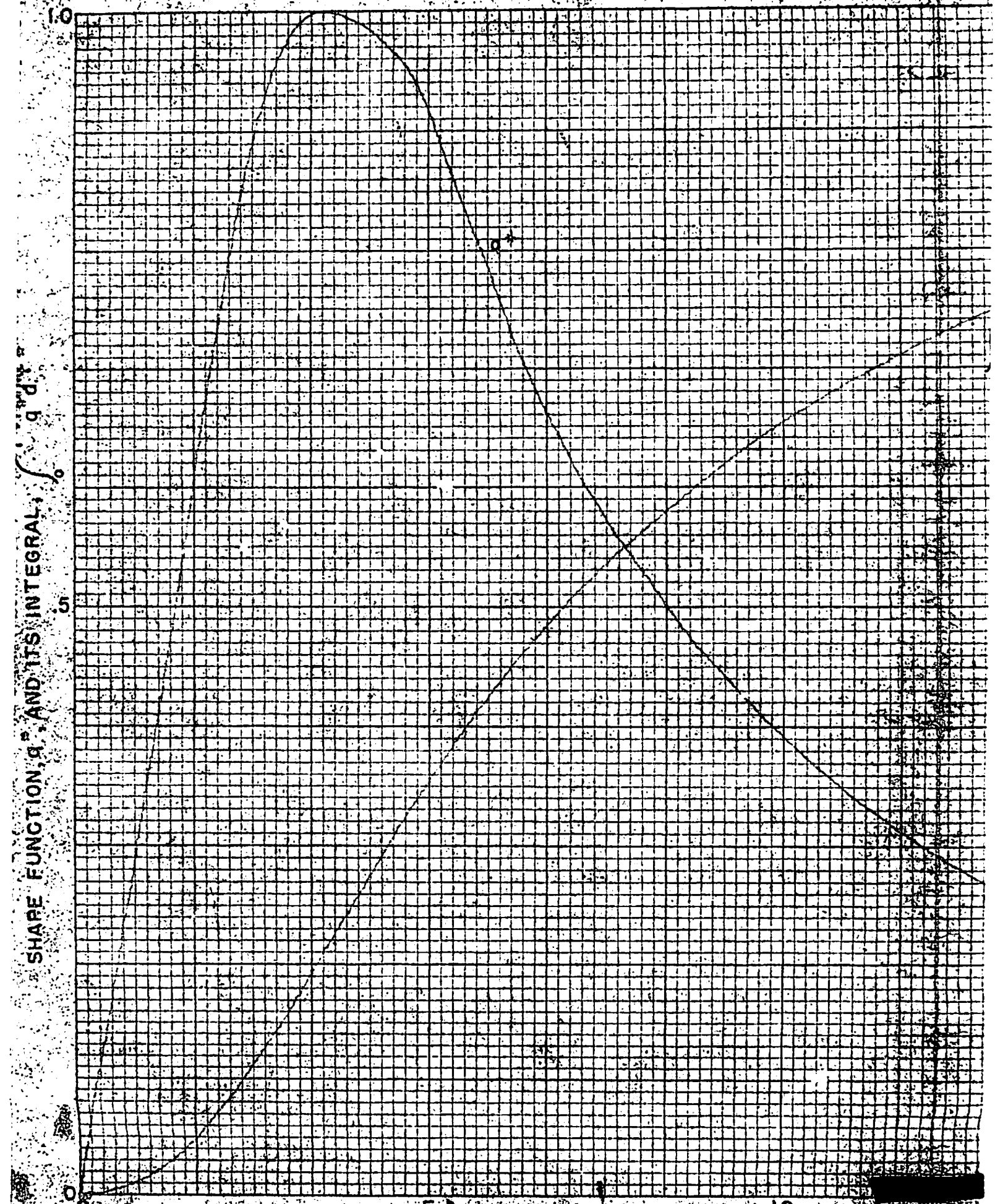

[redacted]

UNCLASSIFIED

Fig. 1

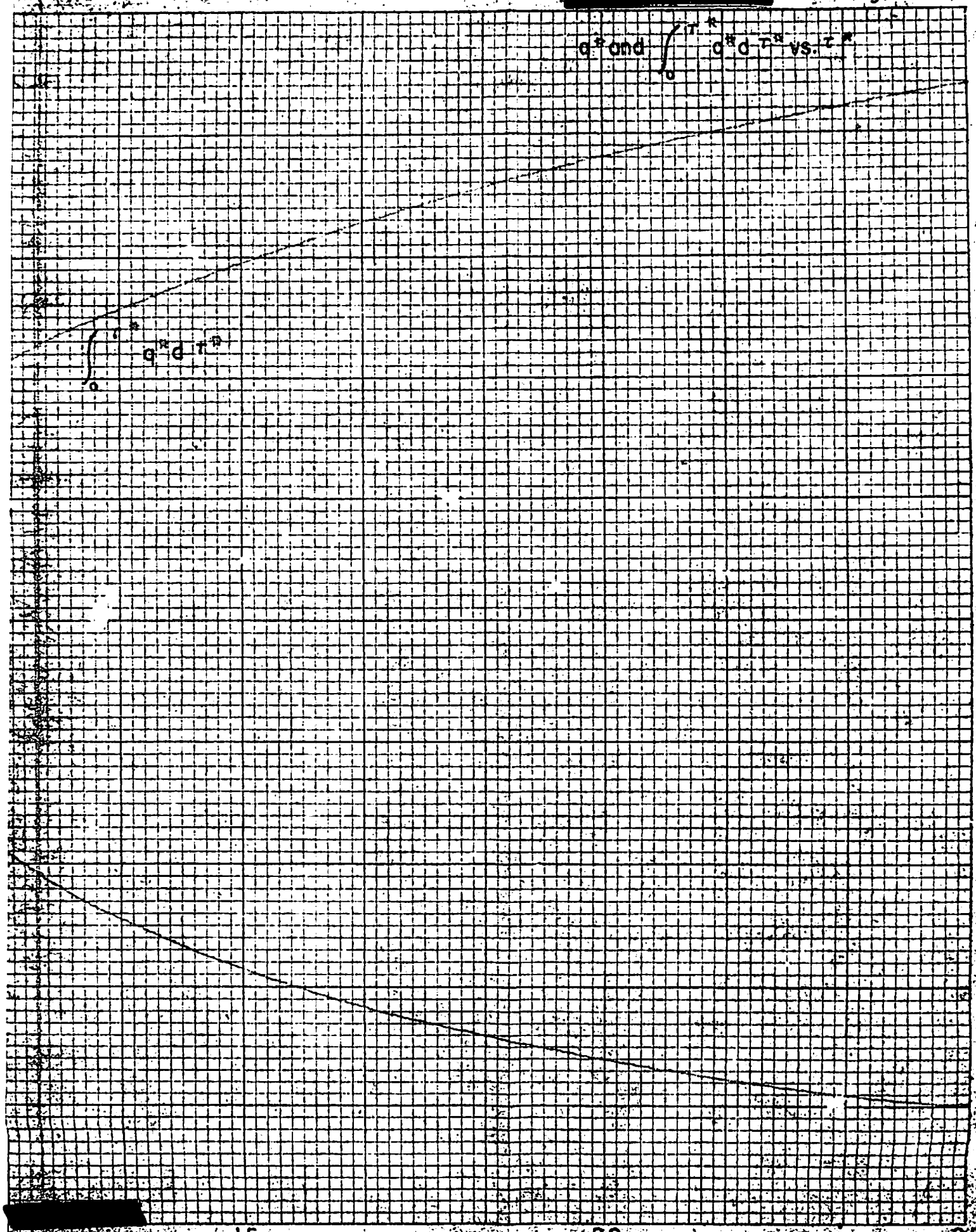
q^* and $\int_0^{\tau^*} q^* d\tau^*$ vs. τ^*
$\int_0^{\tau^*} q^* d\tau^*$
1.5
2.0
2.5
IONLESS TIME τ^*

UNCLASSIFIED

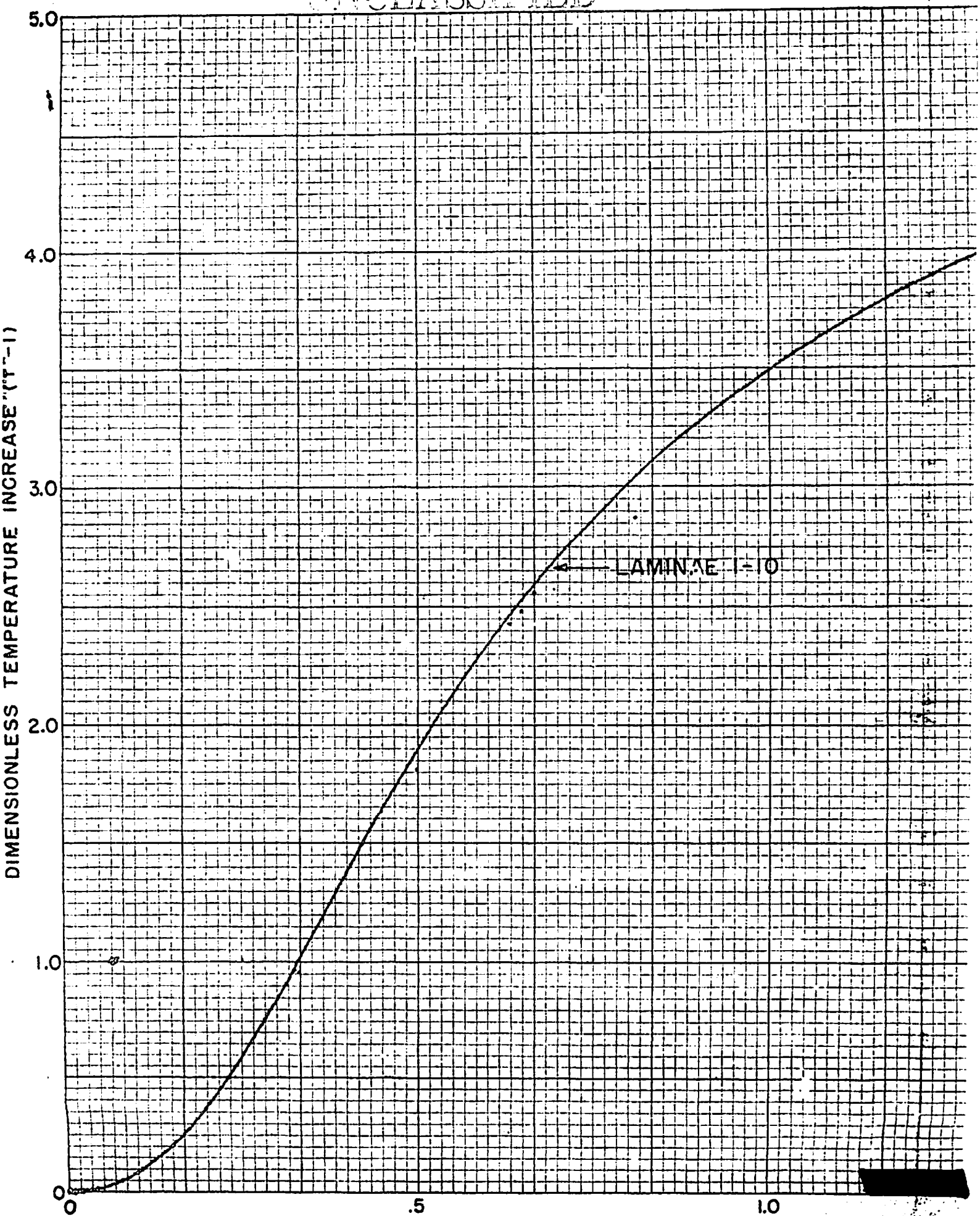

UNCLASSIFIED

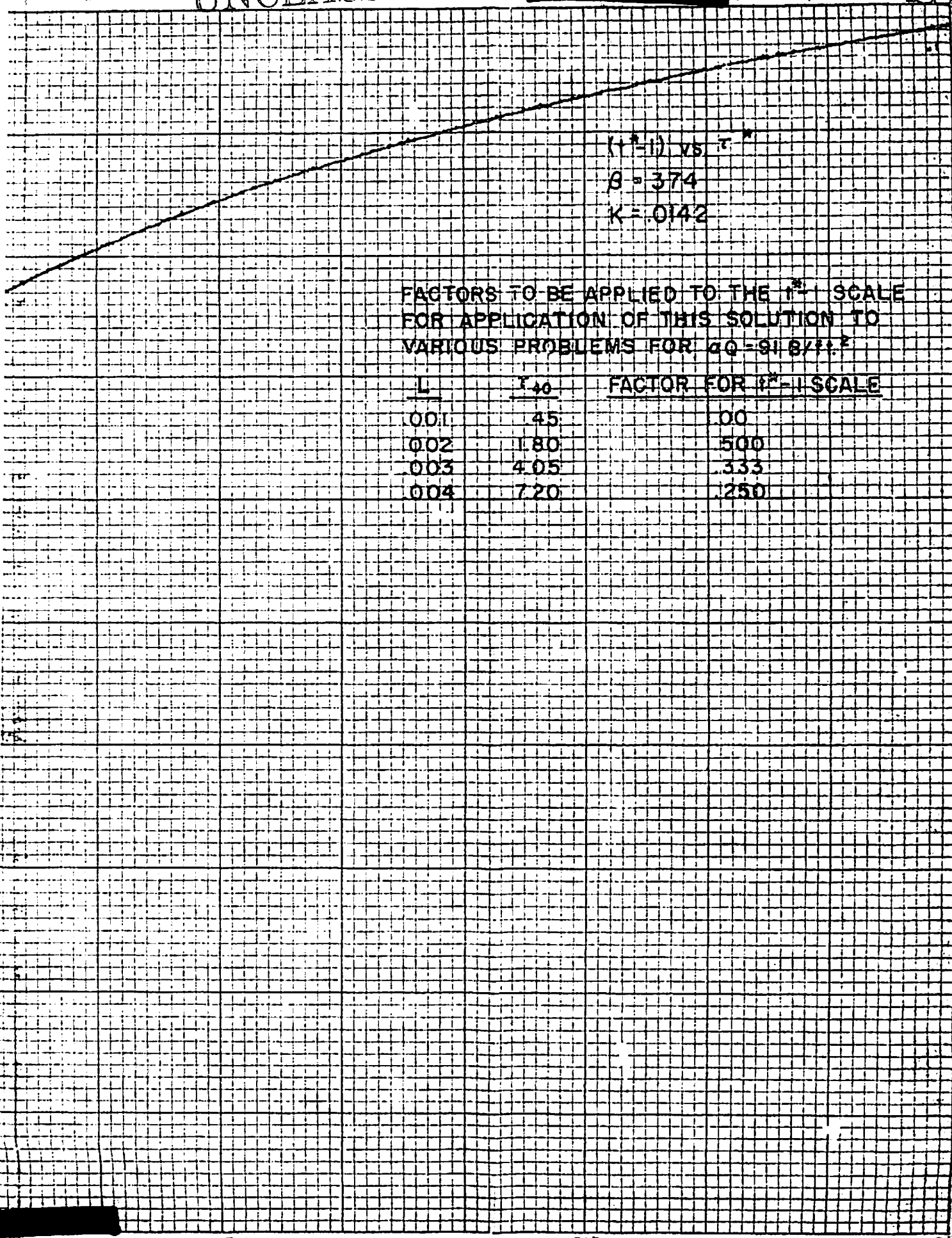

FACTORS TO BE APPLIED TO THE $t^* - 1$ SCALE FOR APPLICATION OF THIS SOLUTION TO VARIOUS PROBLEMS FOR $\alpha Q = 91\ B/ft.^2$

L	τ_{40}	FACTOR FOR $t^* - 1$ SCALE
.001	45	.00
.002	1.80	.500
.003	4.05	.333
.004	7.20	.250

[redacted]

[redacted]

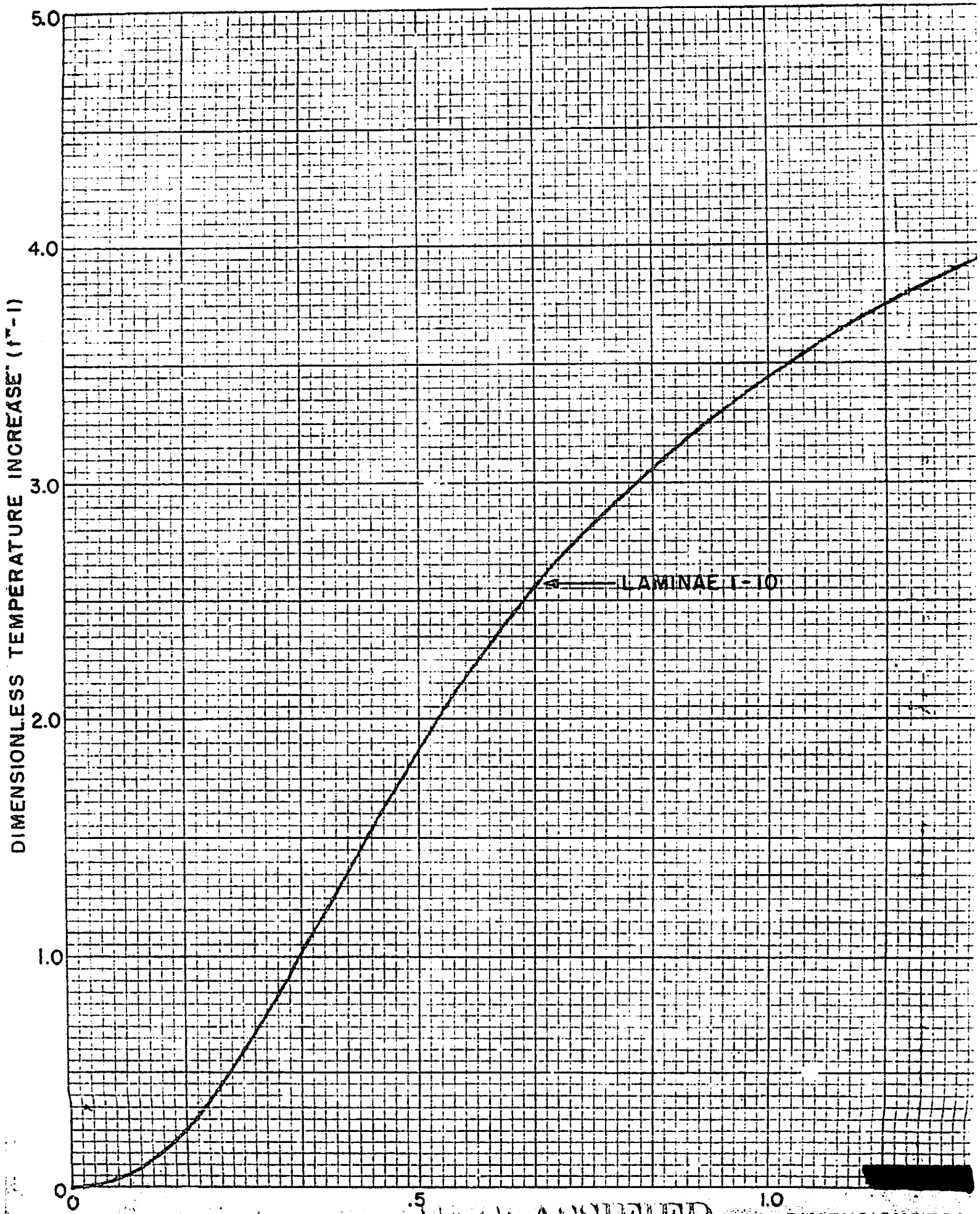

[redacted]

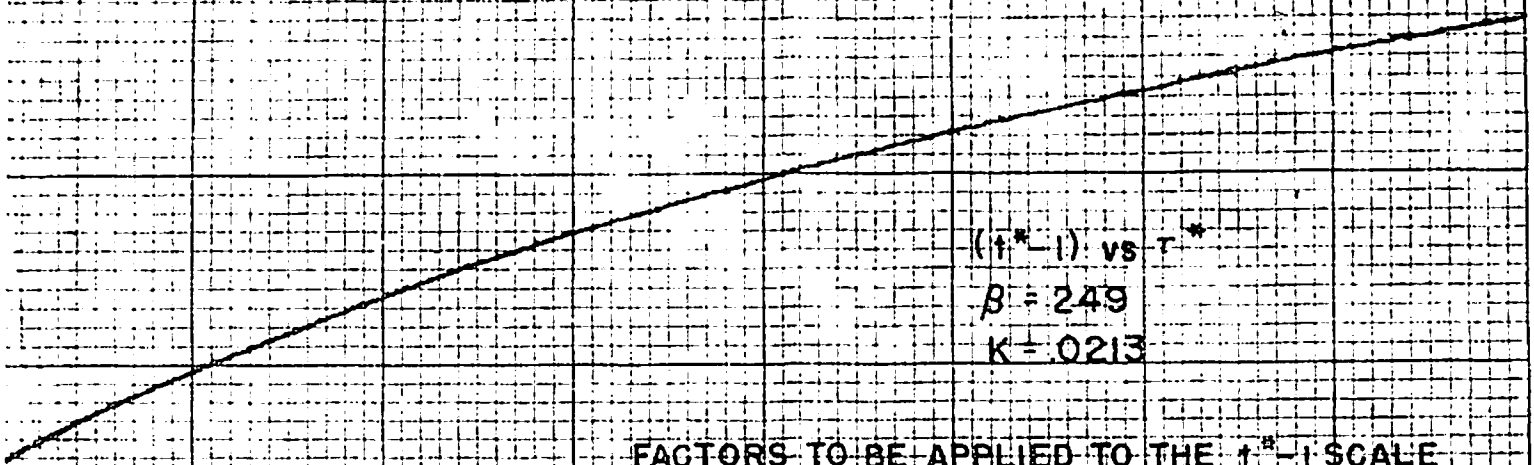

$(t^* - 1)$ vs τ^*

$\beta = 249$

$K = .0213$

FACTORS TO BE APPLIED TO THE $t^* - 1$ SCALE FOR APPLICATION OF THIS SOLUTION TO VARIOUS PROBLEMS FOR $\alpha Q = 91$ B/ft.^{2}

L	τ_{40}	FACTOR FOR $t^* - 1$ SCALE
.001	.30	1.00
.002	1.20	.500
.003	2.70	.333
.004	4.80	.250

[redacted]

1.5 UNCLASSIFIED 2.0 2.5

IONLESS TIME τ^*

UNCLASSIFIED

[redacted]

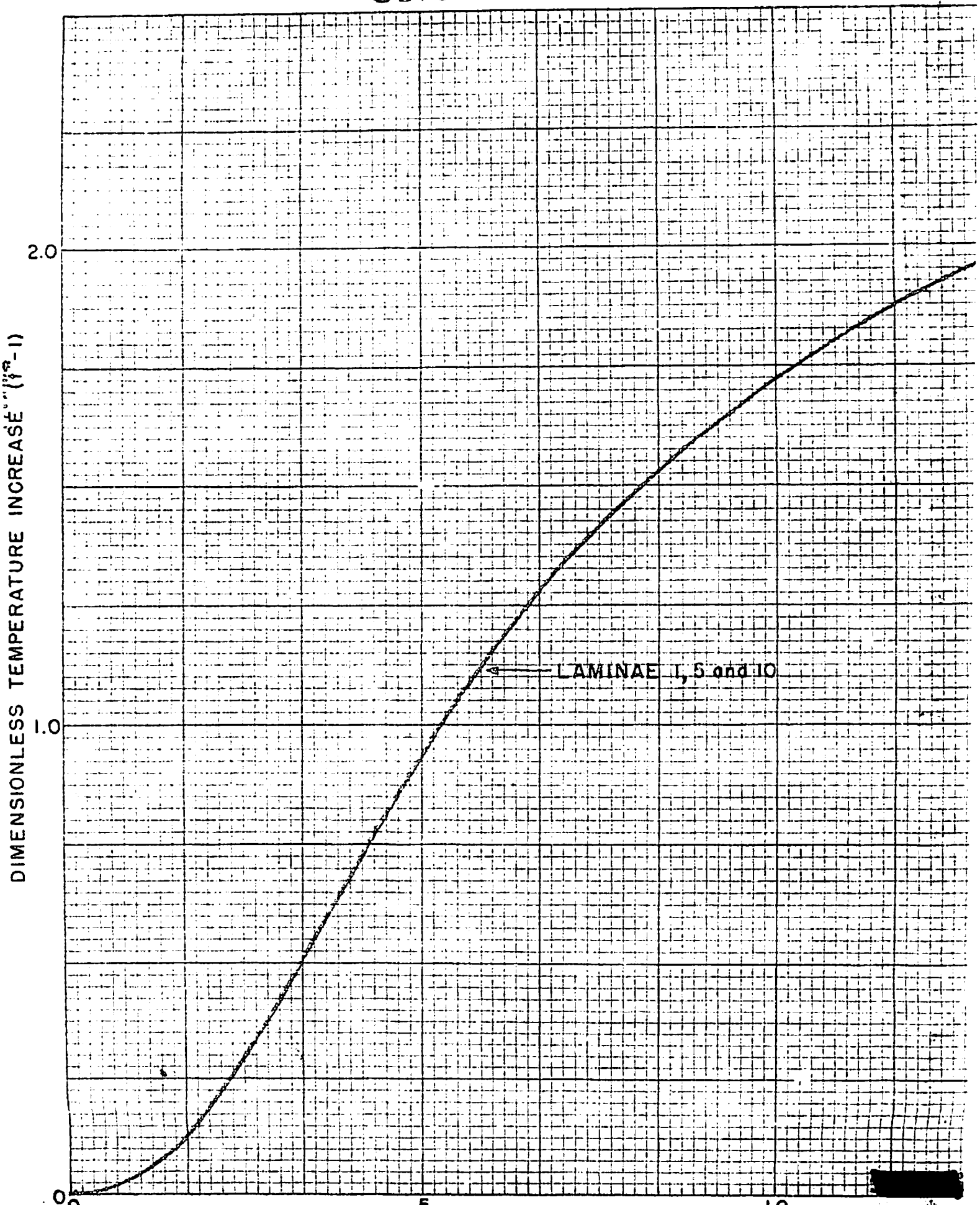

[redacted]

UNCLASSIFIED

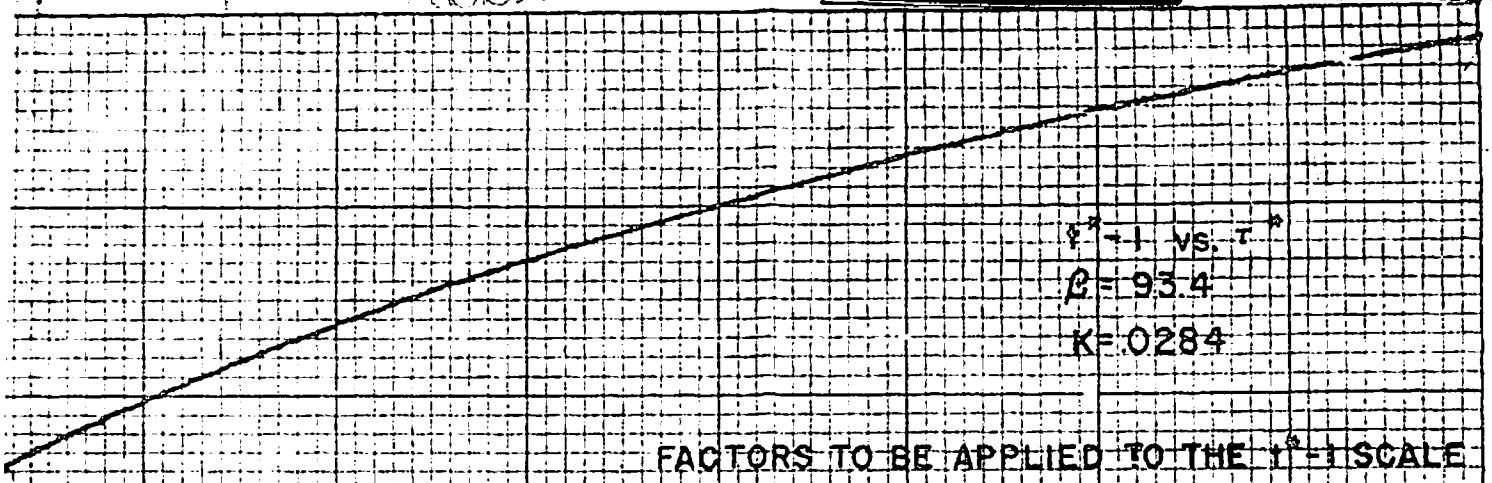

FACTORS TO BE APPLIED TO THE $t^* - 1$ SCALE FOR APPLICATION OF THIS SOLUTION TO VARIOUS PROBLEMS FOR $\alpha Q = 91$ B/ft^2

L	τ_{4D}	FACTOR FOR $t^* - 1$ SCALE
.001	.1125	2.0
.002	45	1.0
.003	1.012	.667
.004	1.80	.500
.007	5.51	.286

[redacted]

UNCLASSIFIED

[redacted]

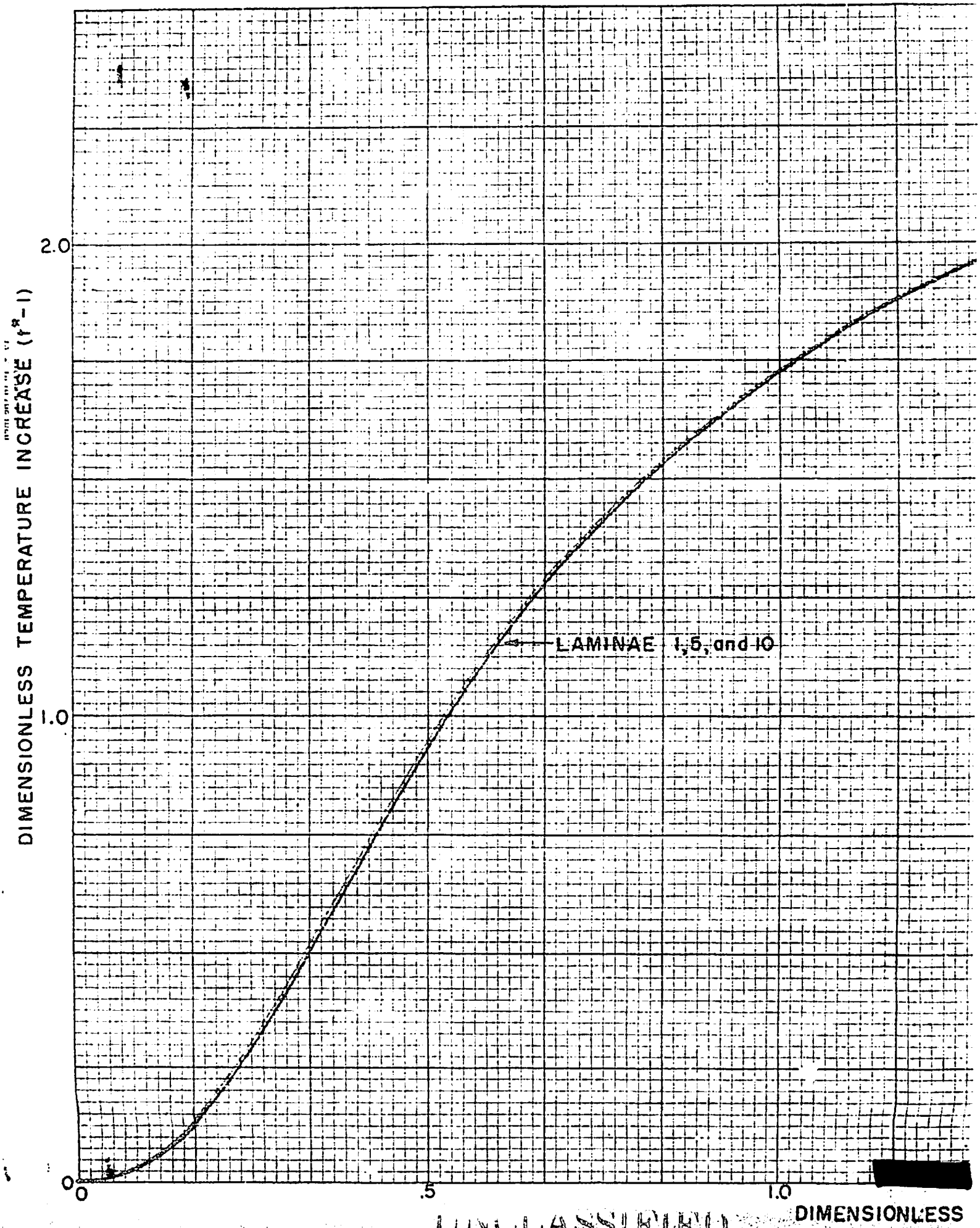

[redacted]

UNCLASSIFIED

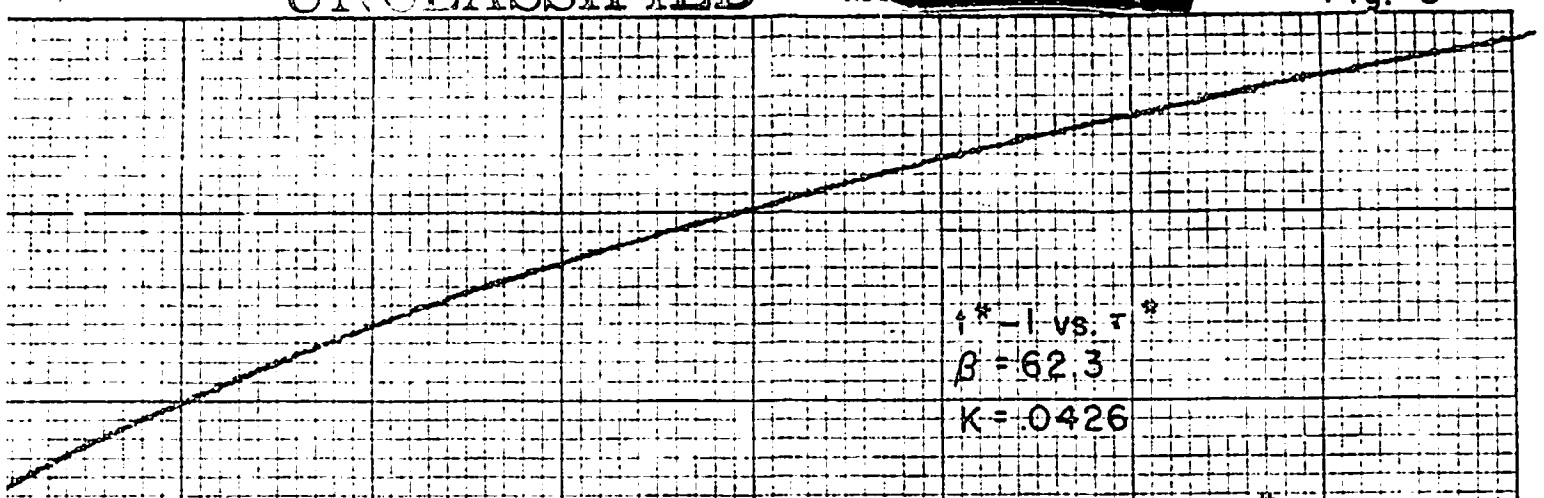

$t^* - 1$ vs. τ^*

$\beta = 62.3$

$K = .0426$

FACTORS TO BE APPLIED TO THE $t^* - 1$ SCALE FOR APPLICATION OF THIS SOLUTION TO VARIOUS PROBLEMS FOR $\alpha Q = 91$ B/ft^2

L	τ_{40}	FACTOR FOR $t^* - 1$ SCALE
.001	.075	2.0
.002	.30	1.0
.003	.675	.667
.004	1.20	.50
.007	3.675	.286
.010	7.50	.20

[redacted]

UNCLASSIFIED

[redacted]

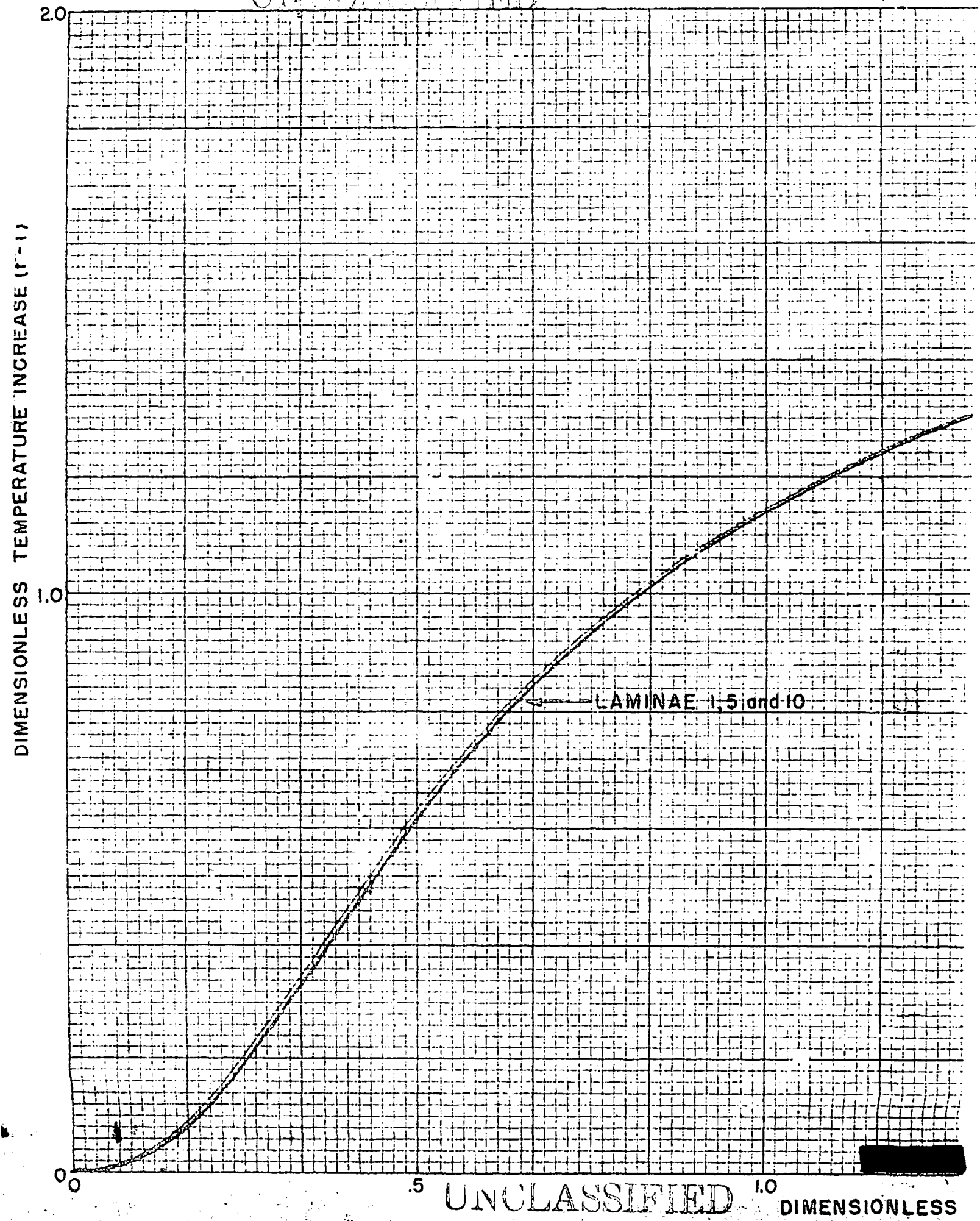

[redacted]

UNCLASSIFIED

$t^* - 1$ vs. τ^*

$\beta = 41.5$

$K = .0426$

FACTORS TO BE APPLIED TO THE $t^* - 1$ SCALE FOR APPLICATION OF THIS SOLUTION TO VARIOUS PROBLEMS FOR $\alpha Q = 91$ B/ft.^{2}

L	τ_{40}	FACTOR FOR $t^* - 1$ SCALE
.001	.05	3.0
.002	.20	1.5
.003	.45	1.0
.004	.80	.75
.007	2.45	.428
.010	5.0	.30

[redacted]

1.5 2.0 2.5

NLESS TIME τ^*

UNCLASSIFIED

[redacted]

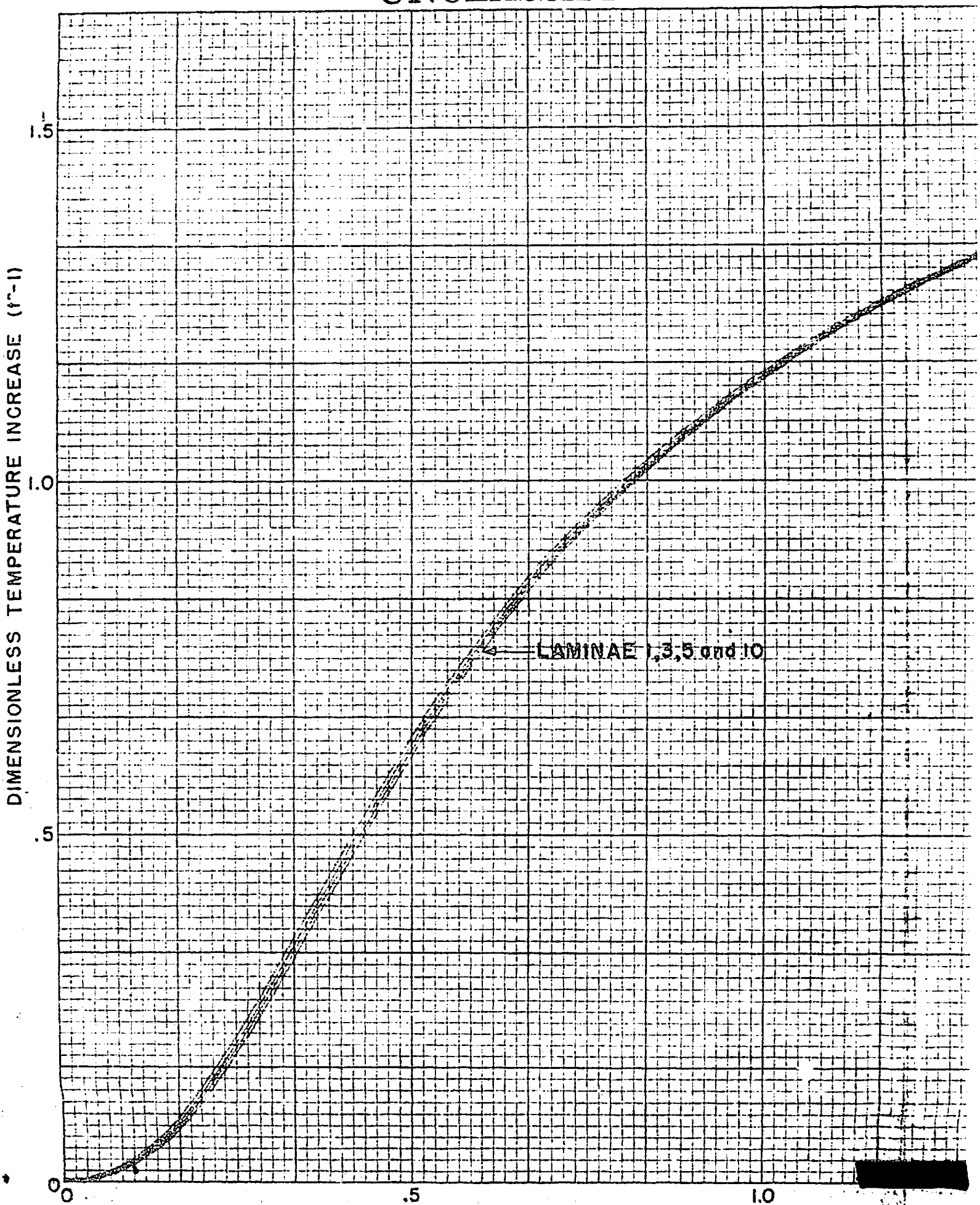

[redacted]

UNCLASSIFIED

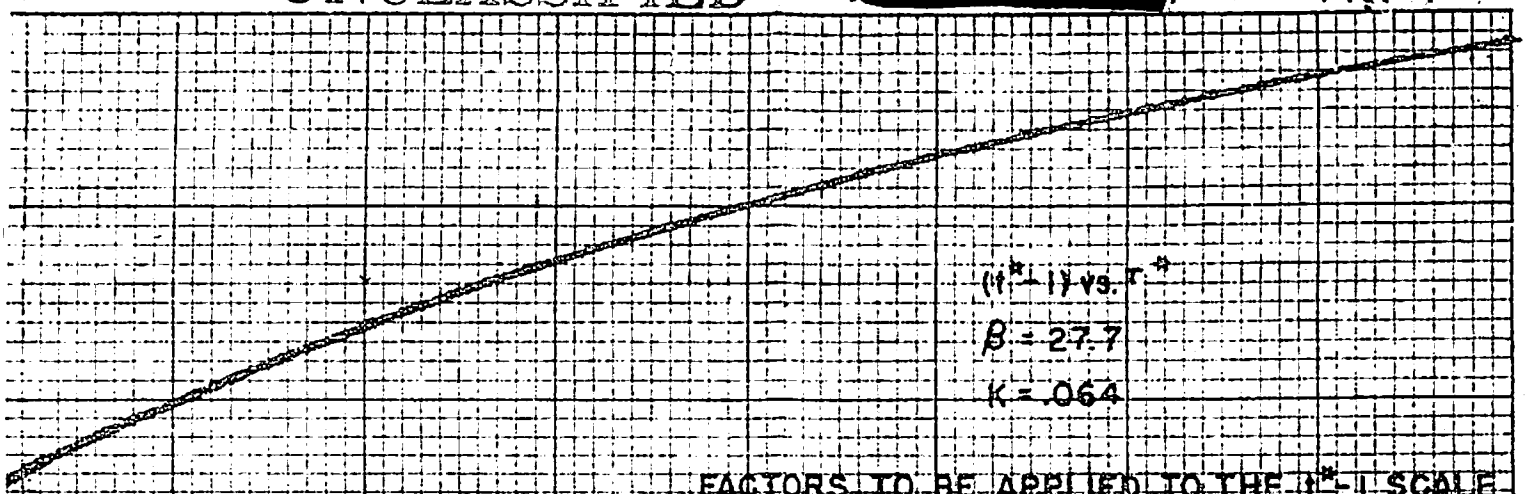

$(t^* - 1)$ vs. τ^*

$\beta = 27.7$

$K = .064$

FACTORS TO BE APPLIED TO THE $t^* - 1$ SCALE FOR APPLICATION OF THIS SOLUTION TO VARIOUS PROBLEMS FOR $dQ = 91$ B/ft.^{2}

L	τ_{40}	FACTOR FOR $t^* - 1$ SCALE
.001	.0333	3.0
.002	.1333	1.5
.003	.30	1.0
.004	.533	.75
.007	1.633	.429
.010	3.333	.30
.020	13.33	.15

[redacted]

[redacted] Fig. 7a

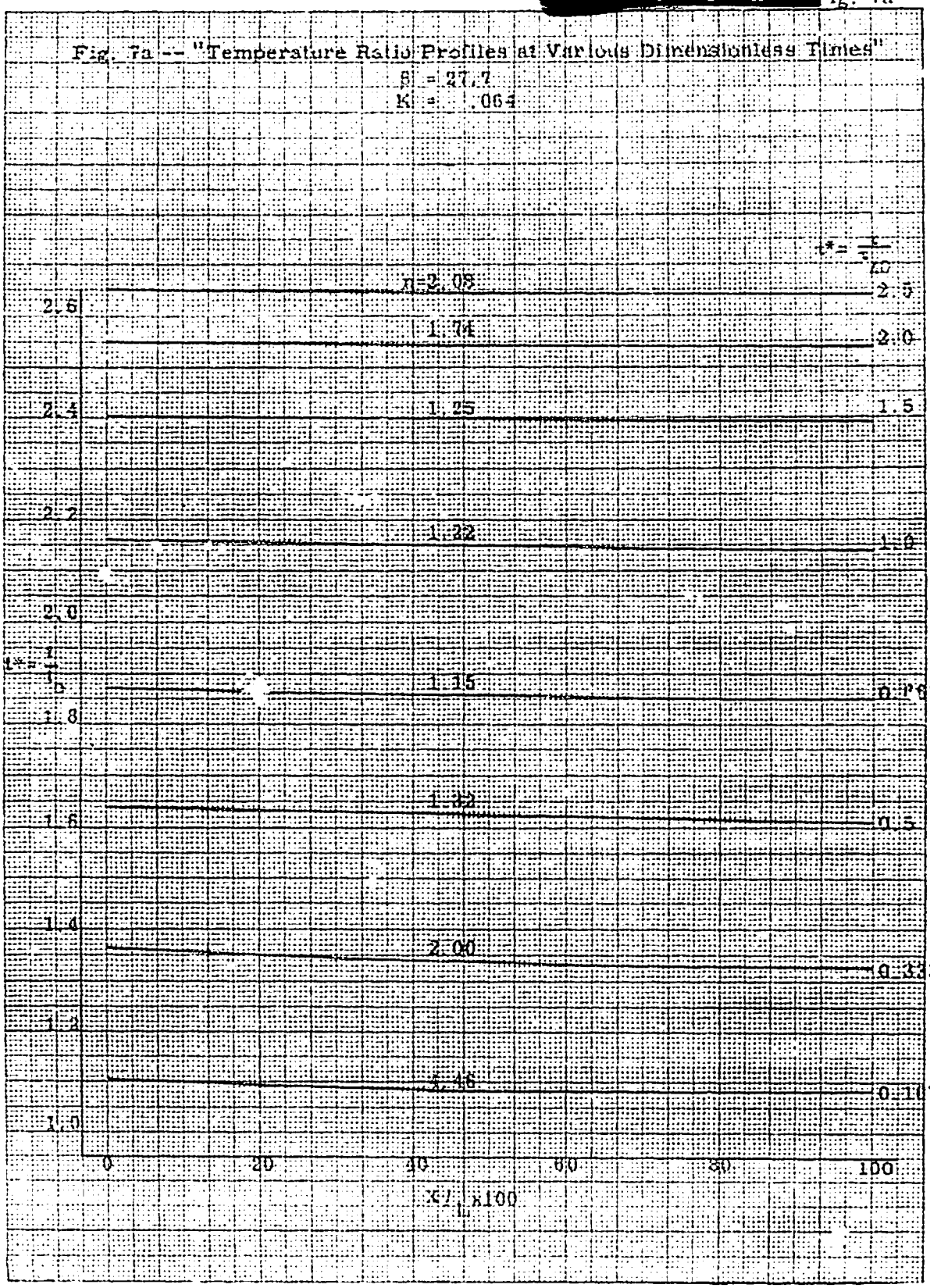

[redacted]

UNCLASSIFIED

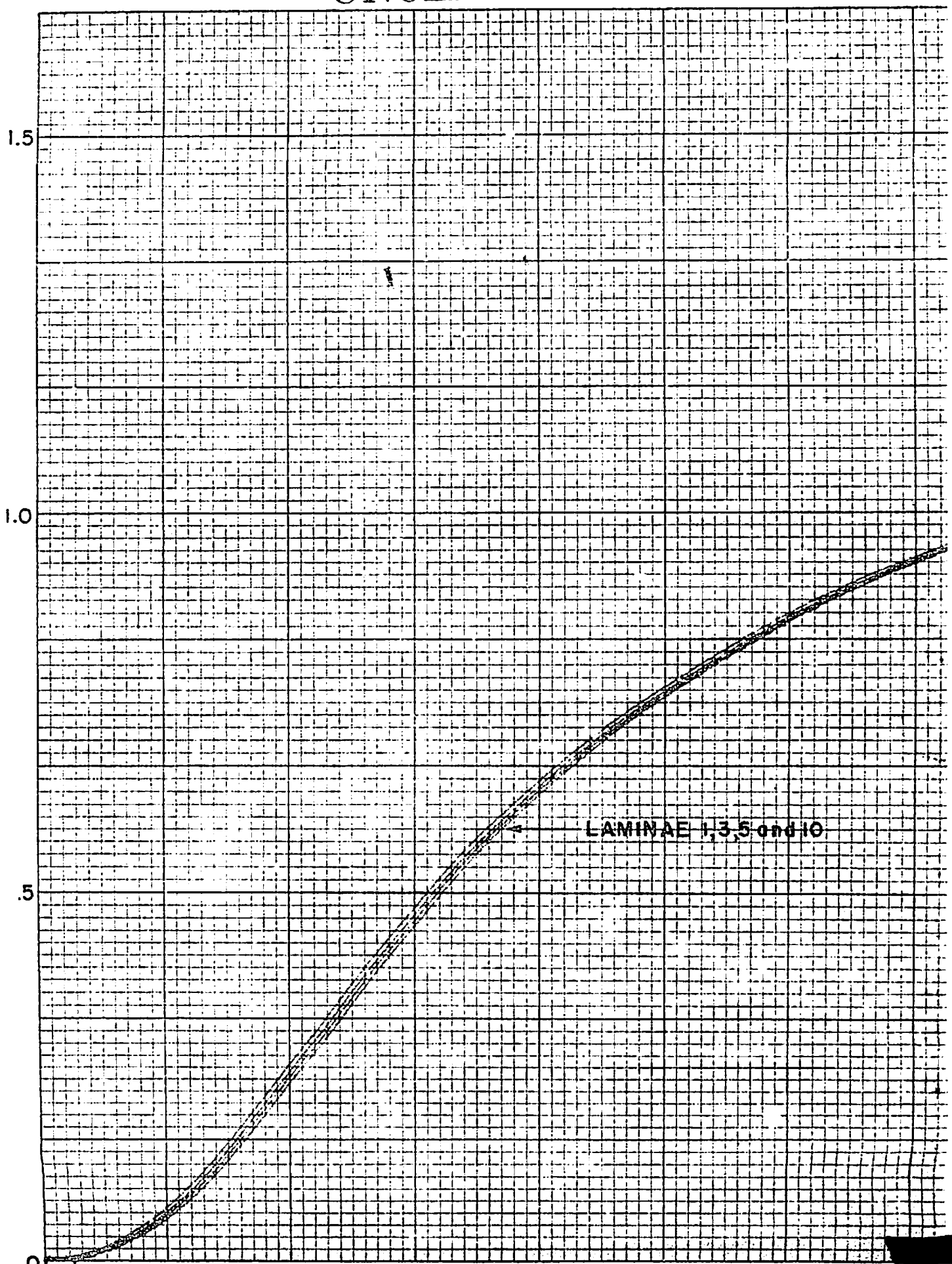

UNCLASSIFIED

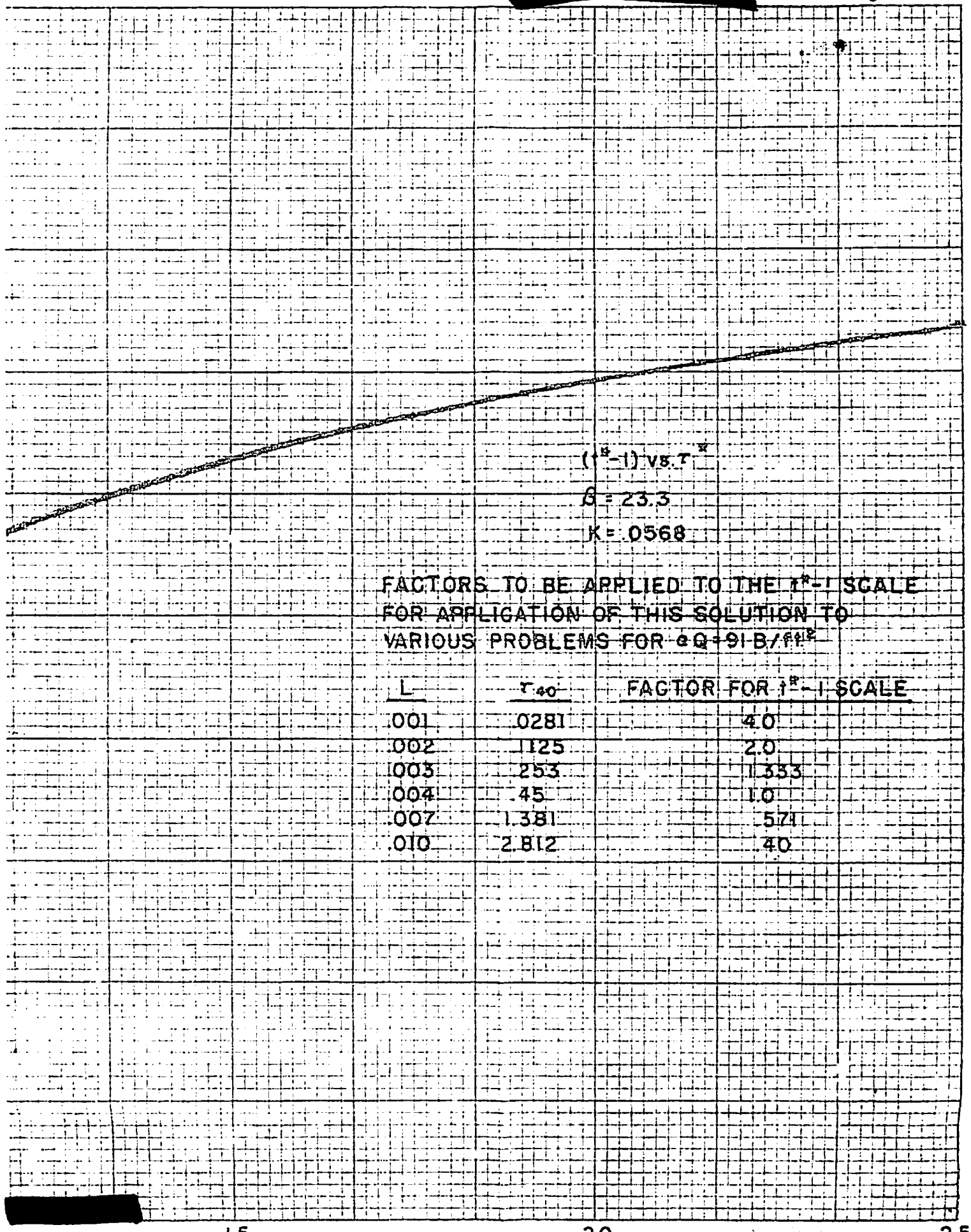
$(t^* - 1)$ vs. τ^*
$\beta = 23.3$
$K = .0568$
FACTORS TO BE APPLIED TO THE $t^* - 1$ SCALE
FOR APPLICATION OF THIS SOLUTION TO
VARIOUS PROBLEMS FOR $aQ = 91 B/f^2$
L | τ_{40} | FACTOR FOR $t^* - 1$ SCALE
.001 | .0281 | 4.0
.002 | .1125 | 2.0
.003 | .253 | 1.333
.004 | .45 | 1.0
.007 | 1.381 | .571
.010 | 2.812 | .40
1.5
2.0
2.5
UNLESS TIME τ^*

[redacted]

[redacted]

Fig. 8a

Fig. 8a -- "Temperature Ratio Profiles at Various Dimensionless Times"

$\beta = 23.3$

$K = .0568$

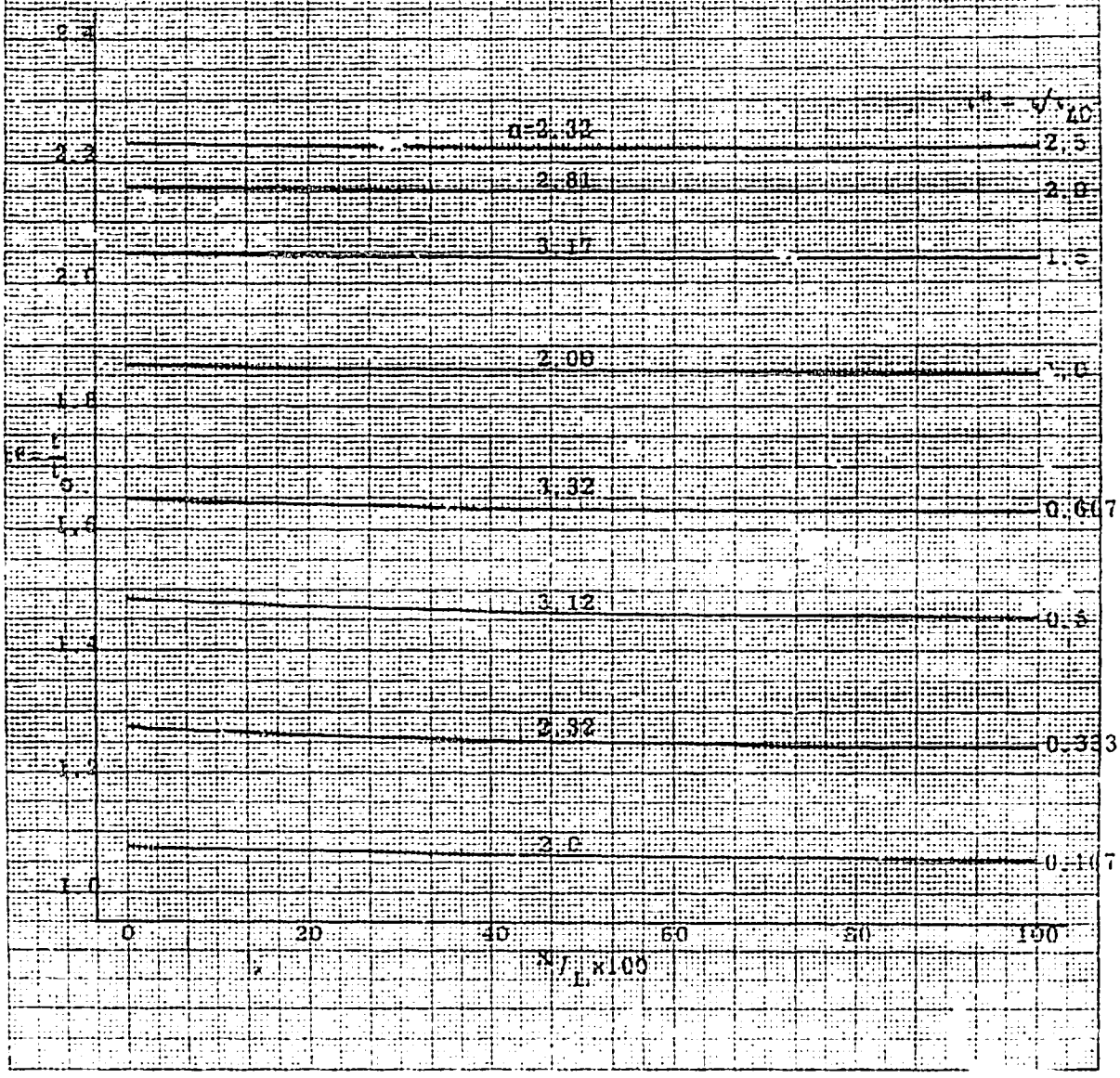

[redacted]

UNCLASSIFIED

[redacted]

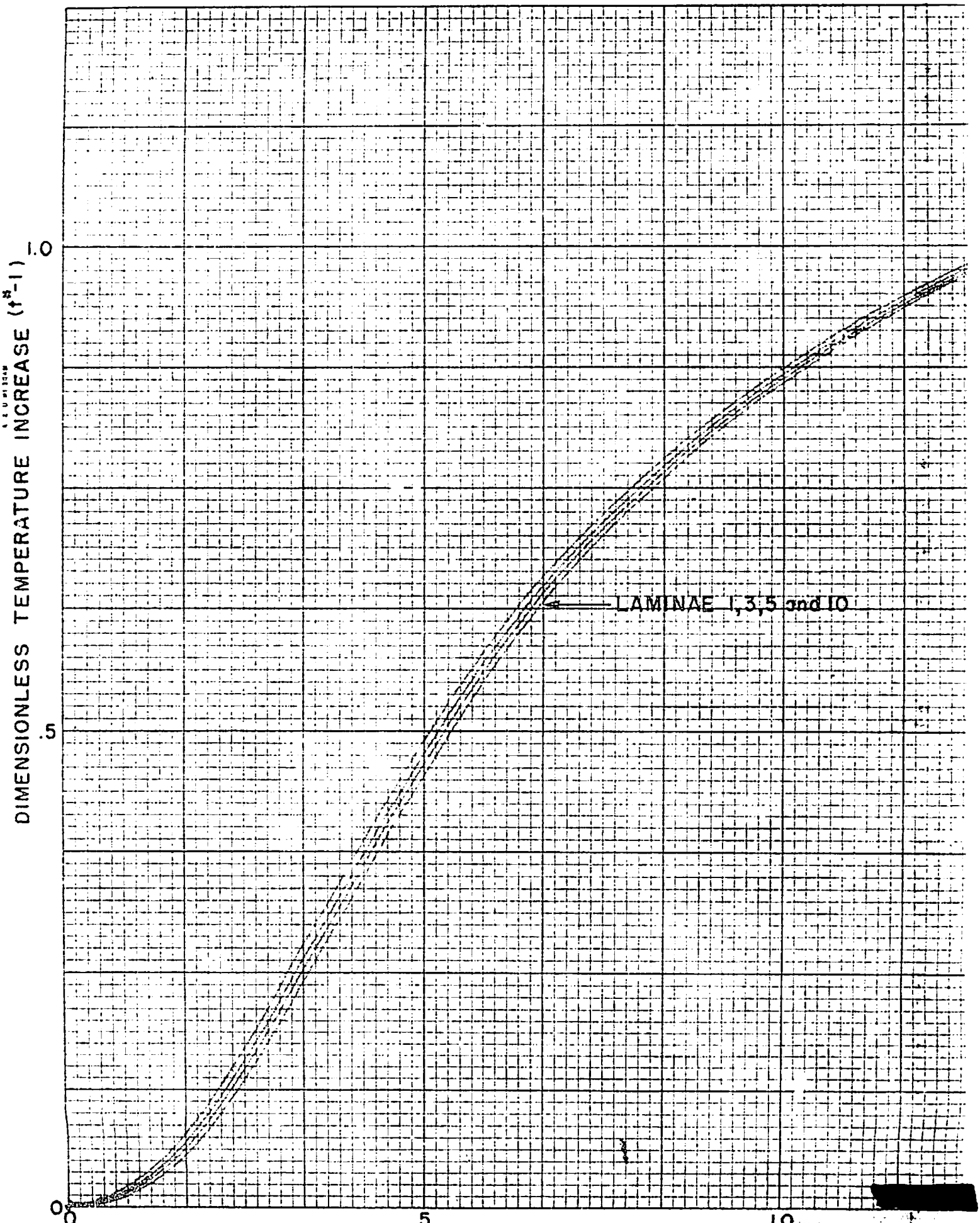

[redacted]

UNCLASSIFIED

$(t^* - 1)$ vs. τ^*

$\beta = 15.6$

$K = .0852$

FACTORS TO BE APPLIED TO THE $t^* - 1$ SCALE FOR APPLICATION OF THIS SOLUTION TO VARIOUS PROBLEMS FOR $\alpha Q = 91$ B/ft.^{2}

L	τ_{40}	FACTOR FOR $t^* - 1$ SCALE
.001	.0188	4.00
.002	.075	2.00
.003	.169	1.333
.004	.30	1.00
.007	.918	.571
.010	1.875	.40
.020	7.5	.20

[redacted]

[redacted]

Fig. 9a

Fig. 9a -- "Temperature Ratio Profiles at Various Dimensionless Times"

$\xi = 15.6$

$K = .0852$

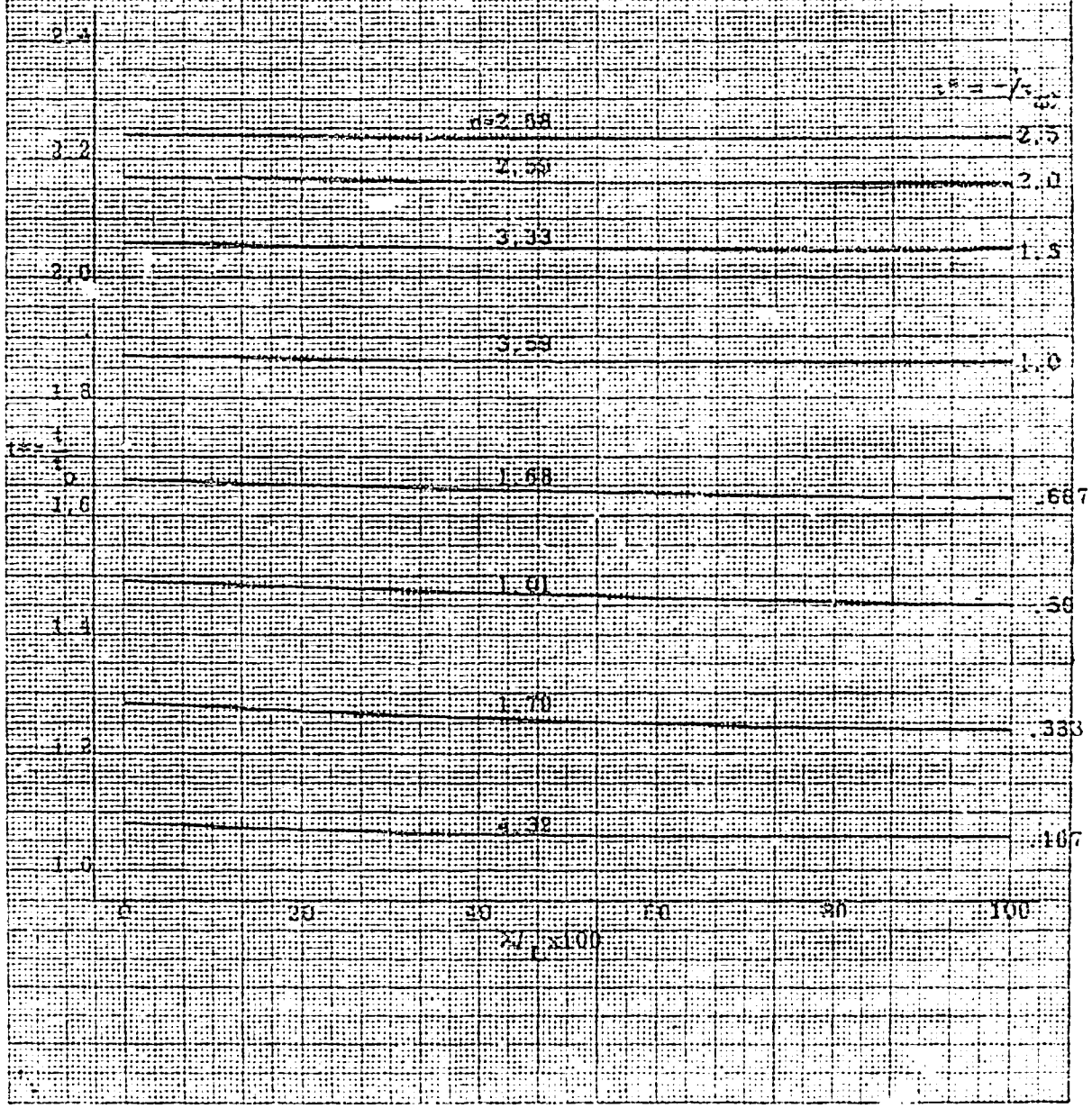

[redacted]

UNCLASSIFIED

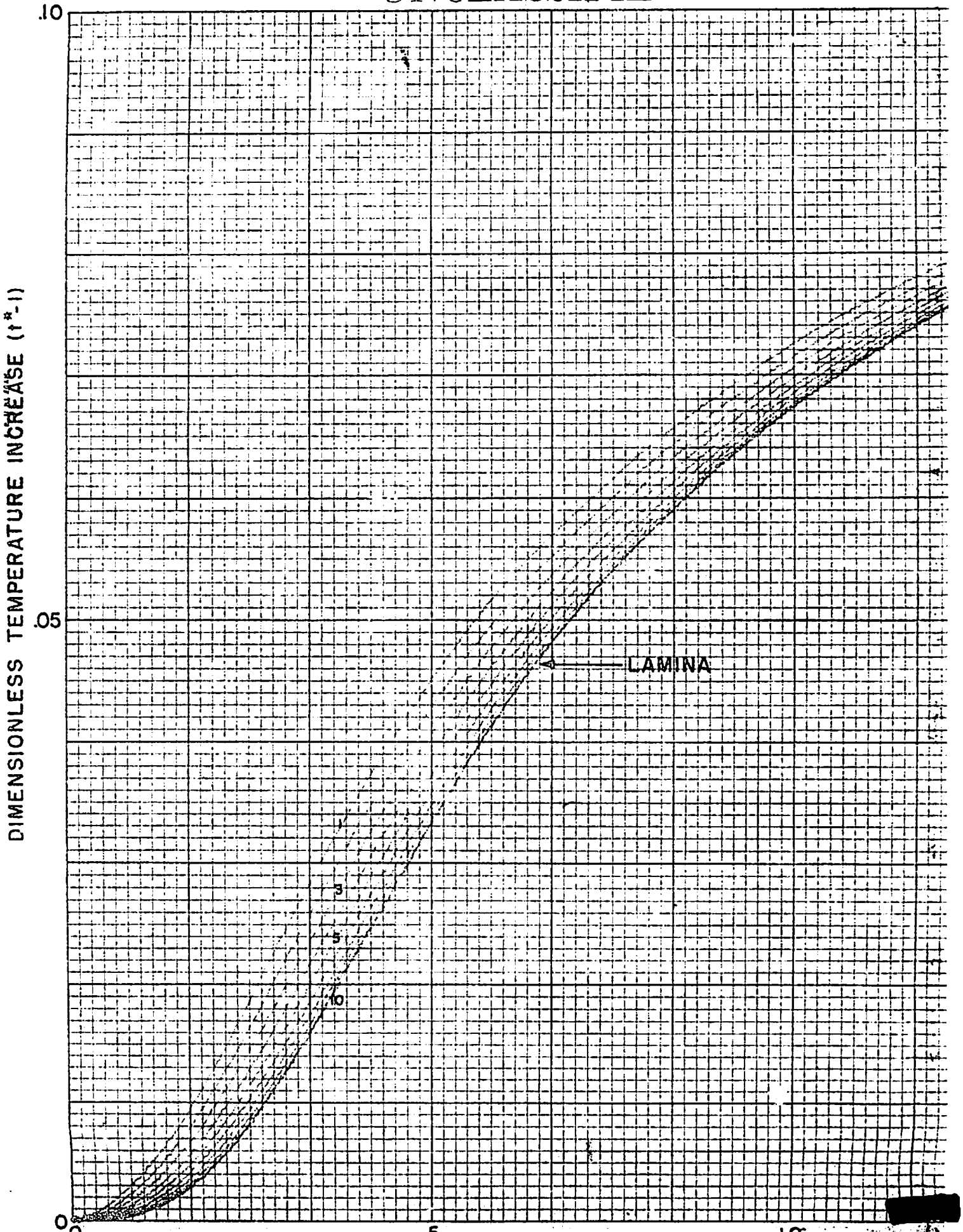

UNCLASSIFIED

Fig. 10

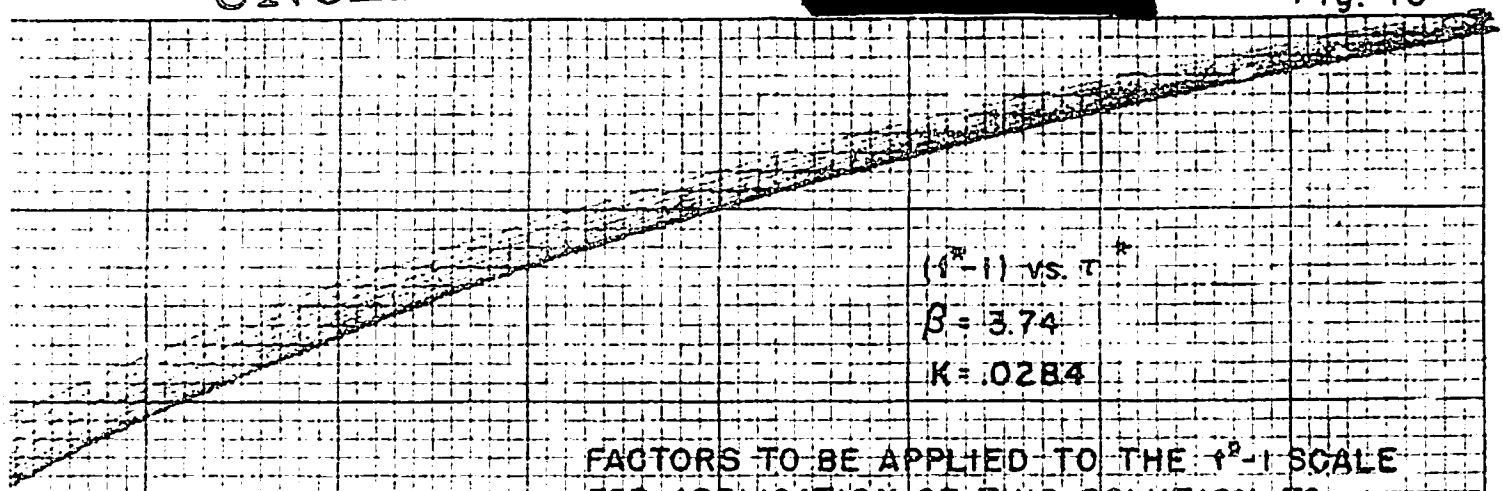

$(t^* - 1)$ vs. τ^*

$\beta = 3.74$

$K = .0284$

FACTORS TO BE APPLIED TO THE $t^* - 1$ SCALE FOR APPLICATION OF THIS SOLUTION TO VARIOUS PROBLEMS FOR $\alpha Q = 91$ B/ft.^{2}

L	τ_{40}	FACTOR FOR $t^* - 1$ SCALE
.001	.0045	50
.002	.018	25
.003	.0405	16.67
.004	.072	12.5
.007	.221	7.14
.010	.45	5.0
.020	1.80	2.5
.030	4.05	1.667

LESS TIME τ^* 1.5 2.0 2.5

UNCLASSIFIED

[redacted]

[redacted] Fig. 10a

Fig. 10a -- "Temperature Ratio Profiles at Various Dimensionless Times"

$\beta = 3.74$

$K = .0284$

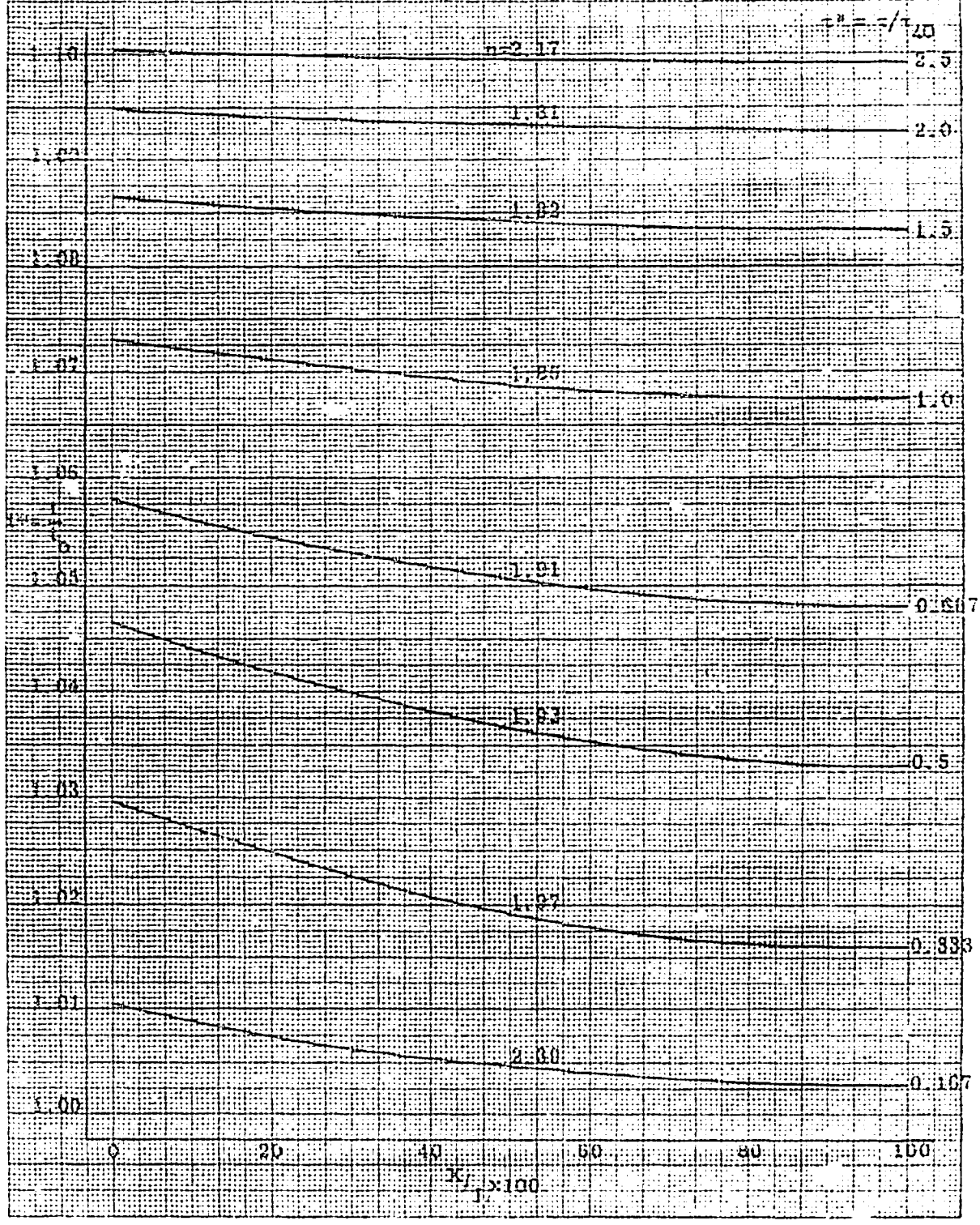

[redacted]

UNCLASSIFIED

UNCLASSIFIED

[redacted]

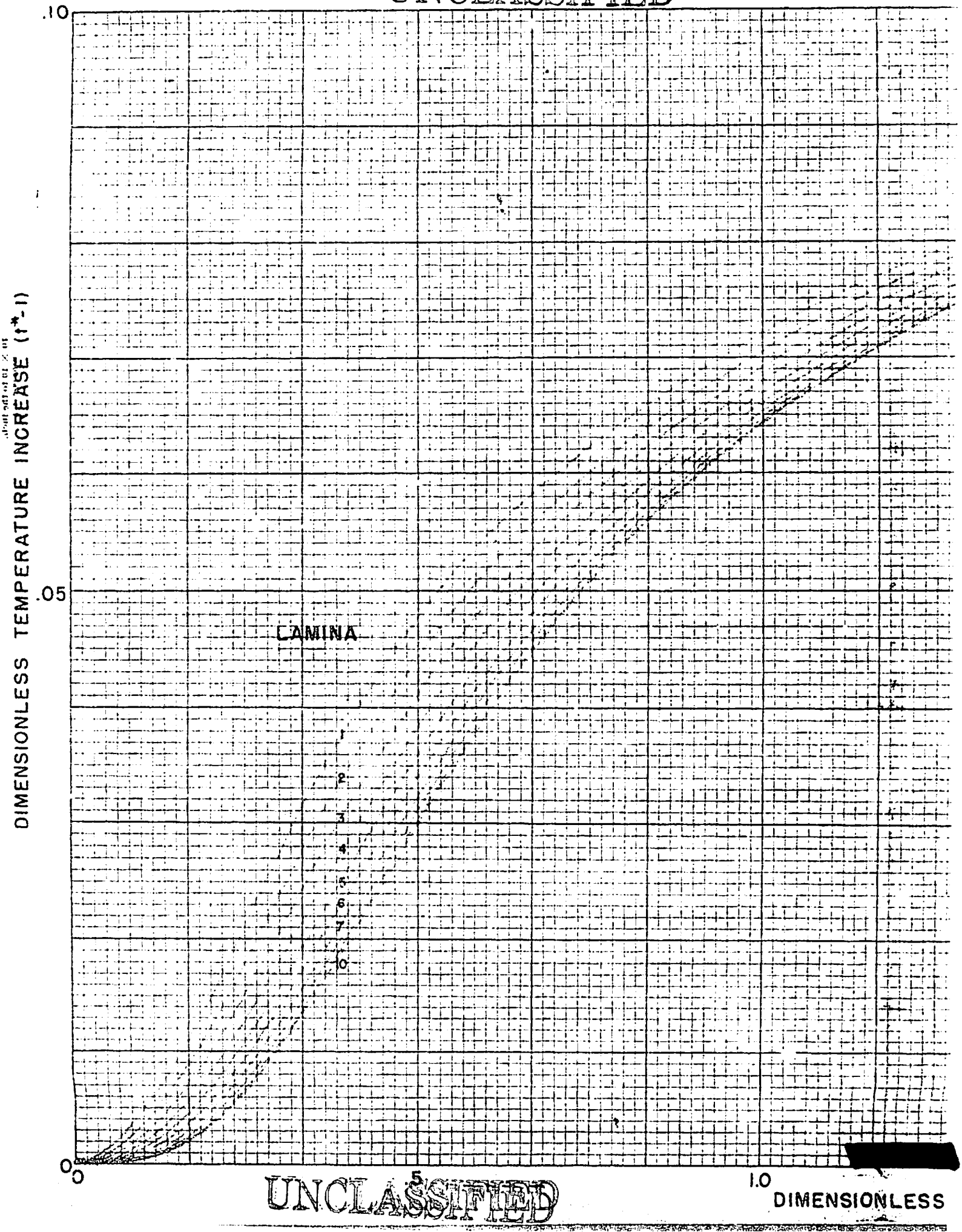

[redacted]

UNCLASSIFIED

$(\tau^* - 1)$ vs. τ^*

$\beta = 2.44$

$K = .0426$

FACTORS TO BE APPLIED TO THE $\tau^* - 1$ SCALE FOR APPLICATION OF THIS SOLUTION TO VARIOUS PROBLEMS FOR $\alpha\, Q = 91\ B/ft^2$

L	τ_{40}	FACTOR FOR $\tau^* - 1$ SCALE
.001	.003	51.1
.002	.0117	25.55
.003	.0262	17.05
.004	.047	12.8
.007	.1485	7.3
.010	.303	5.11
.020	1.175	2.56
.030	2.65	1.705
.040	4.80	1.278

[redacted]

[redacted] Fig. 11a

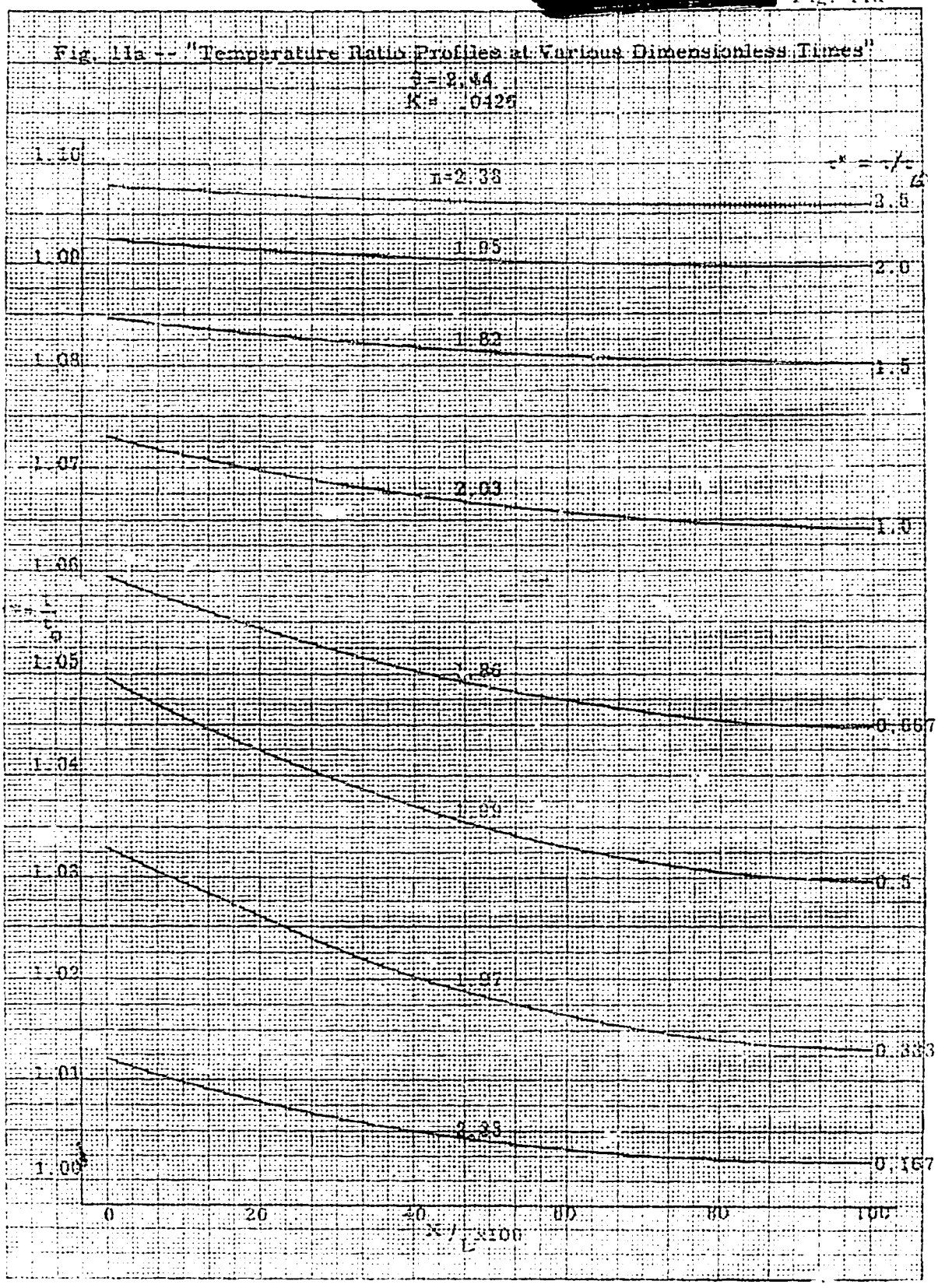

UNCLASSIFIED

[redacted]

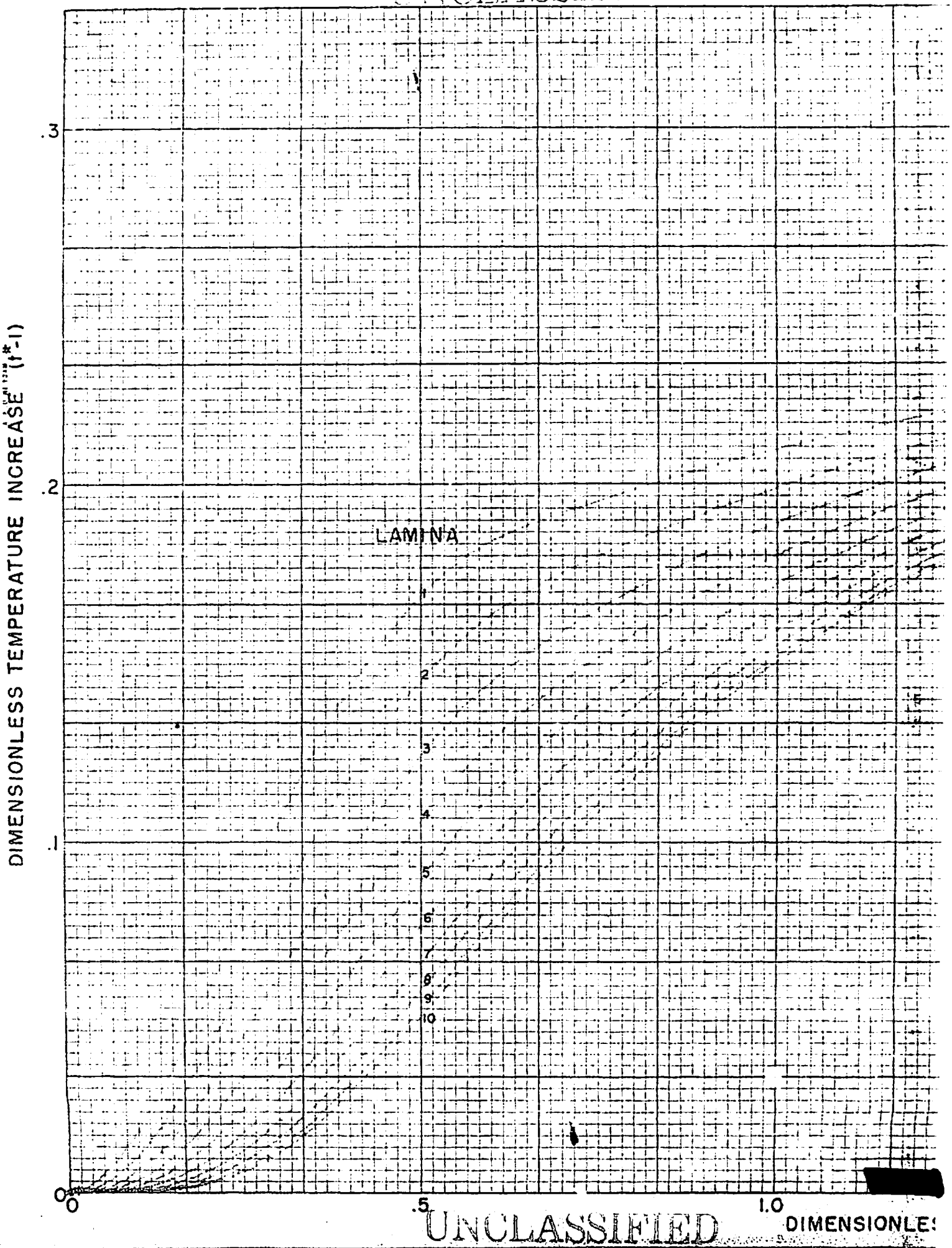

[redacted]

UNCLASSIFIED

$(1^* - 1)$ vs. τ^*

$\beta = .934$

$K = 2.84$

FACTORS TO BE APPLIED TO THE $\tau^* - 1$ SCALE FOR APPLICATION OF THIS SOLUTION TO VARIOUS PROBLEMS FOR $\alpha Q = 91 B/ft^2$

L	τ_{40}	FACTOR FOR $\tau^* - 1$ SCALE
.001	.00125	20.0
.002	.0045	10.0
.003	.0101	6.667
.004	.018	5.0
.007	.055	2.86
.010	.1125	2.0
.020	.45	1.0
.030	1.01	.667
.040	1.8	.500

[redacted]

[redacted] Fig. 12a

Fig. 12a -- "Temperature Ratio Profiles at Various Dimensionless Times"
B = .934
K = .284

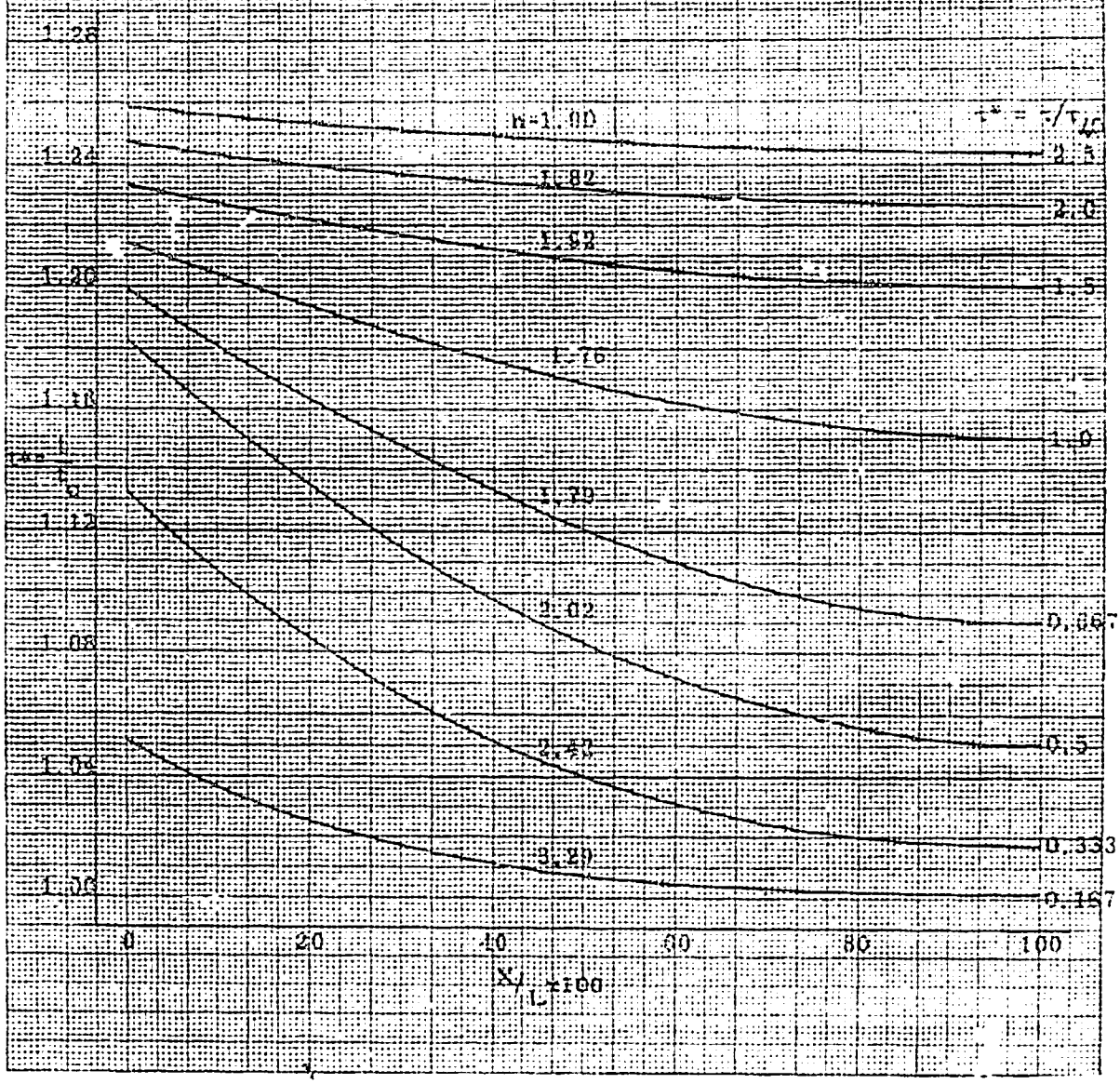

UNCLASSIFIED

[redacted]

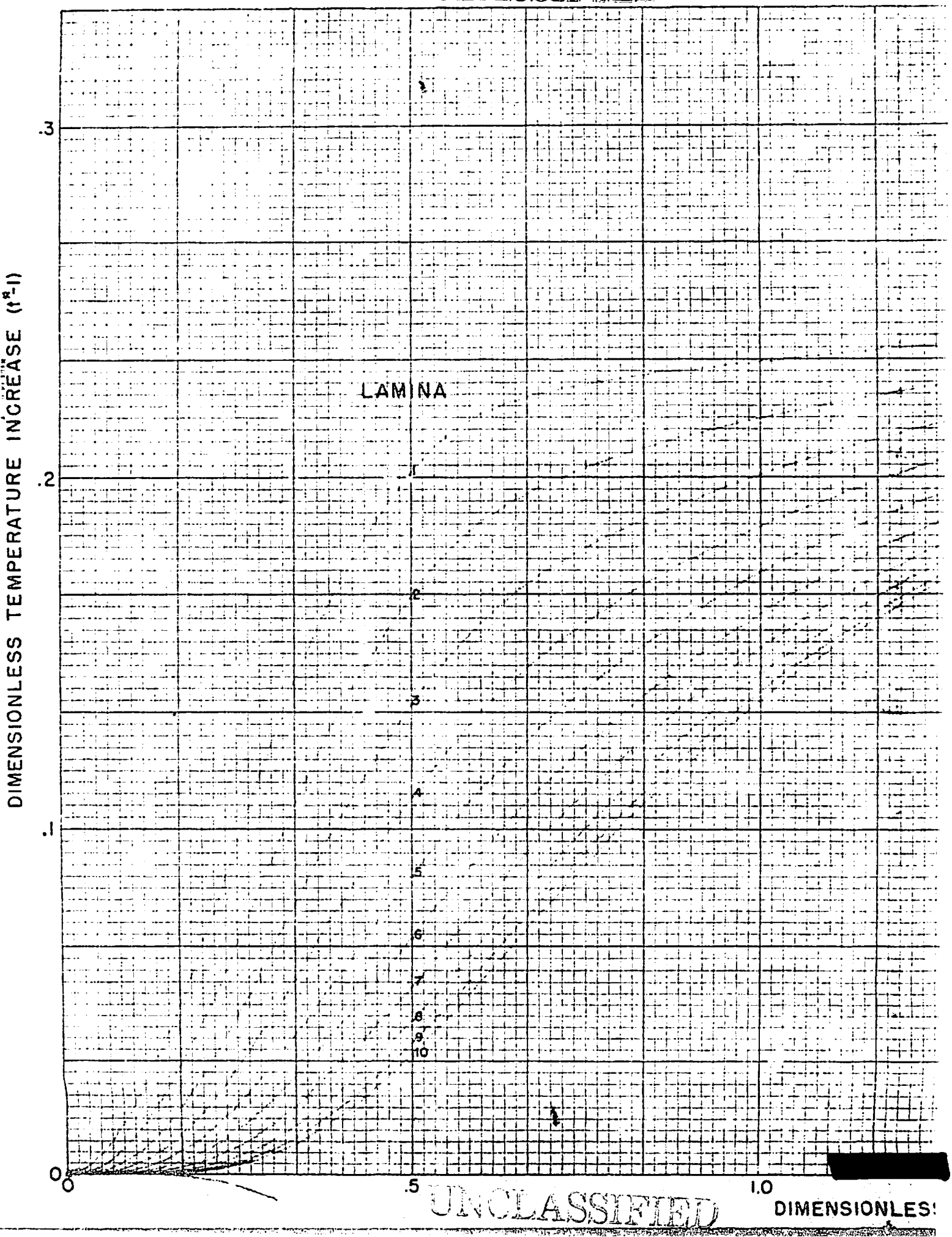

[redacted]

UNCLASSIFIED

$(r^{*}-1)$ vs. τ^{*}

$\beta = .622$

$K = .426$

FACTORS TO BE APPLIED TO THE $r^{*}-1$ SCALE FOR APPLICATION OF THIS SOLUTION TO VARIOUS PROBLEMS FOR $\alpha Q = 91$ B/ft.^{2}

L	τ_{40}	FACTOR FOR $r^{*}-1$ SCALE
.001	.00075	20.0
.002	.0030	10.0
.003	.00675	6.667
.004	.012	5.0
.007	.0367	2.86
.010	.075	2.0
.020	.30	1.0
.030	.675	.667
.040	1.20	.50

[redacted]

[redacted] Fig. 13a

Fig. 13a — "Temperature Ratio Profiles at Various Dimensionless Times"

$\rho_1 = .022$

$K = .425$

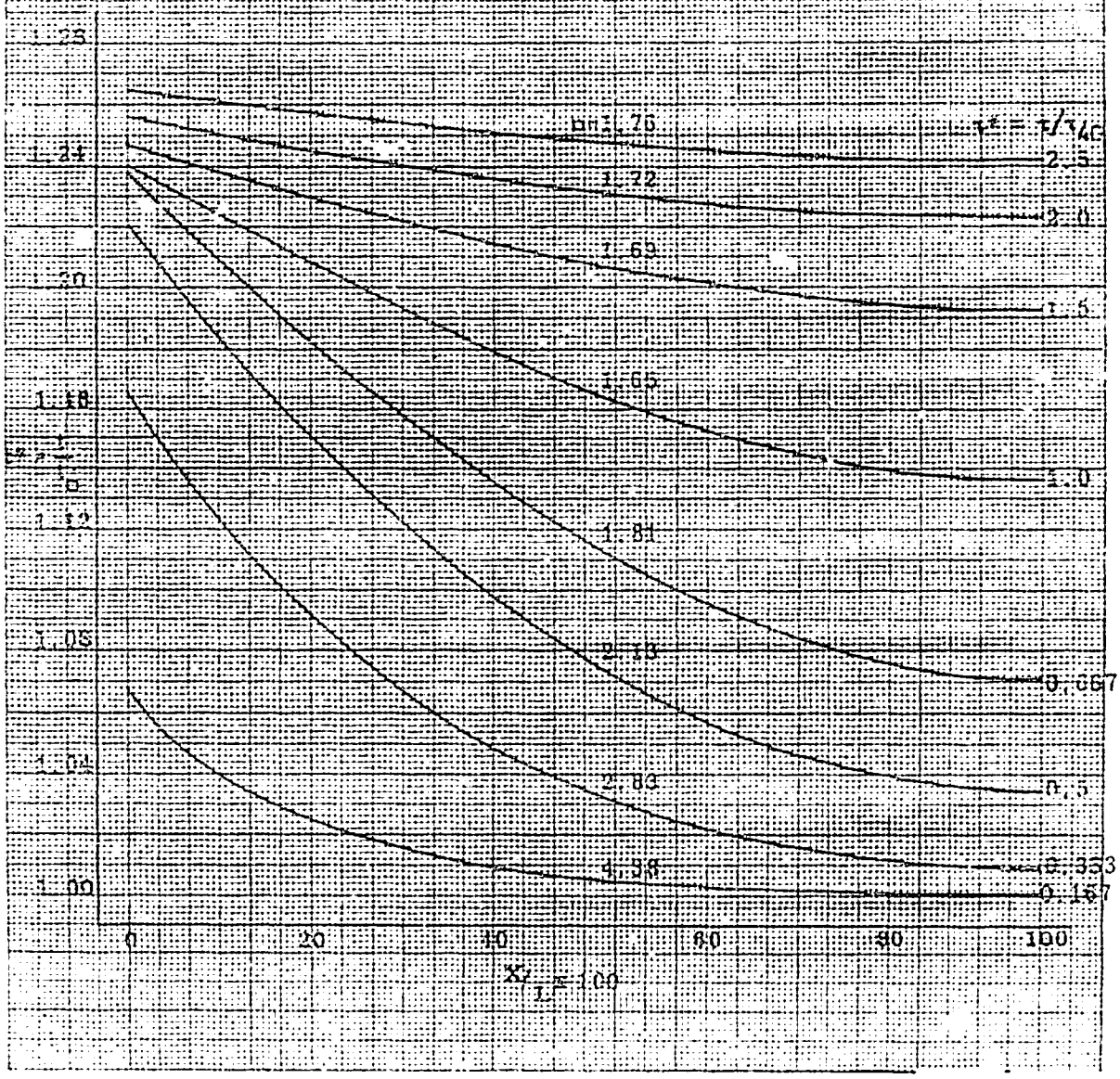

UNCLASSIFIED

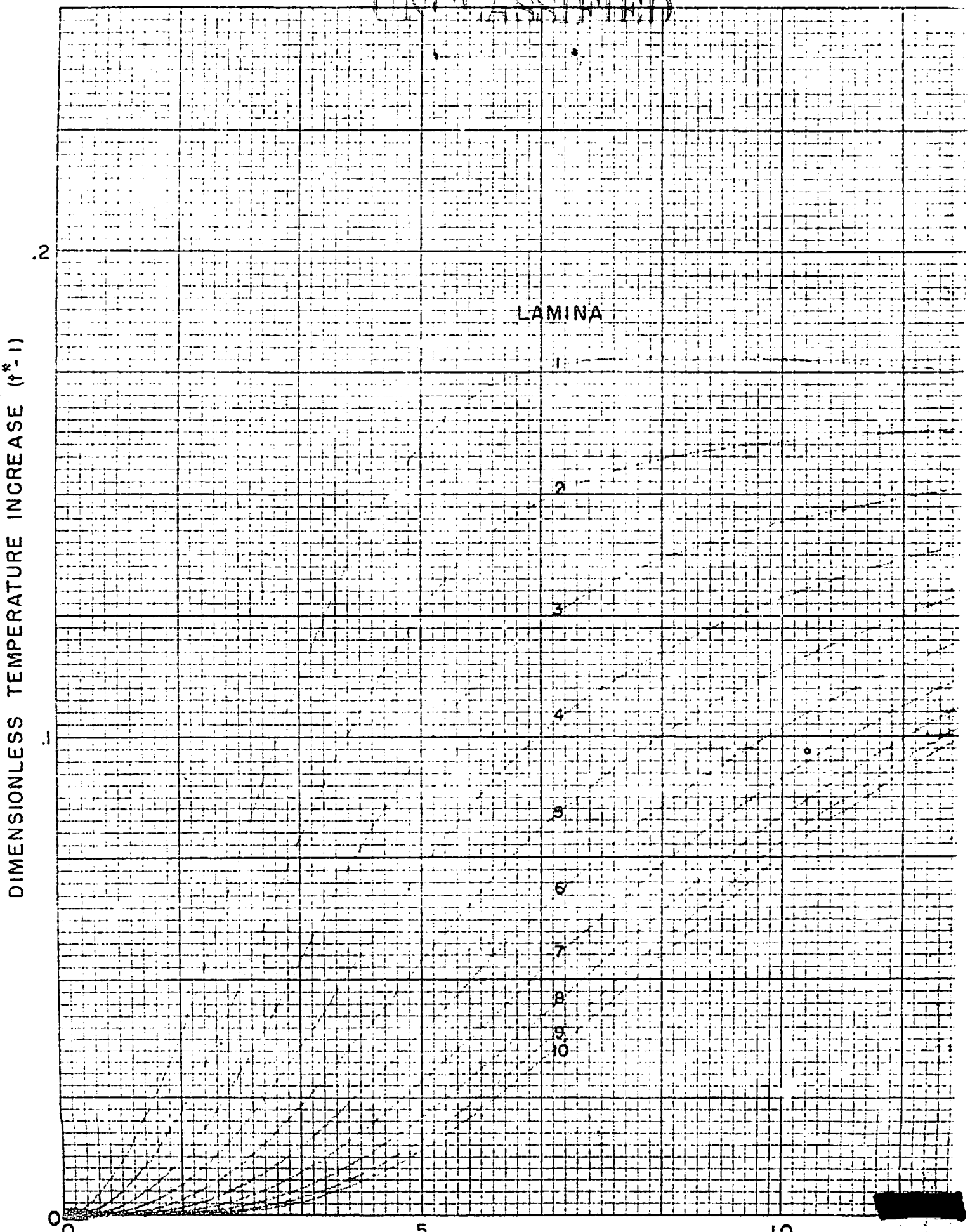

UNCLASSIFIED

$(t^* - 1)$ vs. τ^*

$\beta = .415$

$K = .426$

FACTORS TO BE APPLIED TO THE $t^* - 1$ SCALE FOR APPLICATION OF THIS SOLUTION TO VARIOUS PROBLEMS FOR $\alpha Q = 91$ BZ/ft^2

L	τ_{40}	FACTOR FOR $t^* - 1$ SCALE
.001	.0005	30.0
.002	.0020	15.0
.003	.0045	10.0
.004	.008	7.5
.007	.0245	4.29
.010	.05	3.0
.020	.20	1.5
.030	.45	1.0
.040	.80	.75

[redacted]

LESS TIME τ^* 1.5 2.0 2.5

UNCLASSIFIED

[redacted]

[redacted] 14a

Fig. 14a -- "Temperature Ratio Profiles at Various Dimensionless Times"
B = .410
K = .426

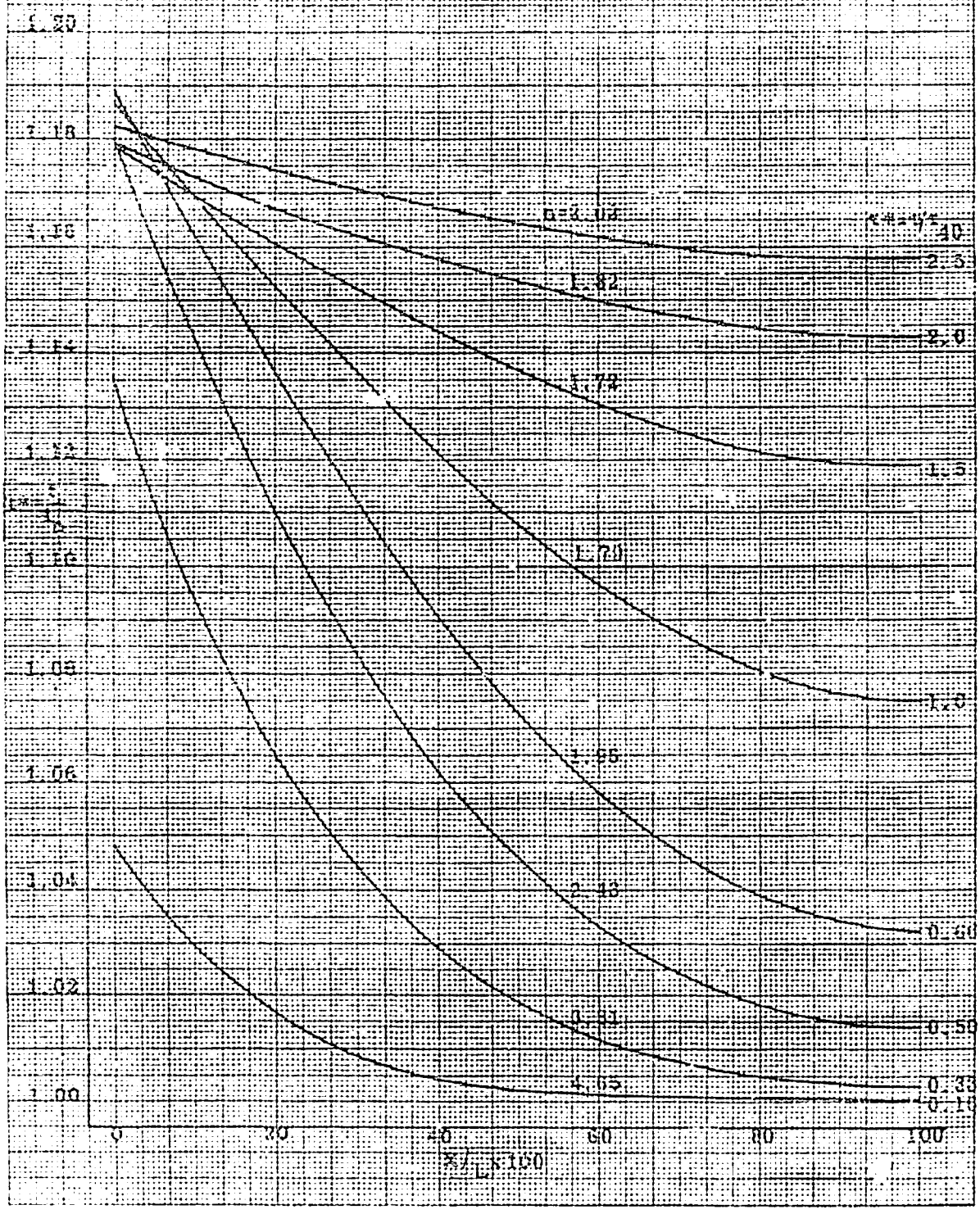

[redacted]

UNCLASSIFIED

UNCLASSIFIED

[redacted]

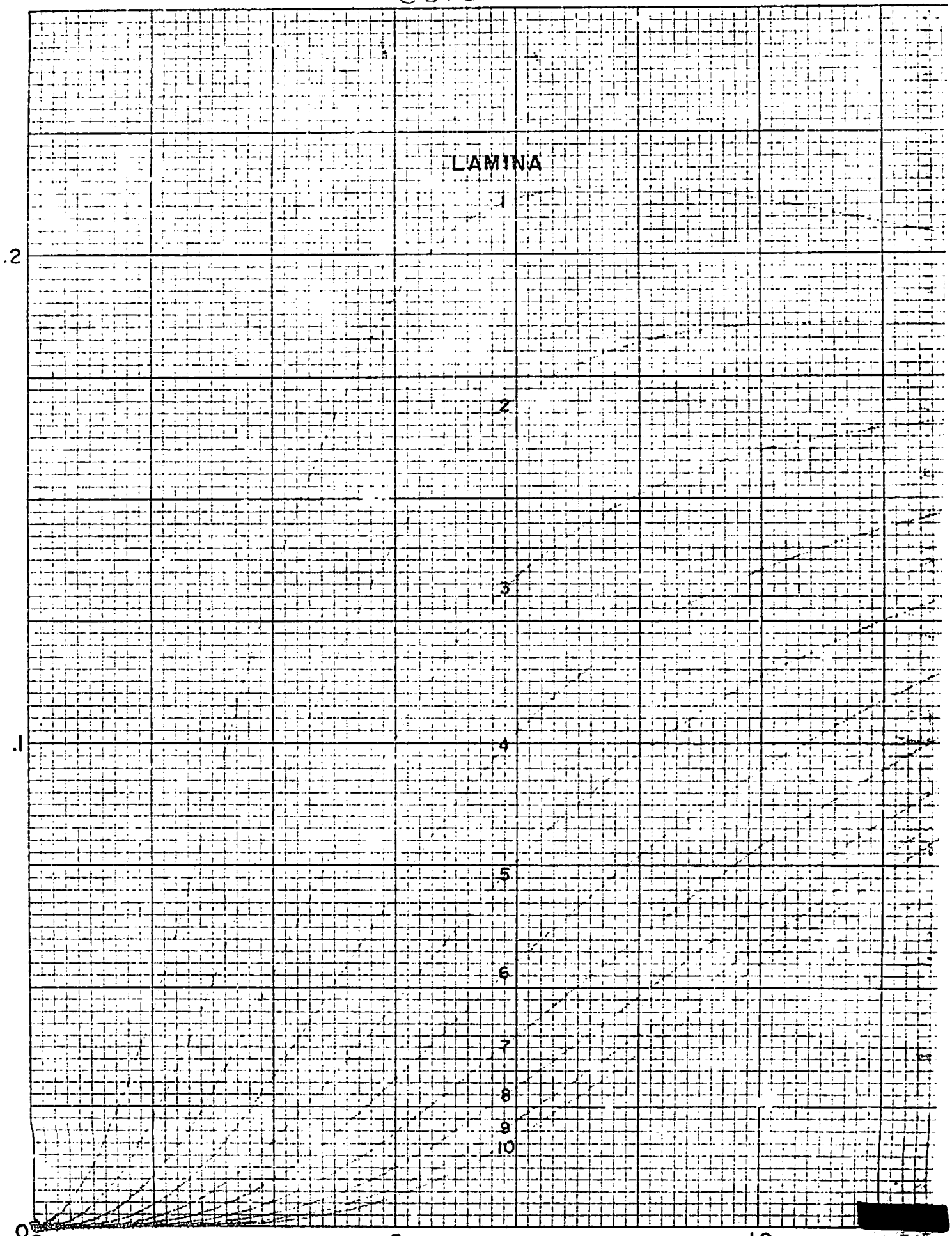

[redacted]

UNCLASSIFIED

$(t^* - 1)$ vs. τ^*

$\beta = .277$

$K = .64$

FACTORS TO BE APPLIED TO THE $t^* - 1$ SCALE FOR APPLICATION OF THIS SOLUTION TO VARIOUS PROBLEMS FOR $\alpha Q = 91$ B/ft^2

L	τ_{40}	FACTOR FOR $t^* - 1$ SCALE
.001	.000333	30.0
.002	.00133	15.0
.003	.003	10.0
.004	.00534	7.5
.007	.0163	4.29
.010	.0333	3.0
.020	.133	1.5
.030	.30	1.0
.040	.533	.75

[redacted]

[redacted] Fig. 15a

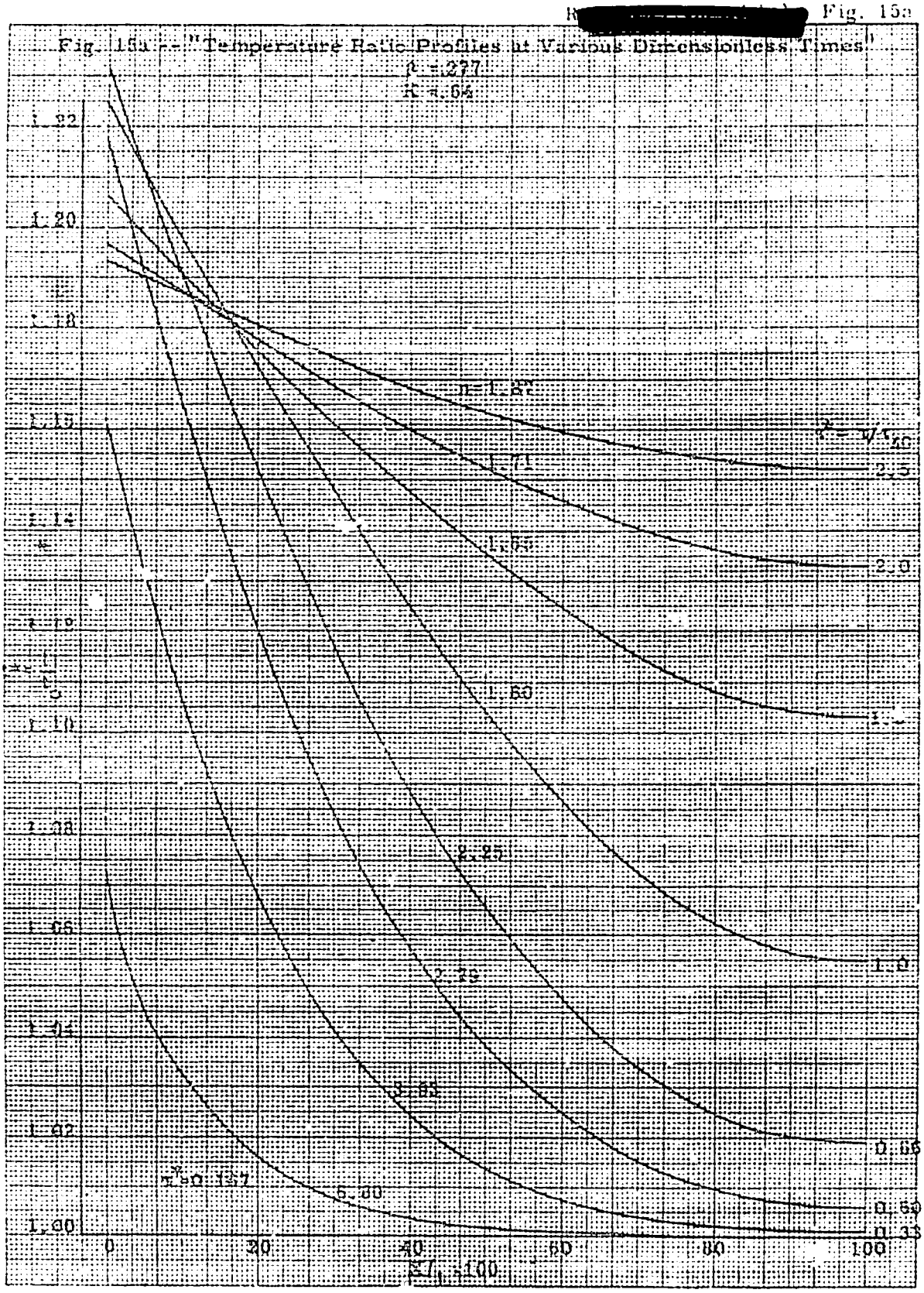

[redacted]

UNCLASSIFIED

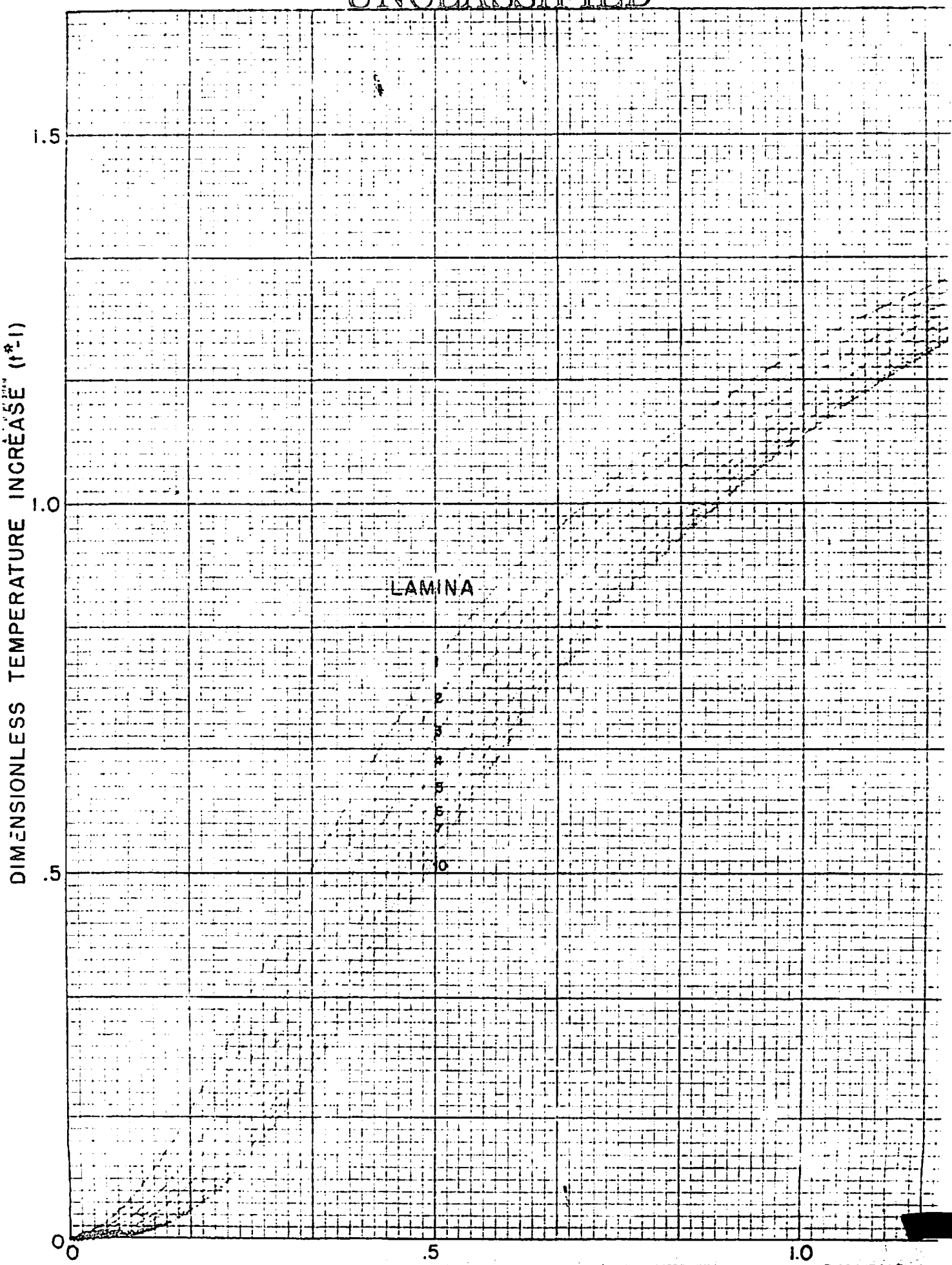

UNCLASSIFIED

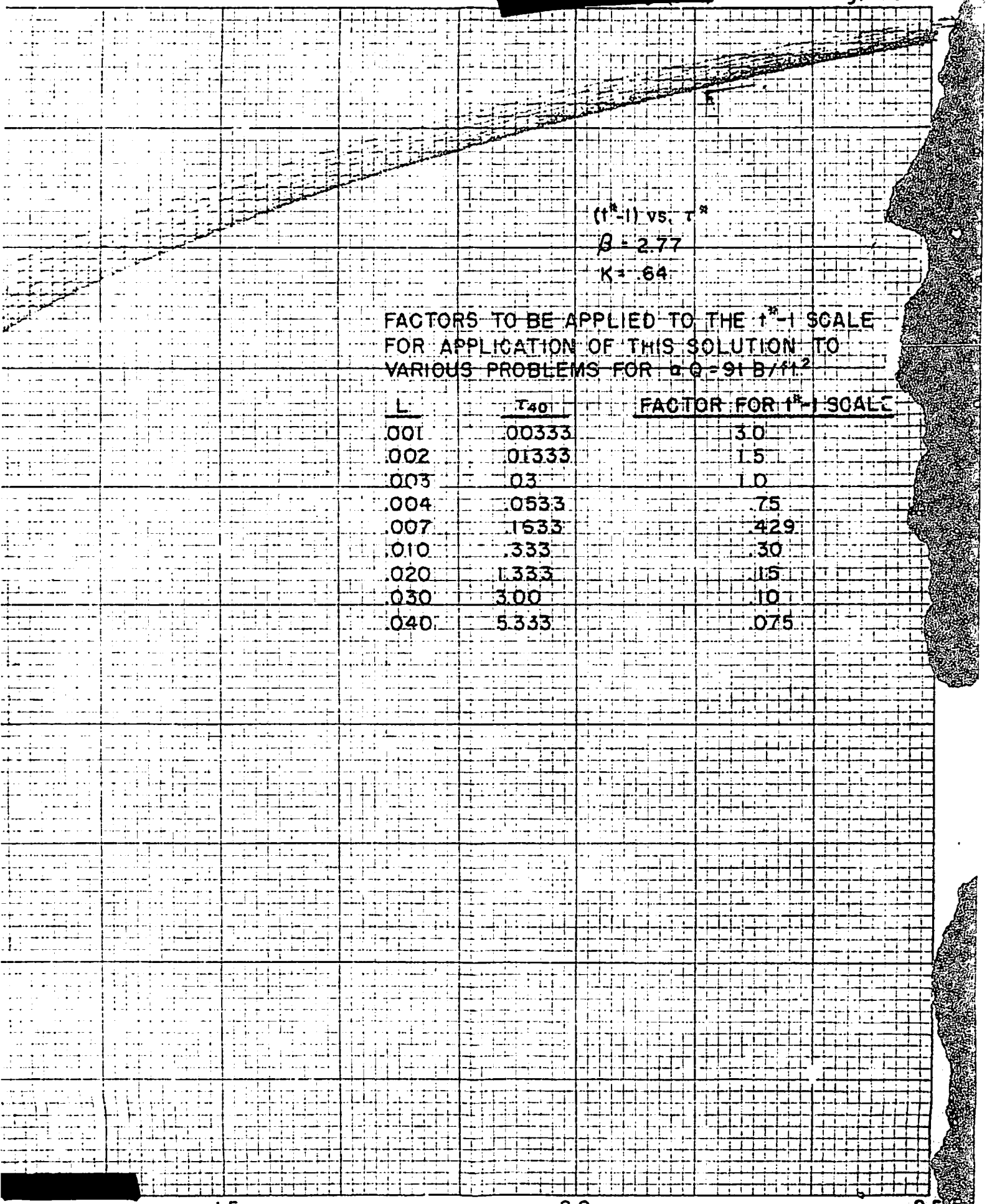

FACTORS TO BE APPLIED TO THE t^*-1 SCALE FOR APPLICATION OF THIS SOLUTION TO VARIOUS PROBLEMS FOR $aQ = 91$ B/ft.^{2}

L	τ_{40}	FACTOR FOR t^*-1 SCALE
.001	.00333	3.0
.002	.01333	1.5
.003	.03	1.0
.004	.0533	.75
.007	.1633	.429
.010	.333	.30
.020	1.333	.15
.030	3.00	.10
.040	5.333	.075

UNCLASSIFIED

[redacted]

[redacted] Fig. 16a

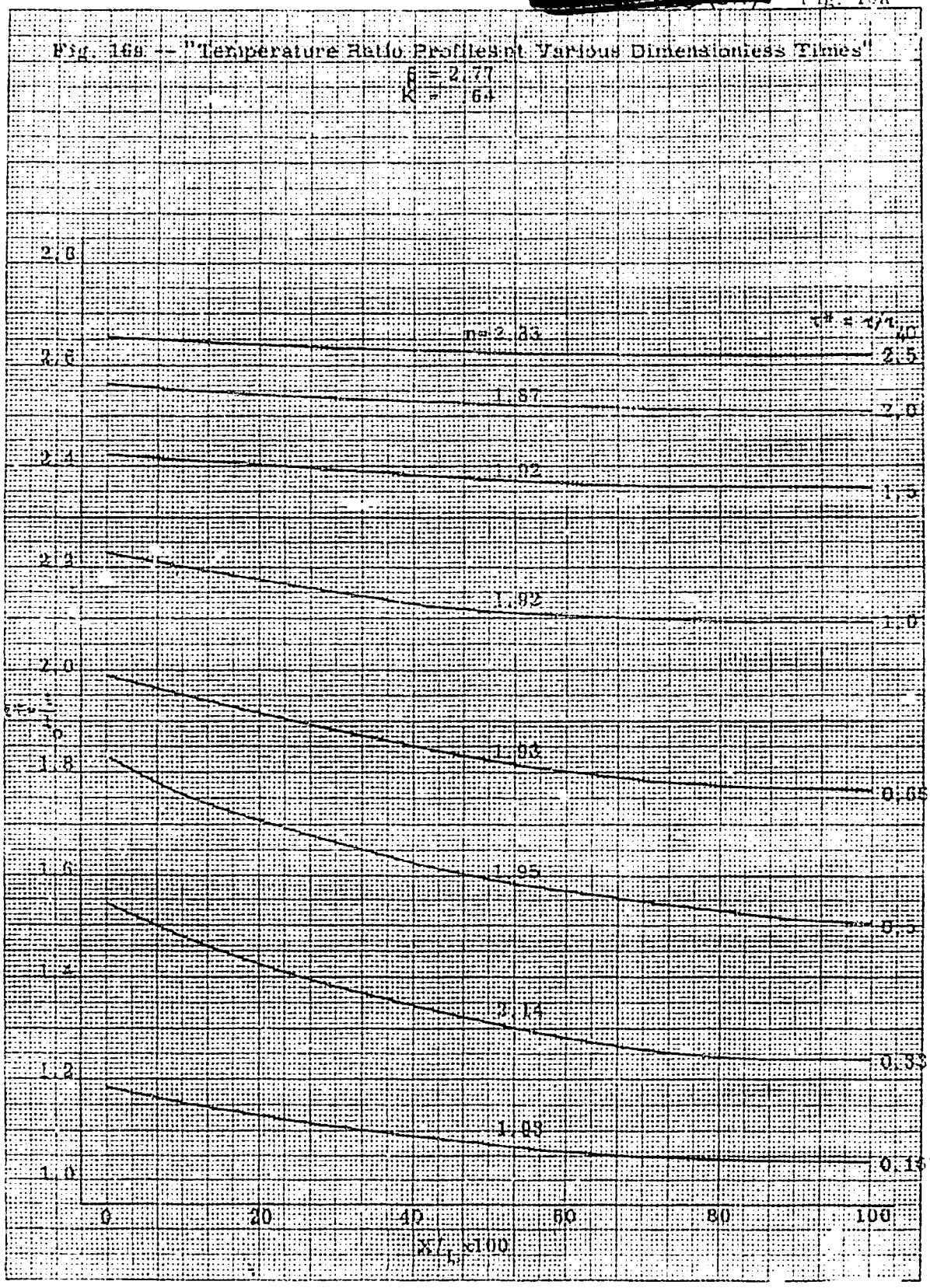

[redacted]

UNCLASSIFIED

UNCLASSIFIED

[redacted]

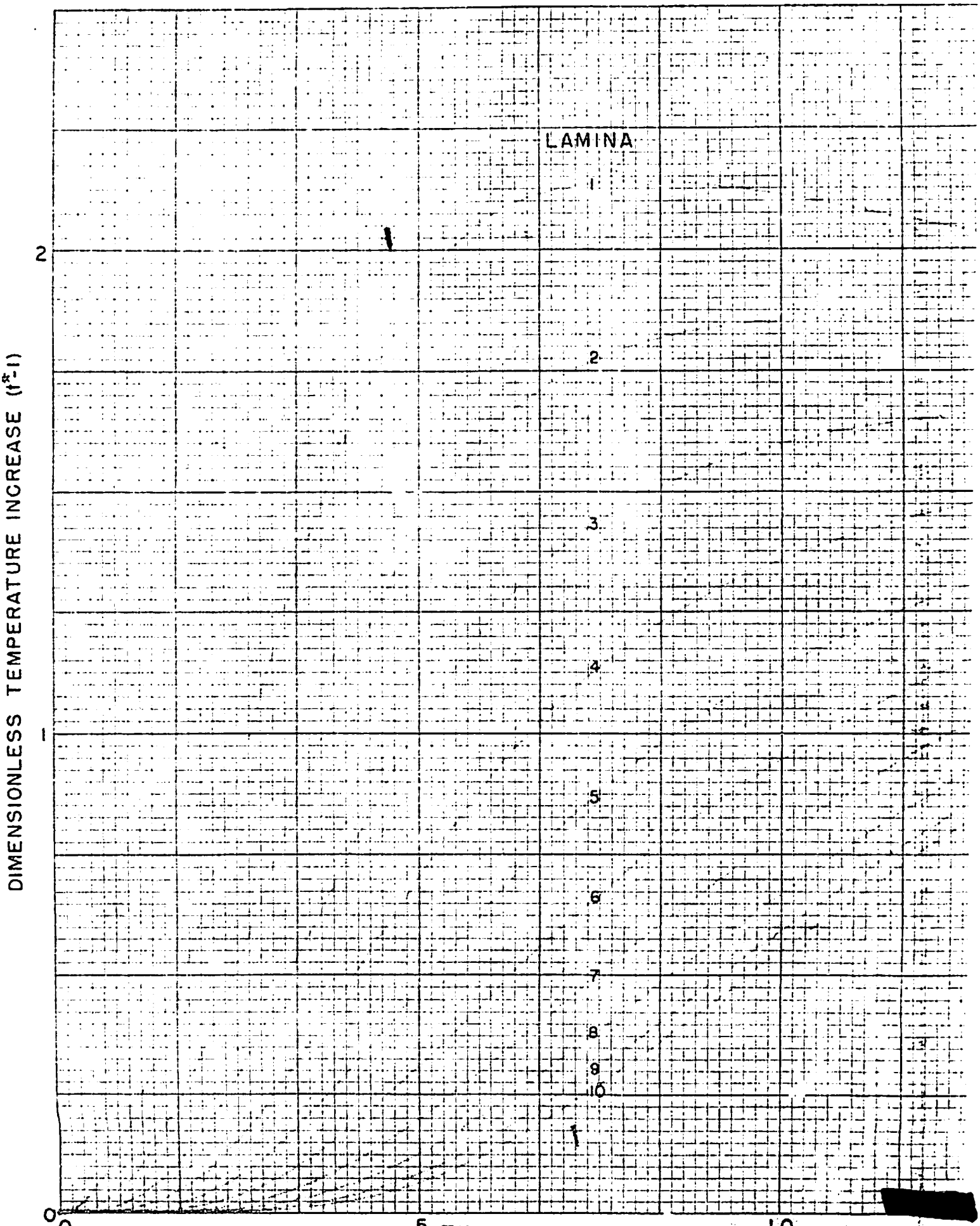

[redacted]

UNCLASSIFIED

$(t^* - 1)$ vs τ^*

$\beta = .277$

$K = 6.4$

FACTORS TO BE APPLIED TO THE t^*-1 SCALE FOR APPLICATION OF THIS SOLUTION TO VARIOUS PROBLEMS FOR $\alpha Q = 91$ B/ft^2

L	τ_{40}	FACTOR FOR t^*-1 SCALE
.001	.000333	3.0
.002	.00133	1.5
.003	.0030	1.0
.004	.00533	.75
.007	.01633	.429
.010	.0333	.30
.020	.1333	.15
.030	.300	.10
.040	.533	.075

1.5 2.0 2.5

ONLESS TIME τ^*

[redacted] [redacted]

Fig. 17a

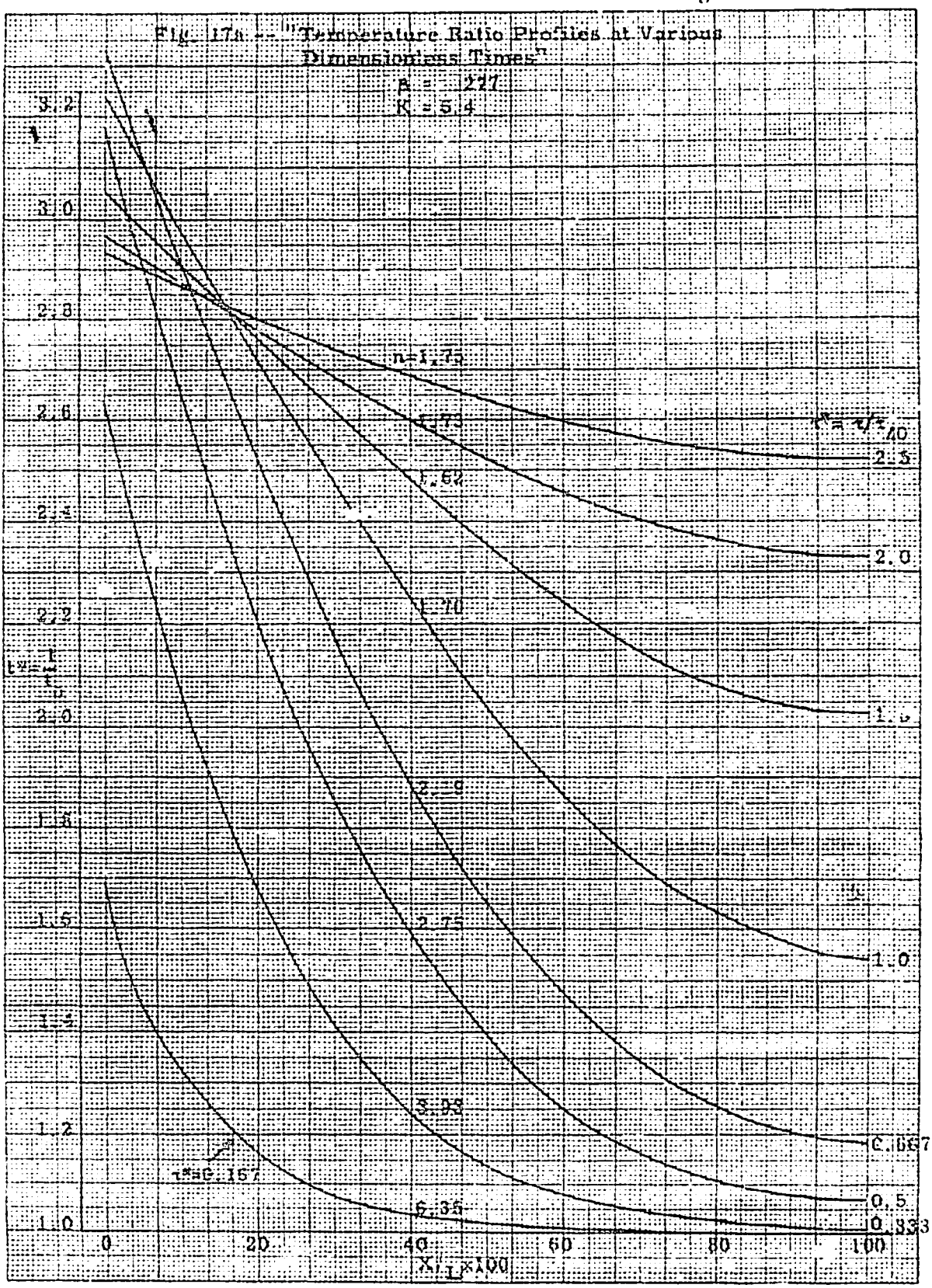

[redacted]

UNCLASSIFIED

[redacted]

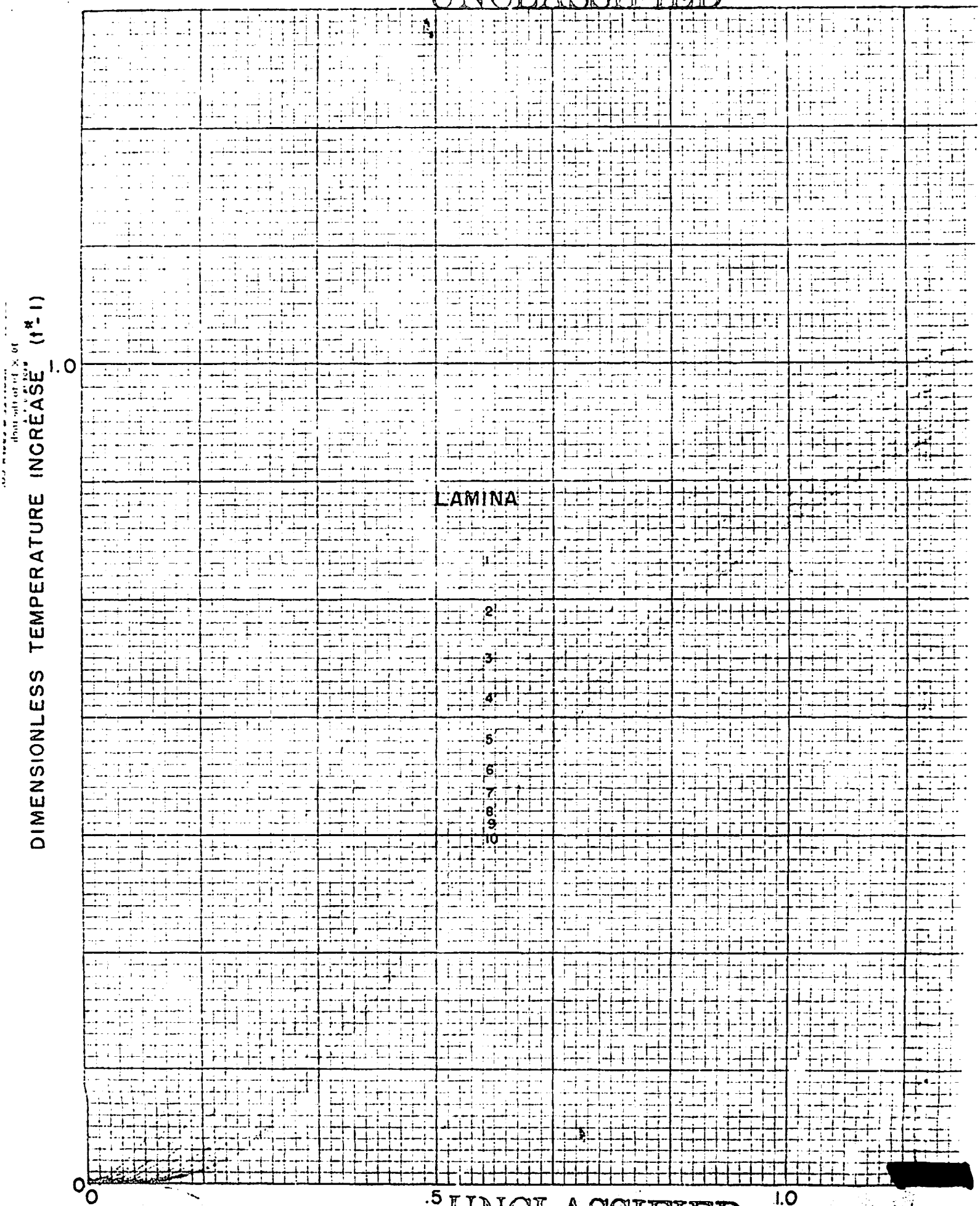

[redacted]

UNCLASSIFIED

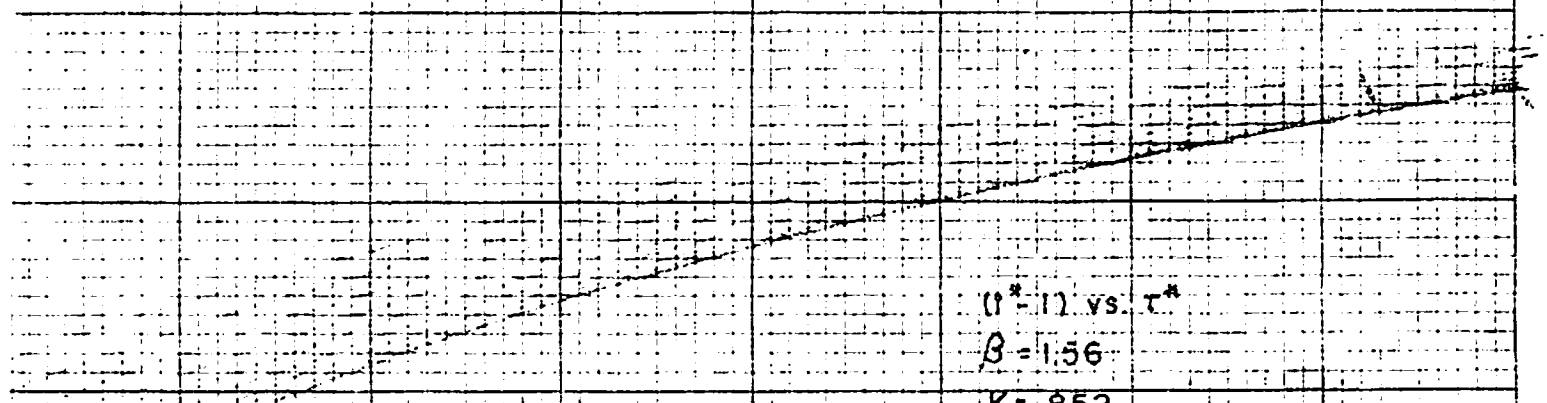

$(t^* - 1)$ vs. τ^*

$\beta = 1.56$

$K = .852$

FACTORS TO BE APPLIED TO THE t^*-1 SCALE FOR APPLICATION OF THIS SOLUTION TO VARIOUS PROBLEMS FOR $\alpha Q = 91$ B/ft.^{2}

L	τ_{40}	FACTOR FOR t^*-1 SCALE
.001	.001875	4.00
.002	.0075	2.00
.003	.01688	1.333
.004	.030	1.00
.007	.0918	.571
.010	.1875	.40
.020	.750	.20
.030	1.688	.133
.040	3.00	.100

[redacted]

1.5 2.0 2.5

ONLESS TIME τ^*

UNCLASSIFIED

[redacted]

[redacted] Fig. 18a

Fig. 18a -- "Temperature Ratio Profiles at Various Dimensionless Times"

$\beta = 1.56$

$K = .652$

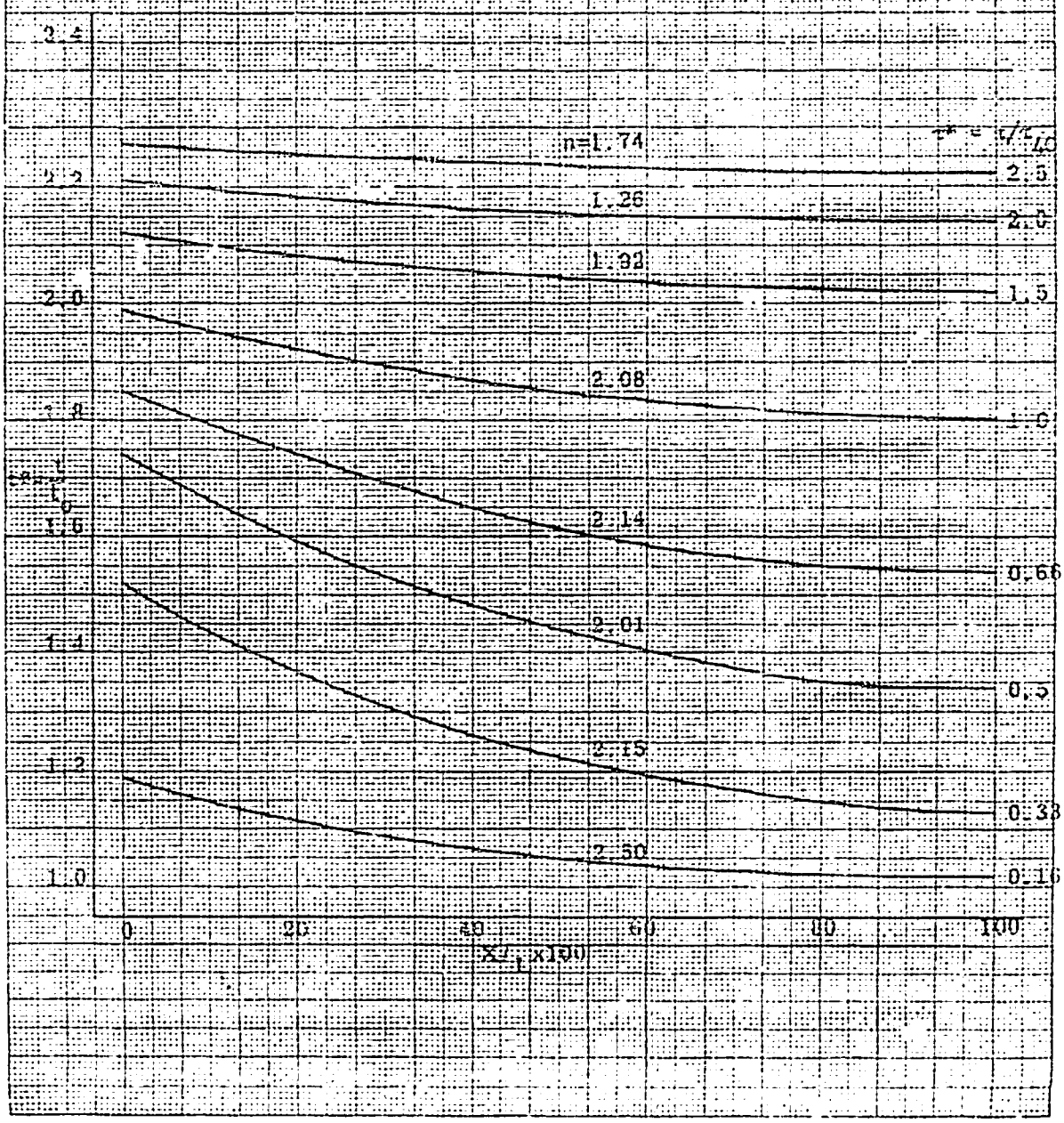

[redacted]

UNCLASSIFIED

UNCLASSIFIED

[redacted]

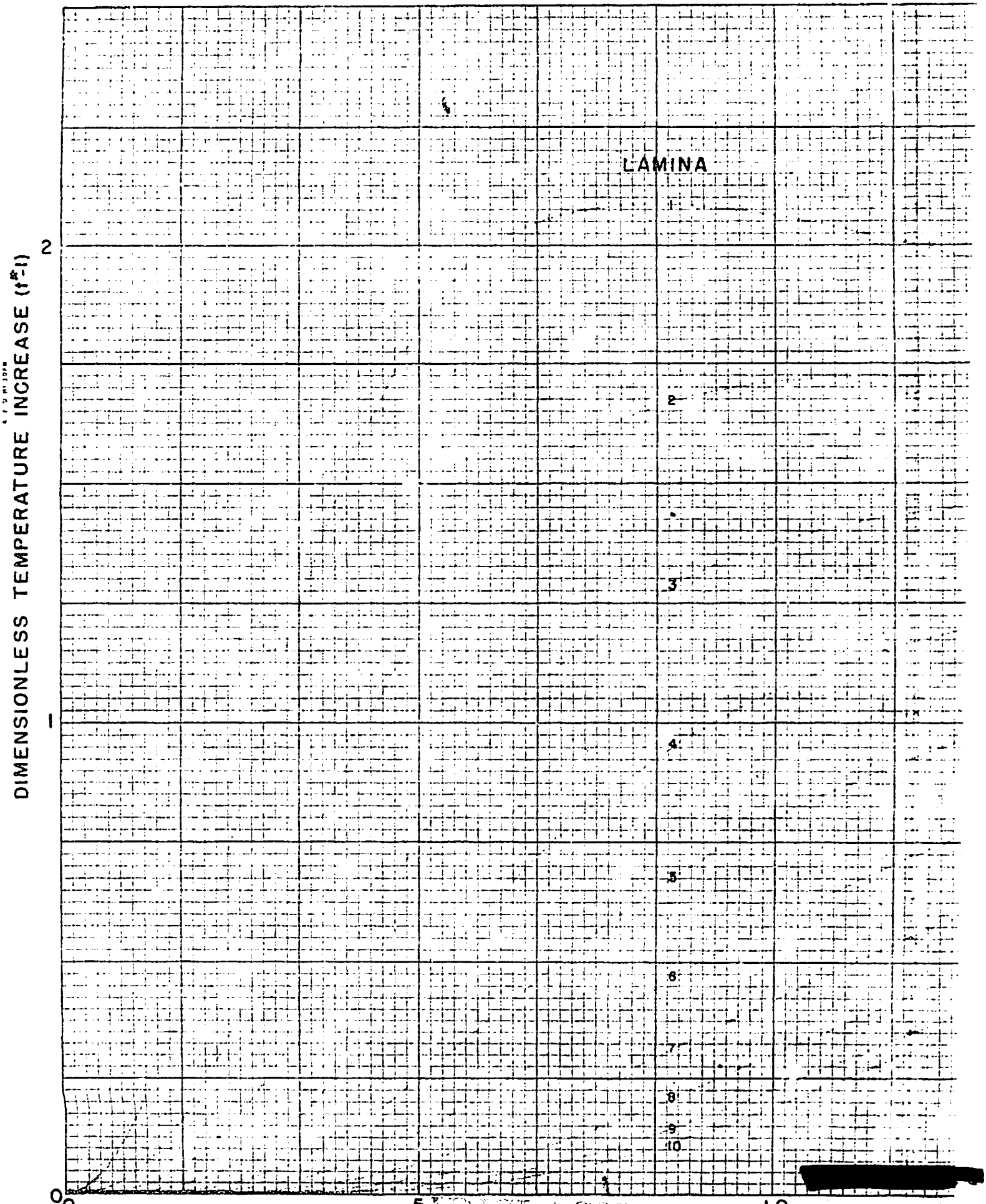

[redacted]

UNCLASSIFIED

$(t^* - 1)$ vs. τ^*

$\beta = .156$

$K = 0.52$

FACTORS TO BE APPLIED TO THE $t^* = 1$ SCALE FOR APPLICATION OF THIS SOLUTION TO VARIOUS PROBLEMS FOR $\alpha Q = 91$ B/ft^2

L	τ_{40}	FACTOR FOR $t^* = 1$ SCALE
.001	.0001875	4.00
.002	.00075	2.00
.003	.001688	1.333
.004	.003	1.00
.007	.00918	.571
.010	.01875	.40
.020	.075	.20
.030	.1688	.133
.040	.300	.100

UNCLASSIFIED

[redacted]

[redacted]

Fig. 19a

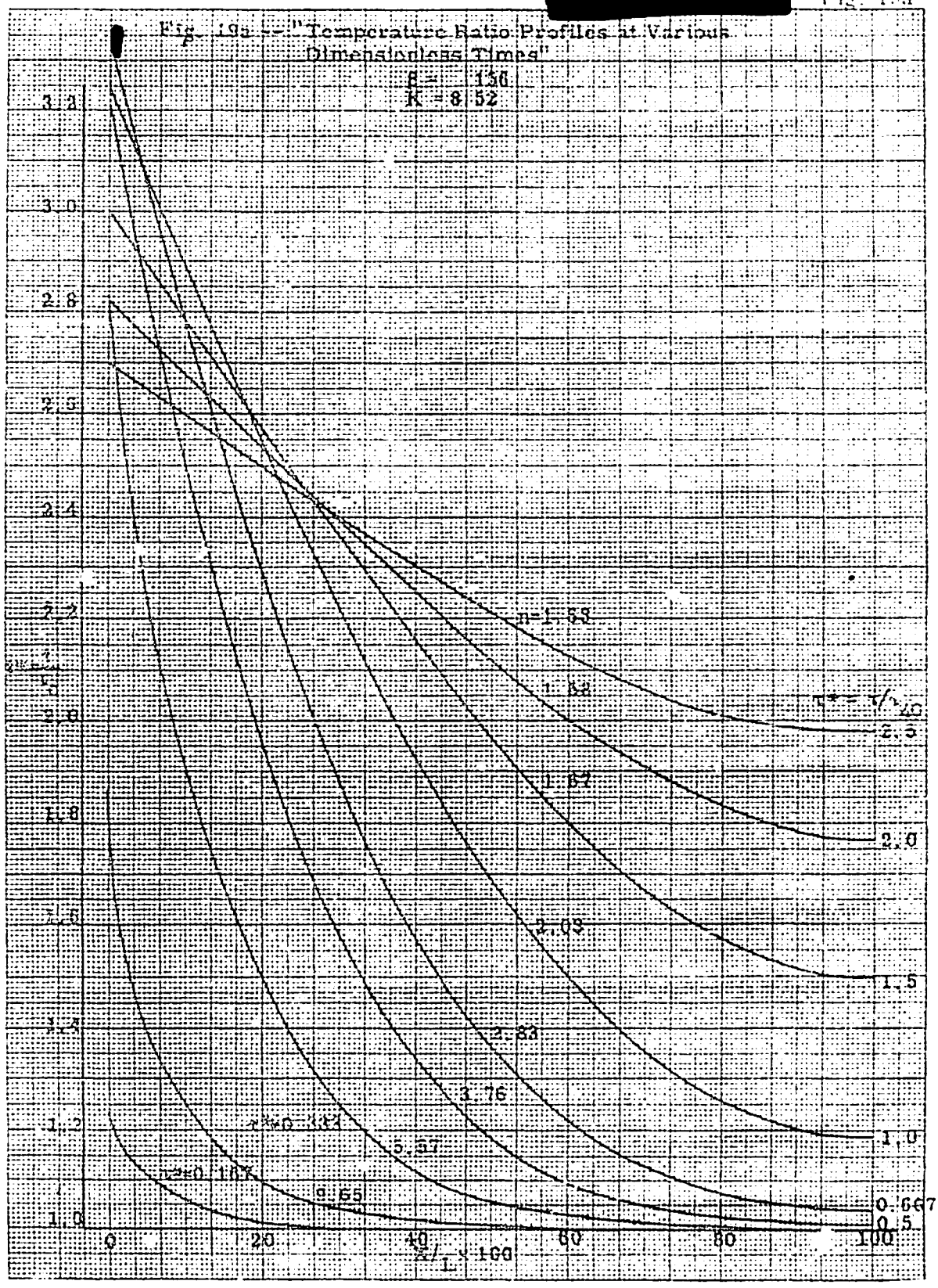

[redacted]

UNCLASSIFIED

K•E LOGARITHMIC 359-111
KEUFFEL & ESSER CO. MADE IN U.S.A.
2 X 2.7 CYCLES

Fig. 20

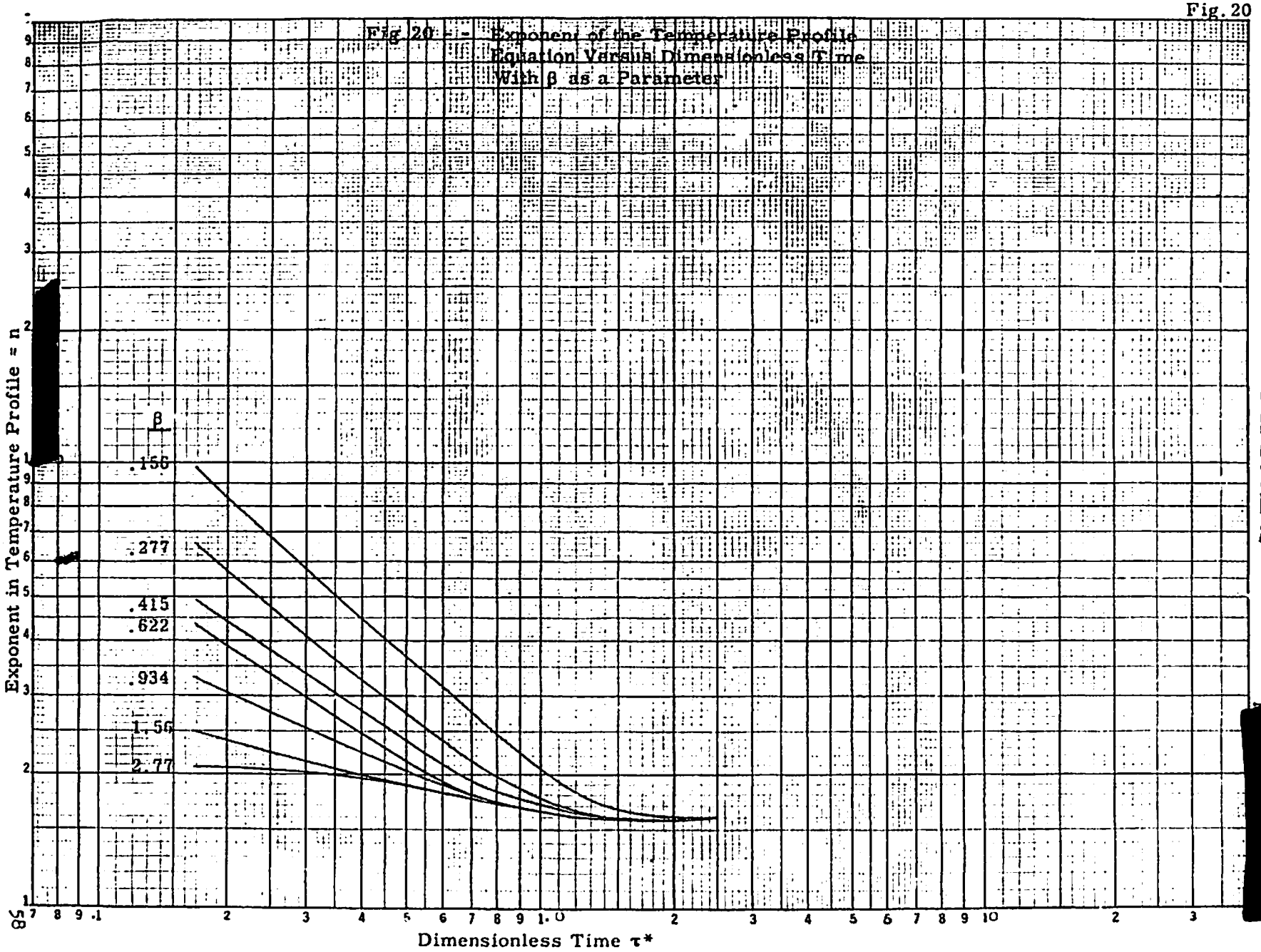

Fig 20 - - Exponent of the Temperature Profile Equation Versus Dimensionless Time With β as a Parameter

UNCLASSIFIED

UNCLASSIFIED

UNCLASSIFIED

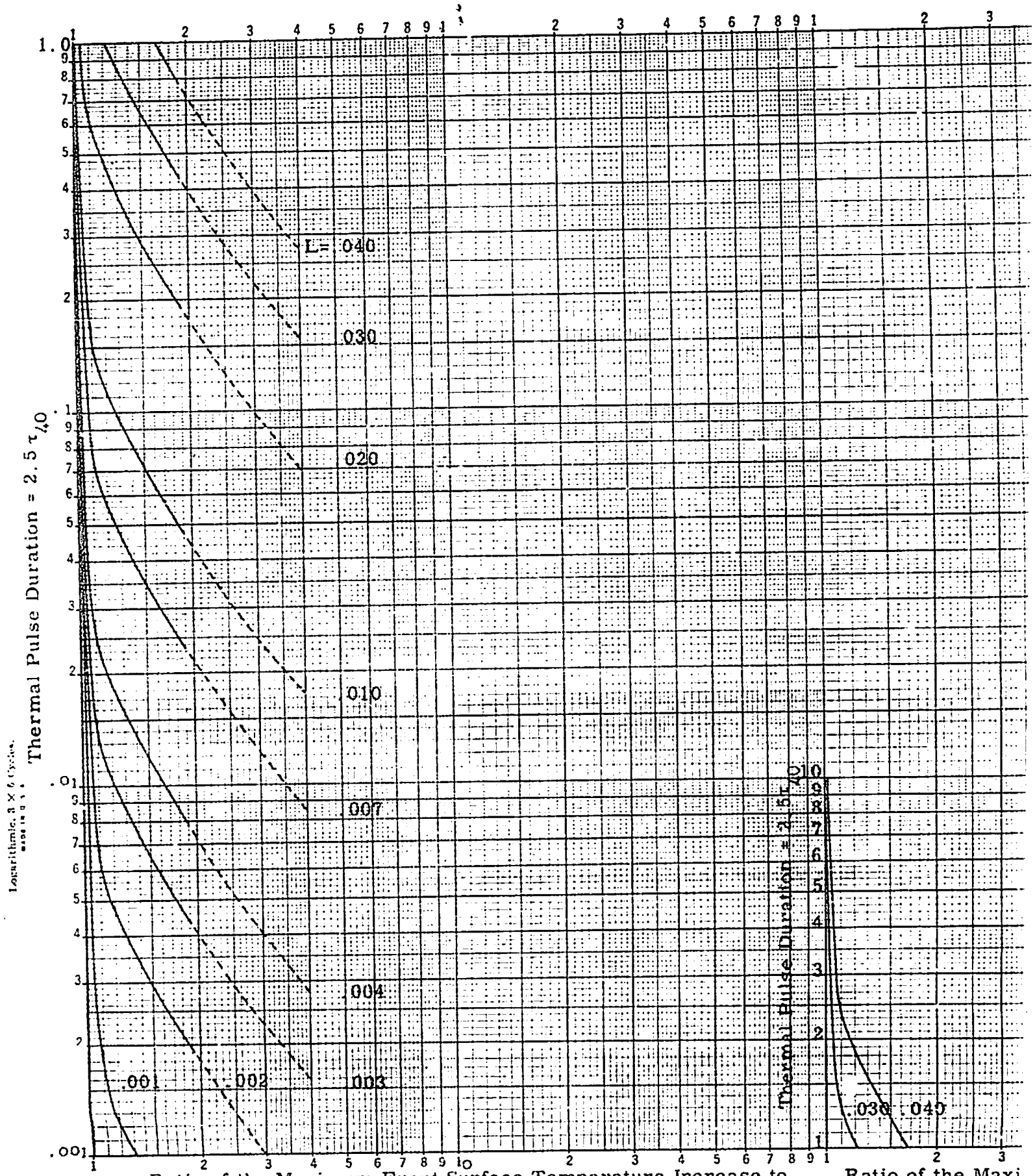

UNCLASSIFIED

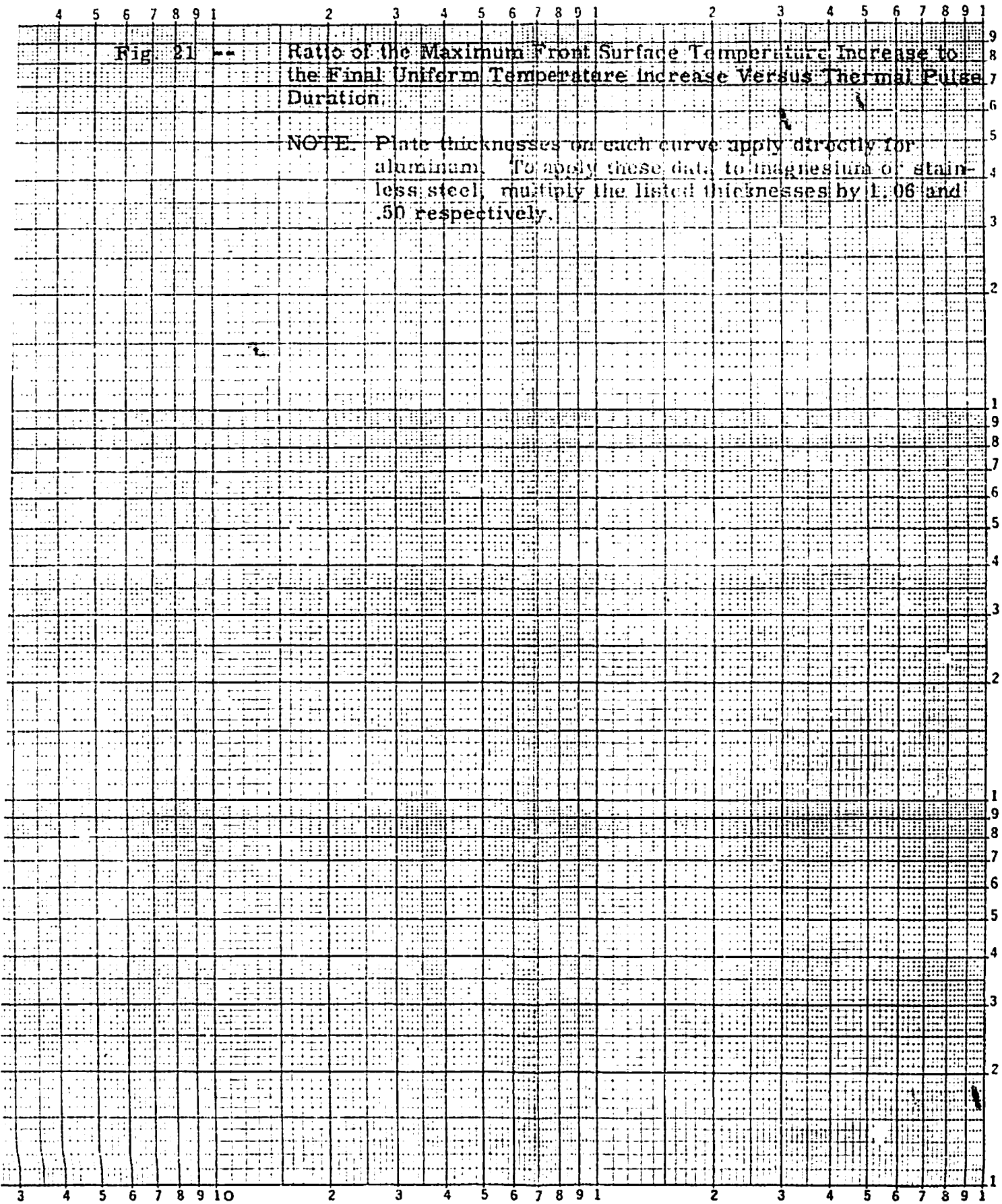
Fig. 21 -- Ratio of the Maximum Front Surface Temperature Increase to the Final Uniform Temperature Increase Versus Thermal Pulse Duration.
NOTE. Plate thicknesses on each curve apply directly for aluminum. To apply these data to magnesium or stainless steel, multiply the listed thicknesses by 1.06 and .50 respectively.
Maximum Front Surface Temperature
he Final Uniform Temperature Increase

UNCLASSIFIED

THERMAL STRESSES IN

FRONT SURFACE REDUCED STRESS:

$$\frac{\sigma_z \ (1-\upsilon)}{\delta E t_0 (t_F^* - t_R^*)} = -\left\{1 - \frac{1}{n+1} - \frac{3n}{(n+1)(n+2)}\right\}$$

REAR SURFACE REDUCED STRESS:

$$\frac{\sigma_z \ (1-\upsilon)}{\delta E t_0 (t_F^* - t_R^*)} = -\left\{-\frac{1}{n+1} + \frac{3n}{(n+1)(n+2)}\right\}$$

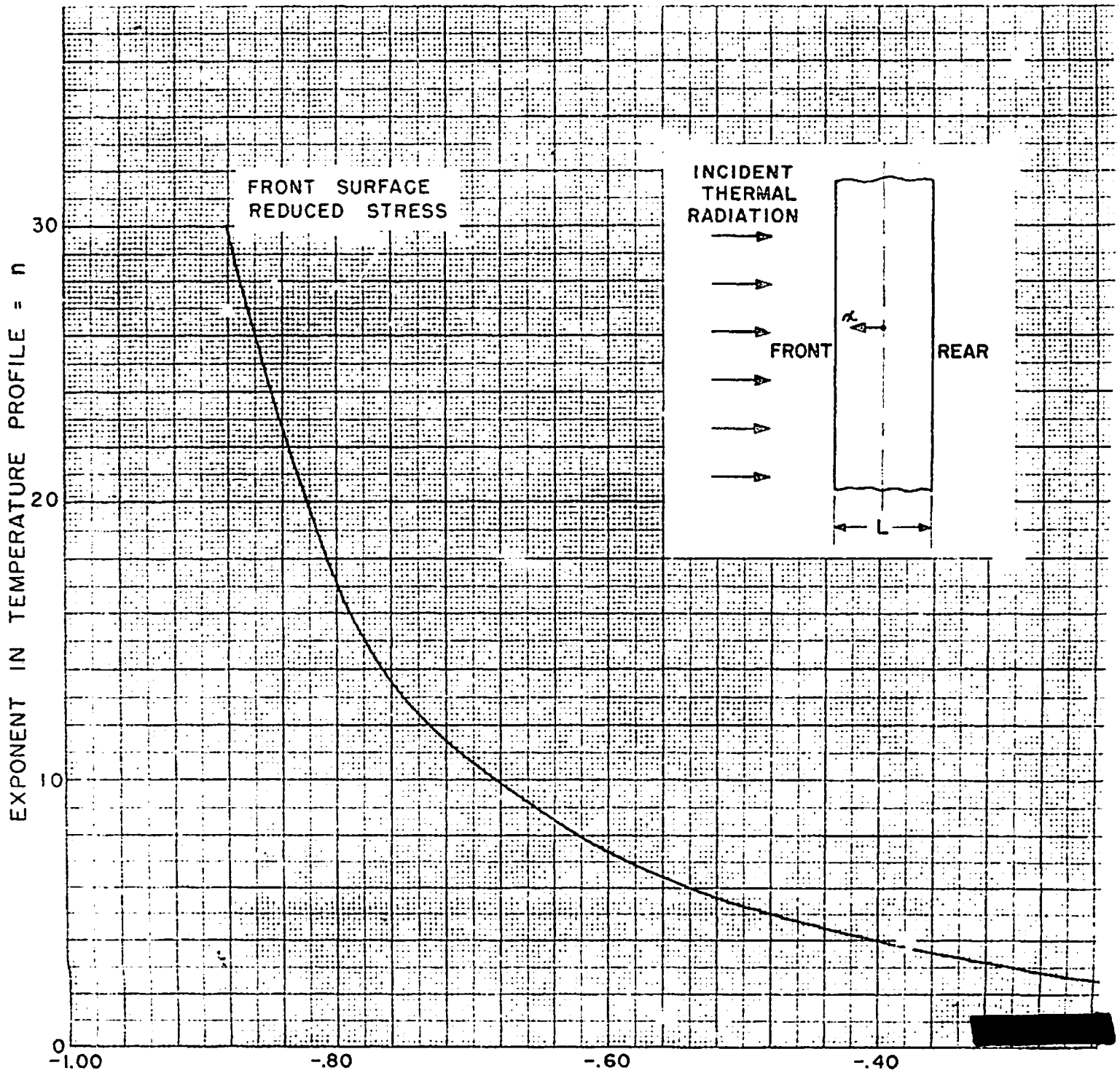

UNCLASSIFIED

IN A FREE PLATE

UNCLASSIFIED

MAXIMUM INTERIOR REDUCED STRESS:

$$\frac{\sigma_{Z\,max}(1-\nu)}{\delta E t_0 (t_F^* - t_R^*)} = -\left\{ (1-n)\left[\frac{6}{(n+1)(n+2)}\right]^{\frac{n}{n-1}} + \frac{2n-2}{(n+1)(n+2)} \right\}$$

POSITION OF MAXIMUM INTERIOR REDUCED STRESS: $n \neq 1$

$$\frac{x_{max}}{L} = \left\{ \left[\frac{6}{(n+1)(n+2)}\right]^{\frac{1}{n-1}} - \frac{1}{2} \right\}$$

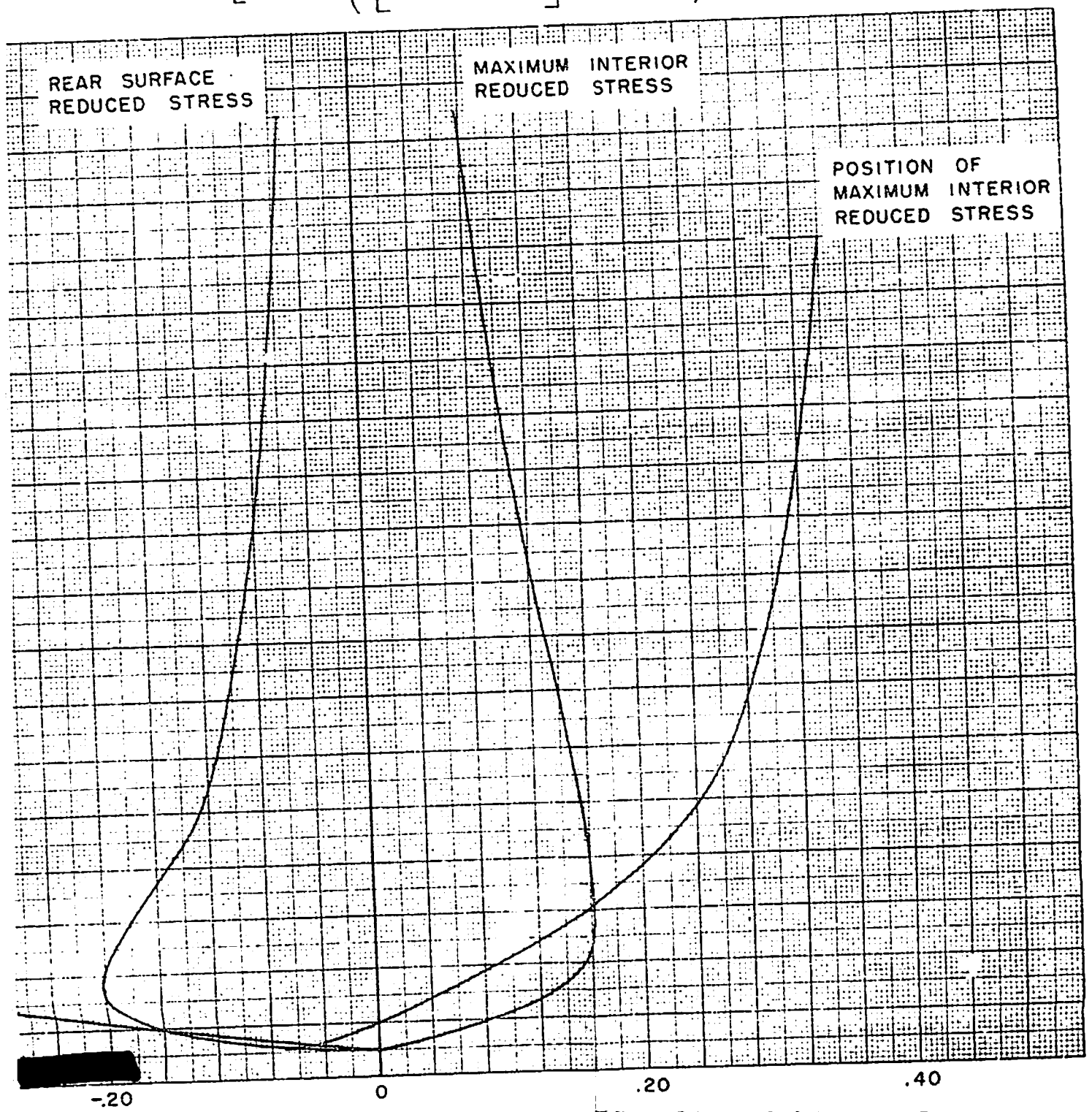

[redacted]

TRESS = $\frac{\sigma_z (1-\nu)}{\delta E t_0 (t_F^* - t_R^*)}$ and $\frac{x}{L}$

UNCLASSIFIED

[redacted]

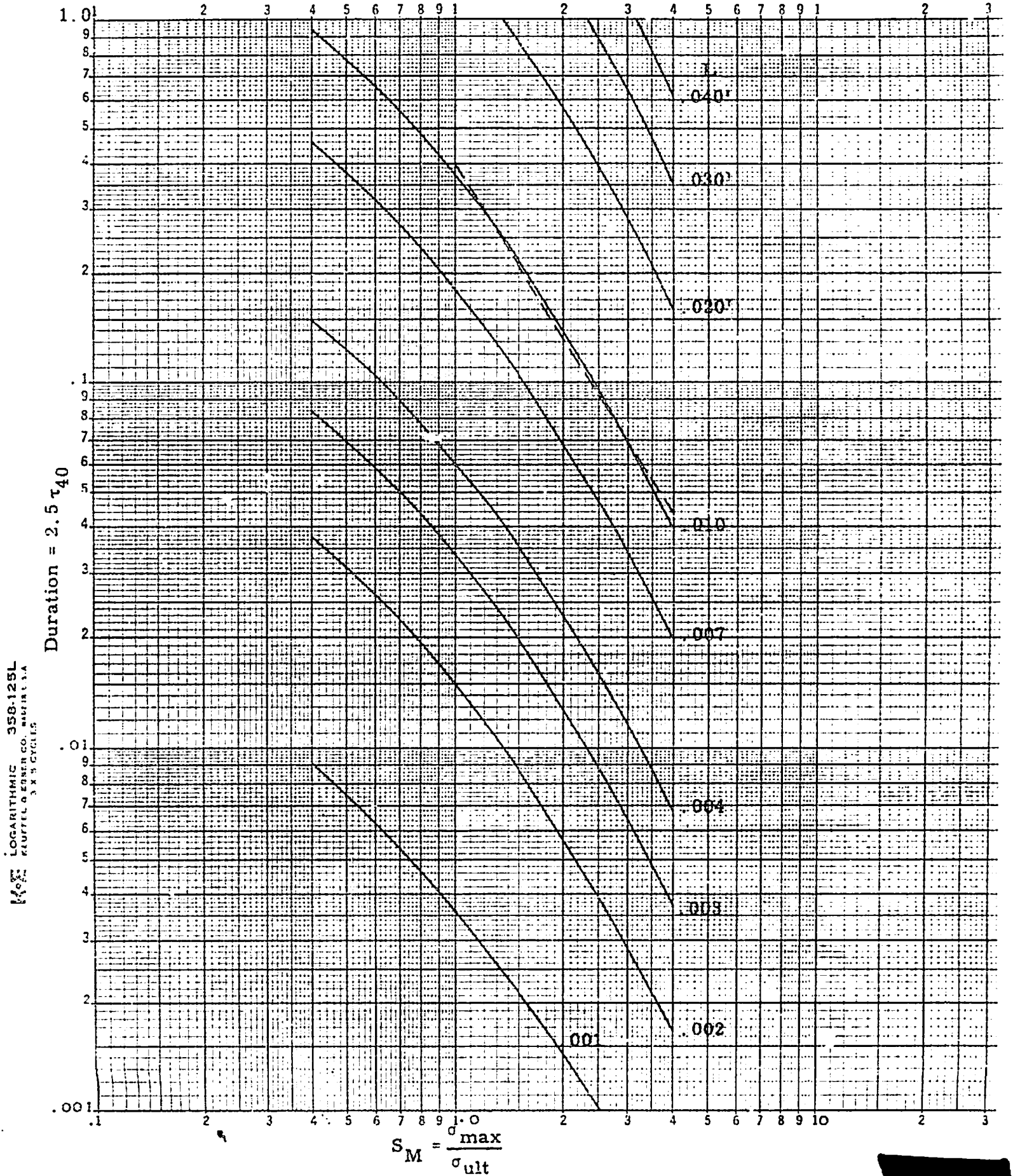

[redacted]

[redacted]

Figure 23

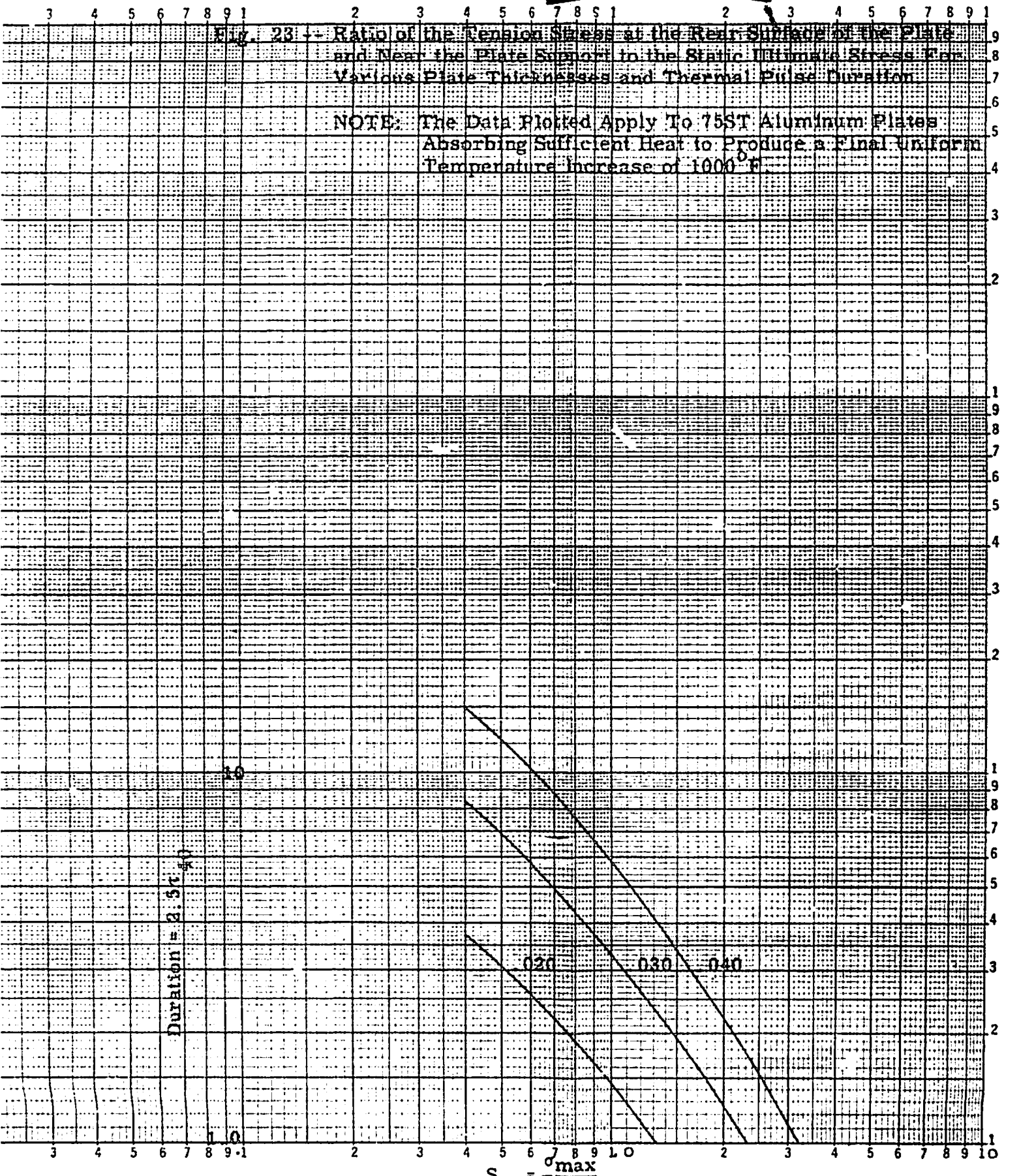

Fig. 23 -- Ratio of the Tension Stress at the Rear Surface of the Plate and Near the Plate Support to the Static Ultimate Stress For Various Plate Thicknesses and Thermal Pulse Duration

NOTE: The Data Plotted Apply To 75ST Aluminum Plates Absorbing Sufficient Heat to Produce a Final Uniform Temperature Increase of 1000°F

[redacted] UNCLASSIFIED

[redacted]

[redacted] Fig. 24

Fig. 24 -- Maximum Tension Stresses On the Rear Surface Near the Edge of a Nonuniformly Heated 75ST Aluminum Plate Fixed at its Edges.

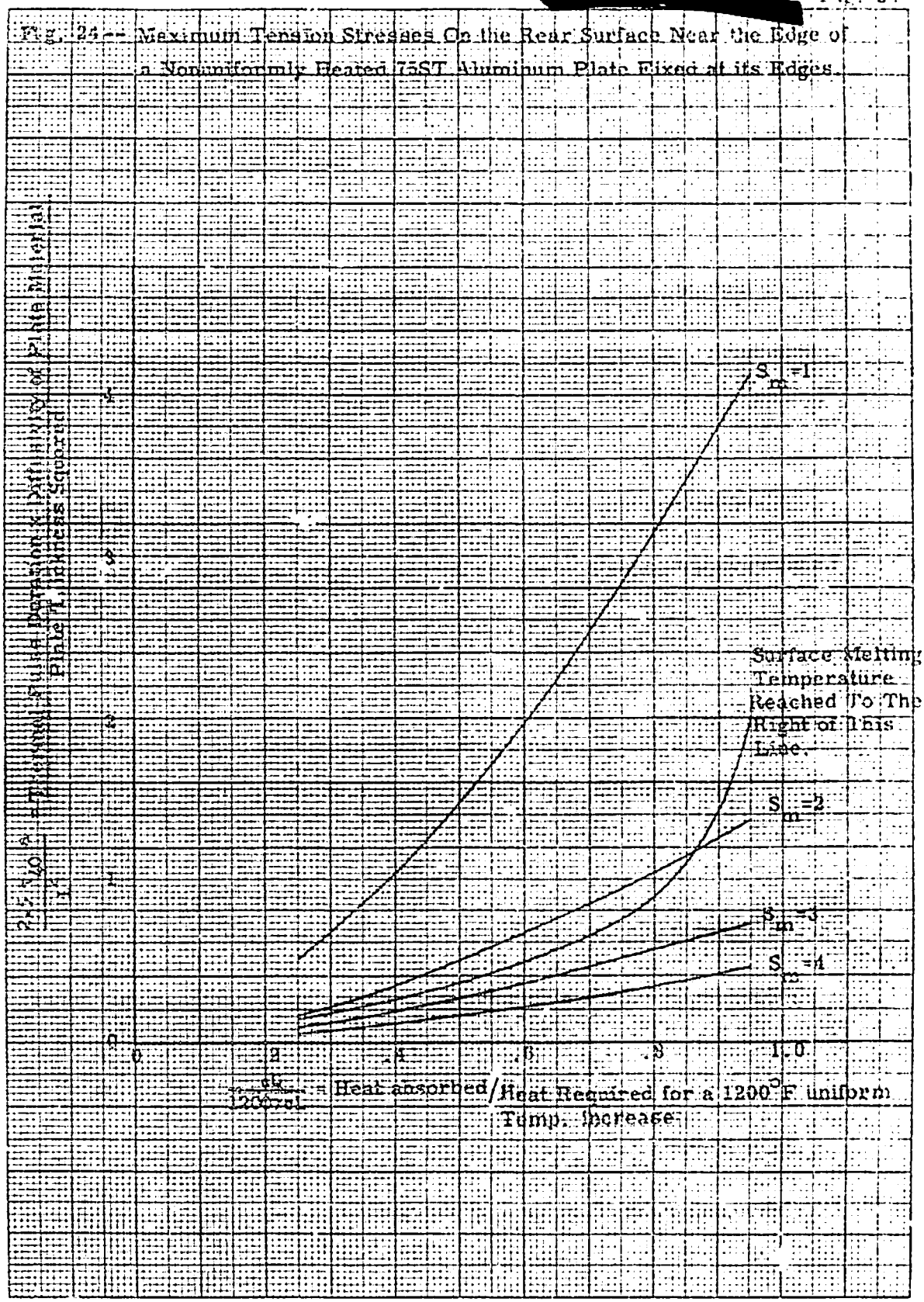

K&E 10 X 10 TO THE ½ INCH 359-11 KEUFFEL & ESSER CO.

[redacted]

[redacted]

Fig. 25

Fig. 25-Maximum Tension Stresses On The Rear Surface Near the Edge of a Nonuniformly Heated JS-1H Magnesium Plate Fixed at Its Edges.

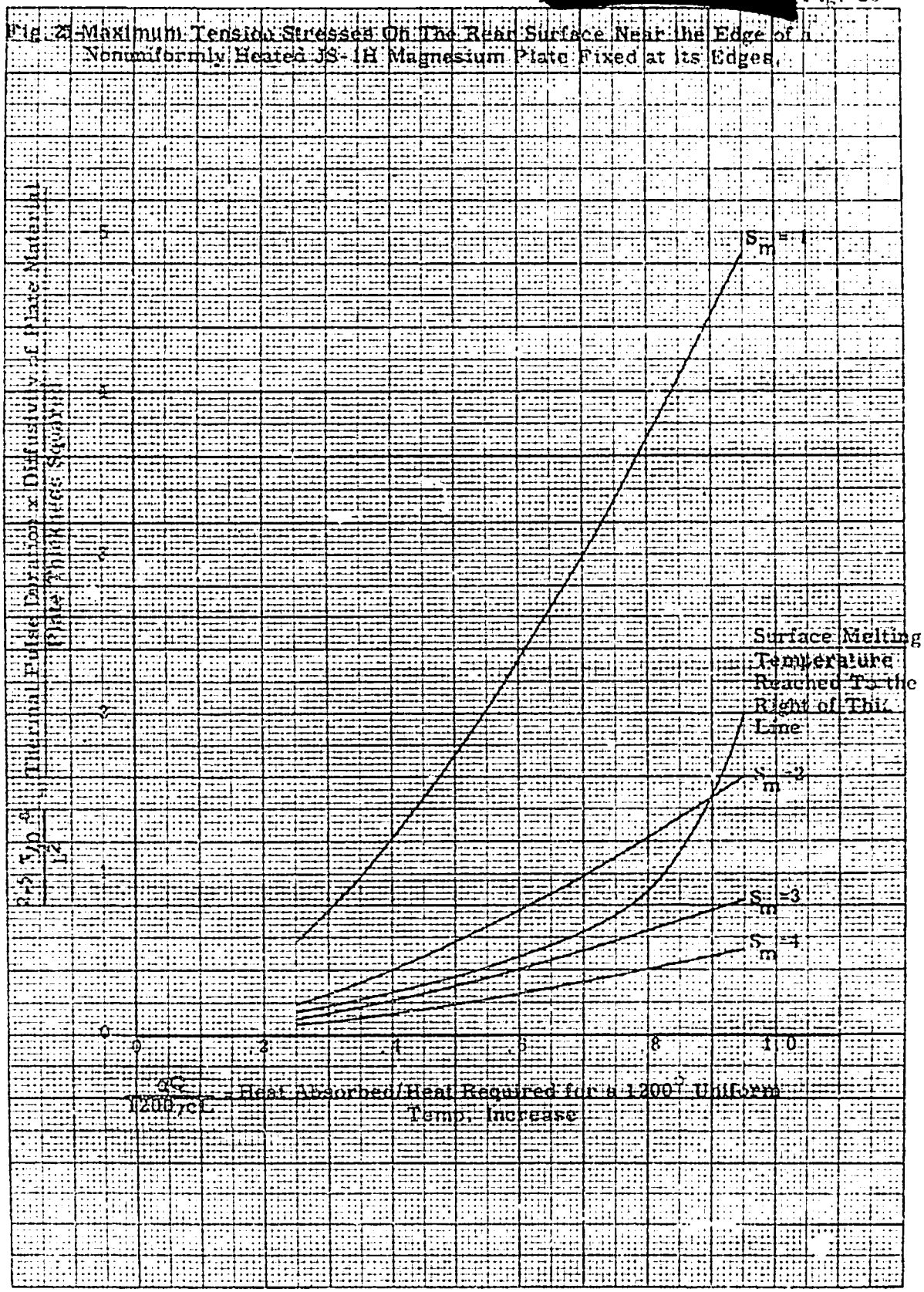

[redacted]

UNCLASSIFIED

[redacted]

[redacted]

Fig. 26

Fig. 26 Maximum Tension Stresses On the Rear Surface Near the Edge of a Nonuniformly Heated 18-8 Stainless Steel Plate Fixed at its Edges

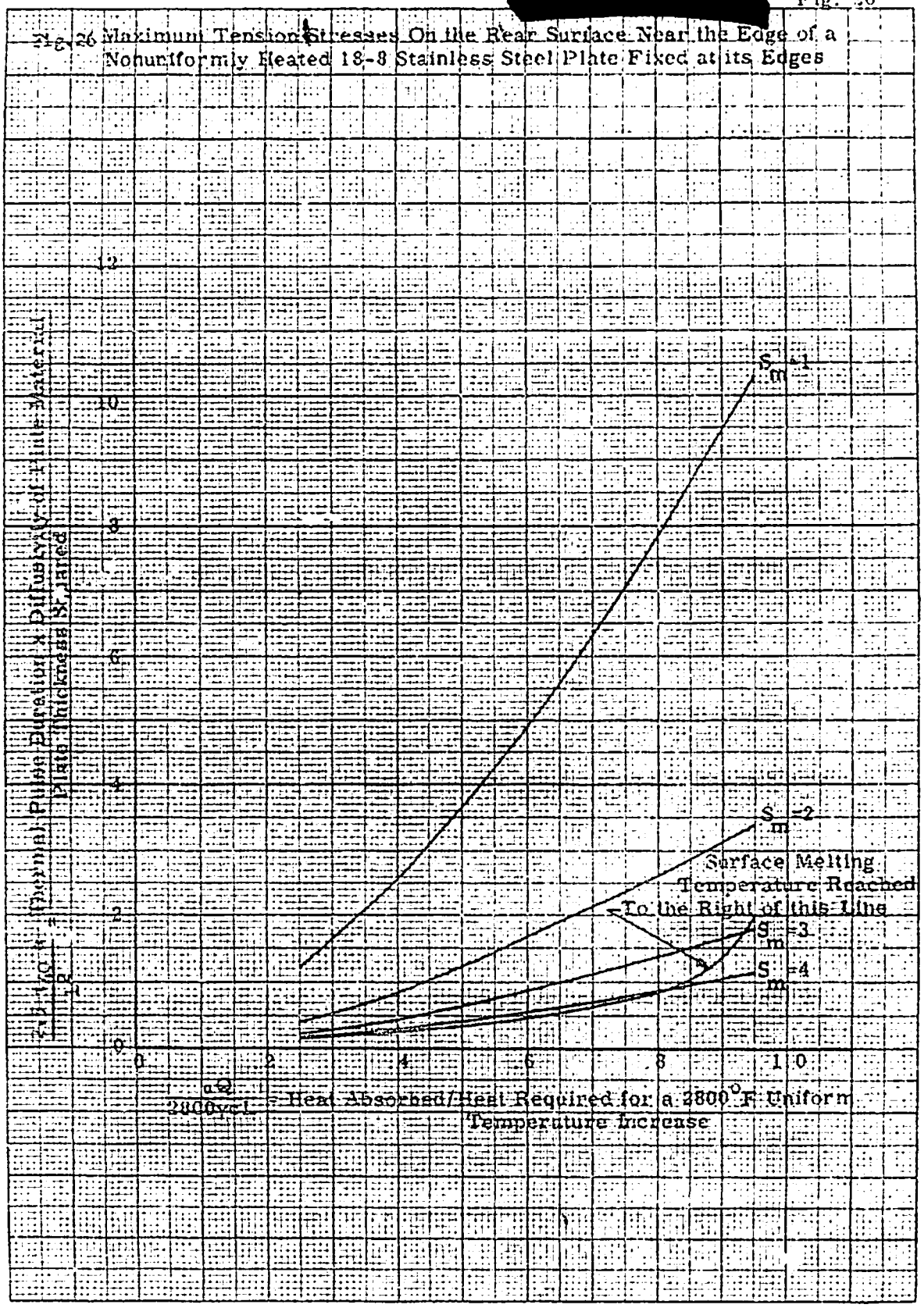

[redacted]

UNCLASSIFIED

[redacted] Fig. 27

Time Variations of Front and Rear Surface Temperature and Stress For a Typical Case of Nonuniform heating which produces large stresses in an Aluminum Plate.

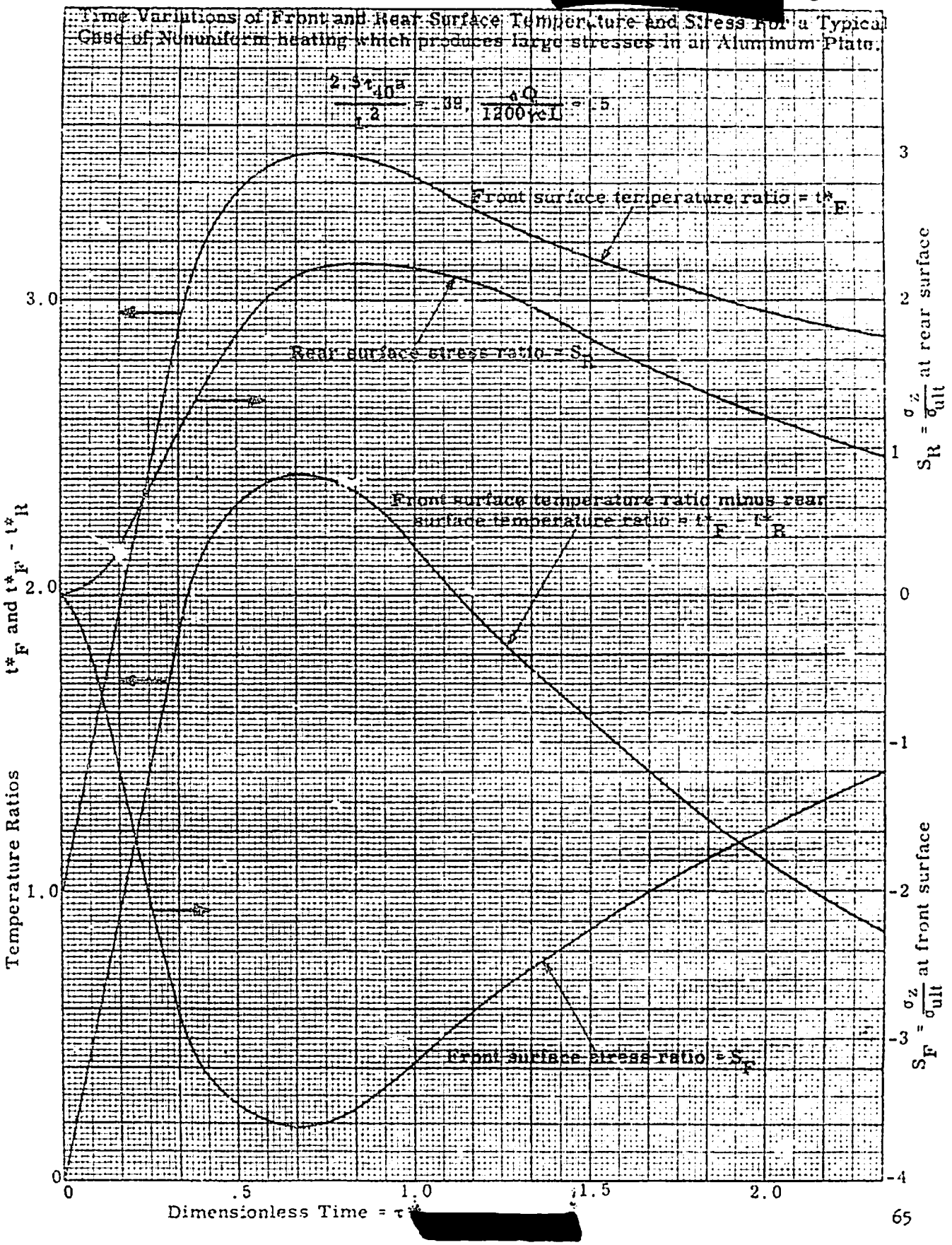

UNCLASSIFIED

[redacted]

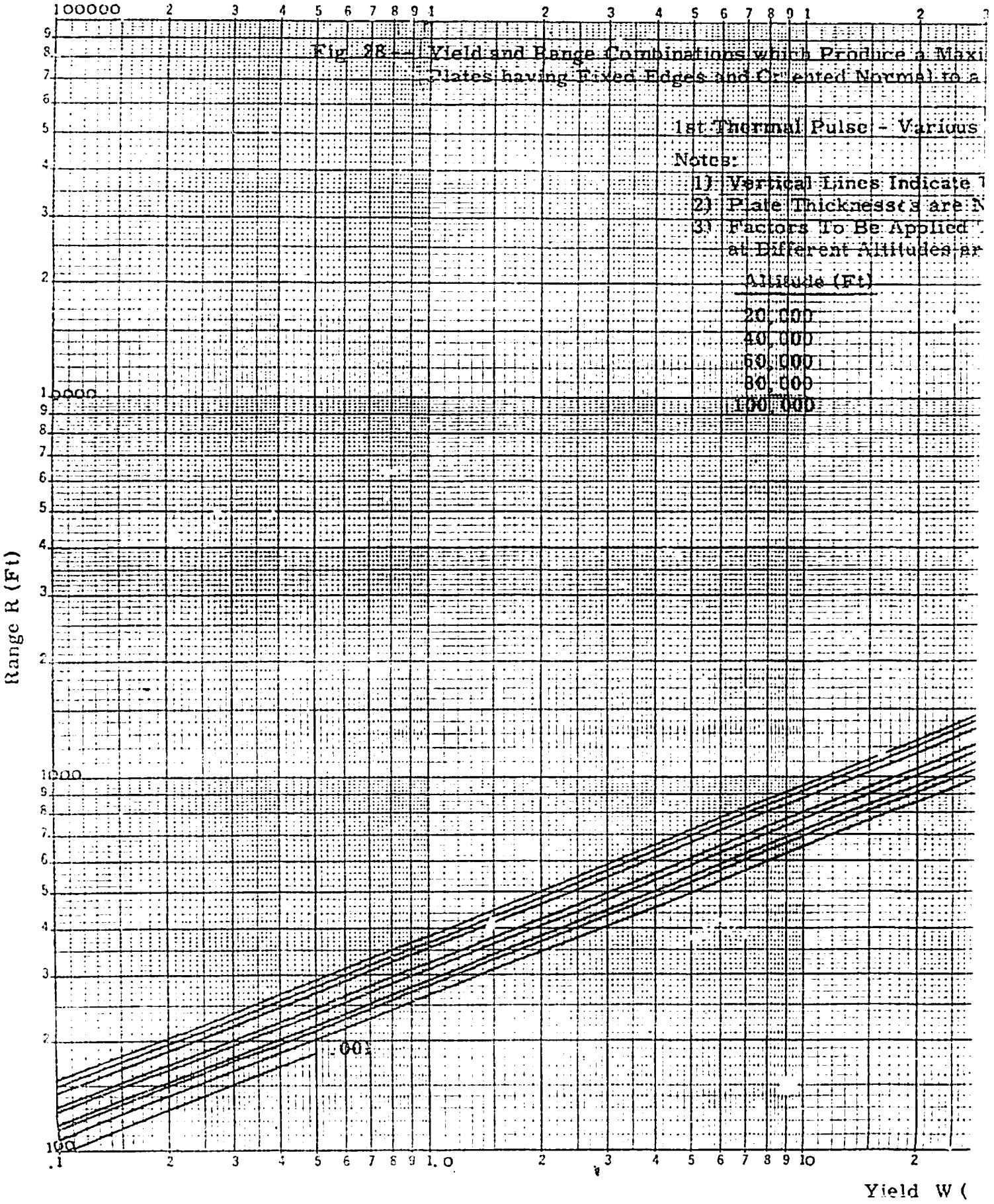

UNCLASSIFIED

[redacted]

[redacted] Fig. 28

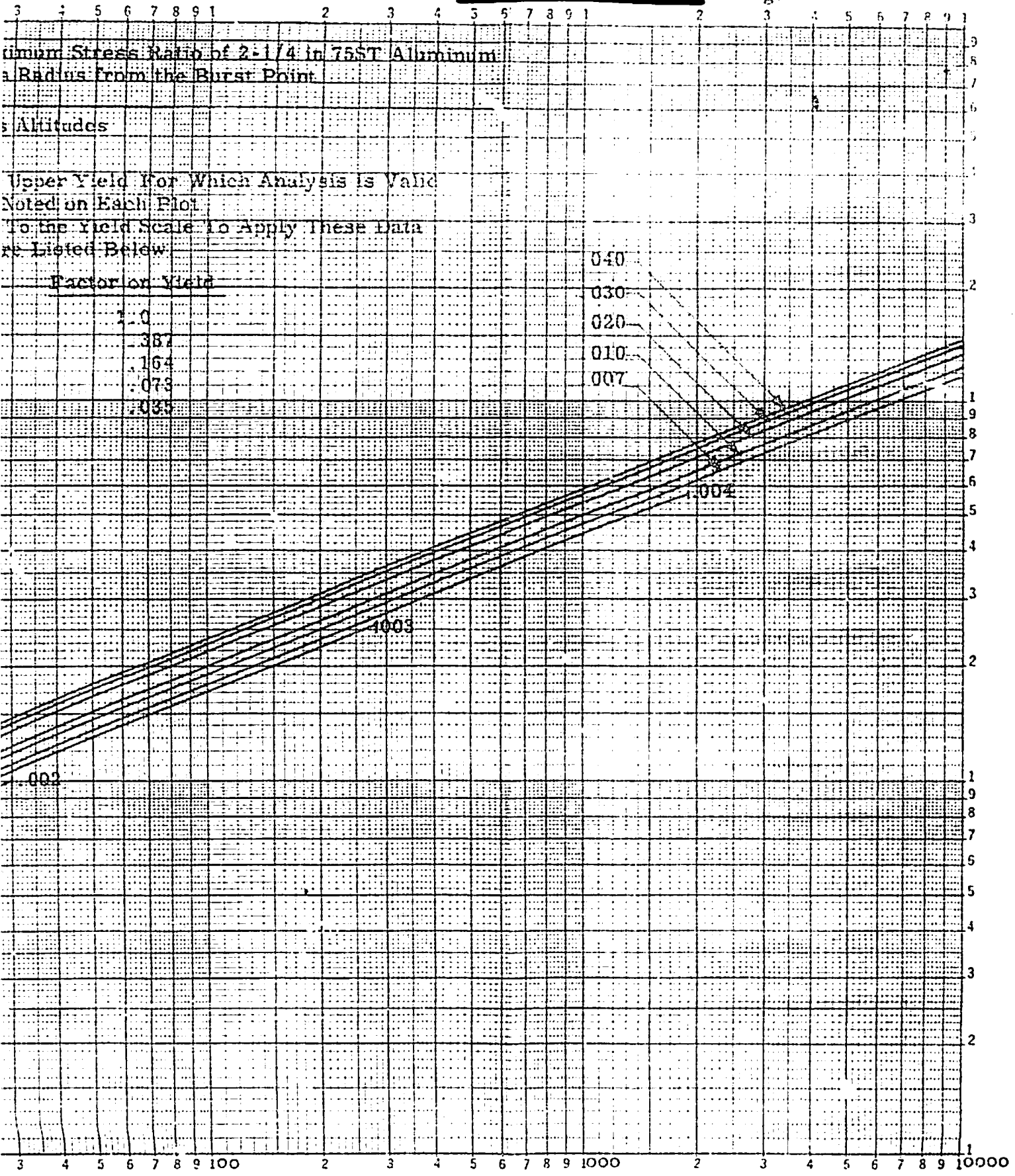

UNCLASSIFIED

[redacted]

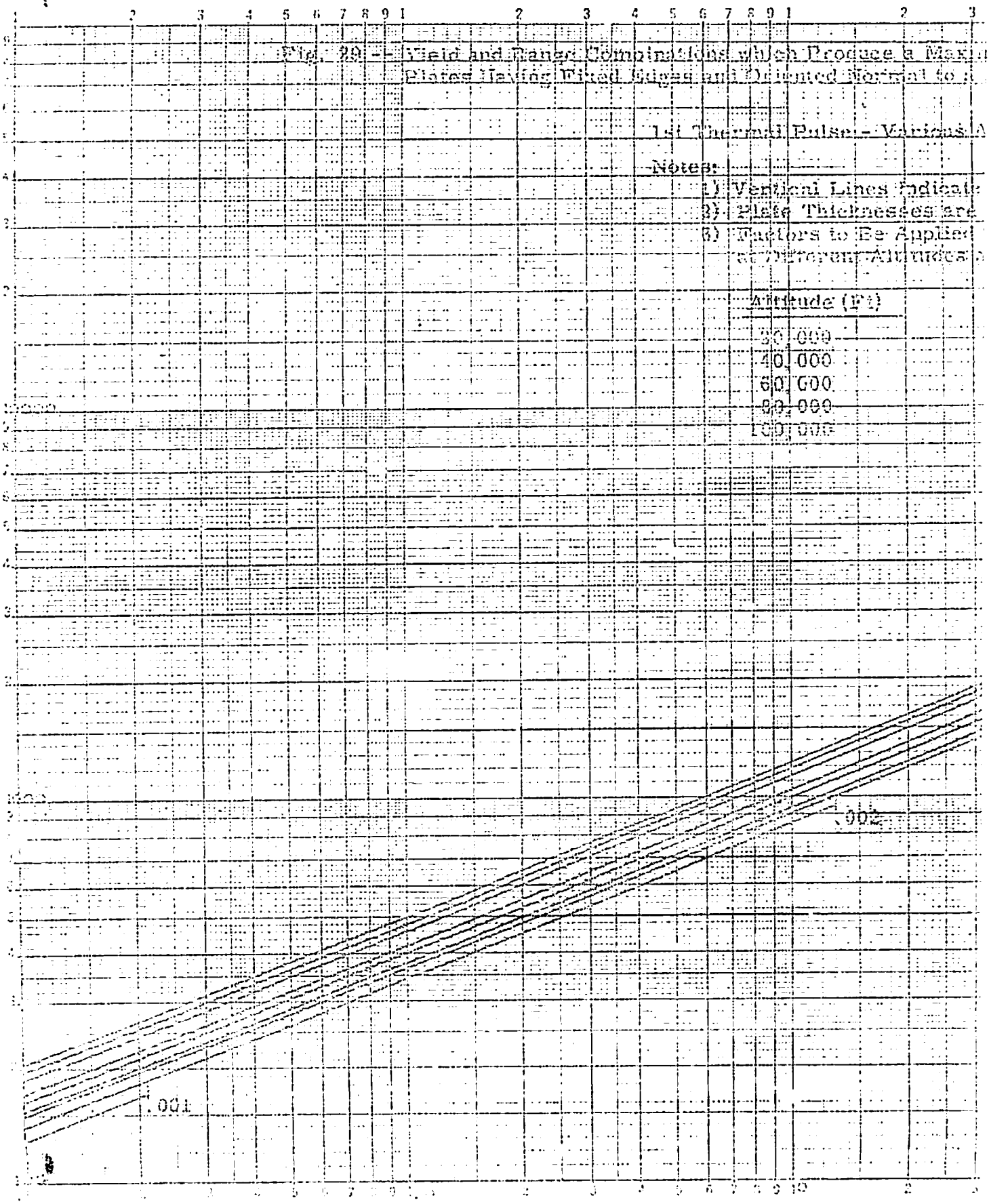

UNCLASSIFIED

[redacted]

[redacted] Fig. 29

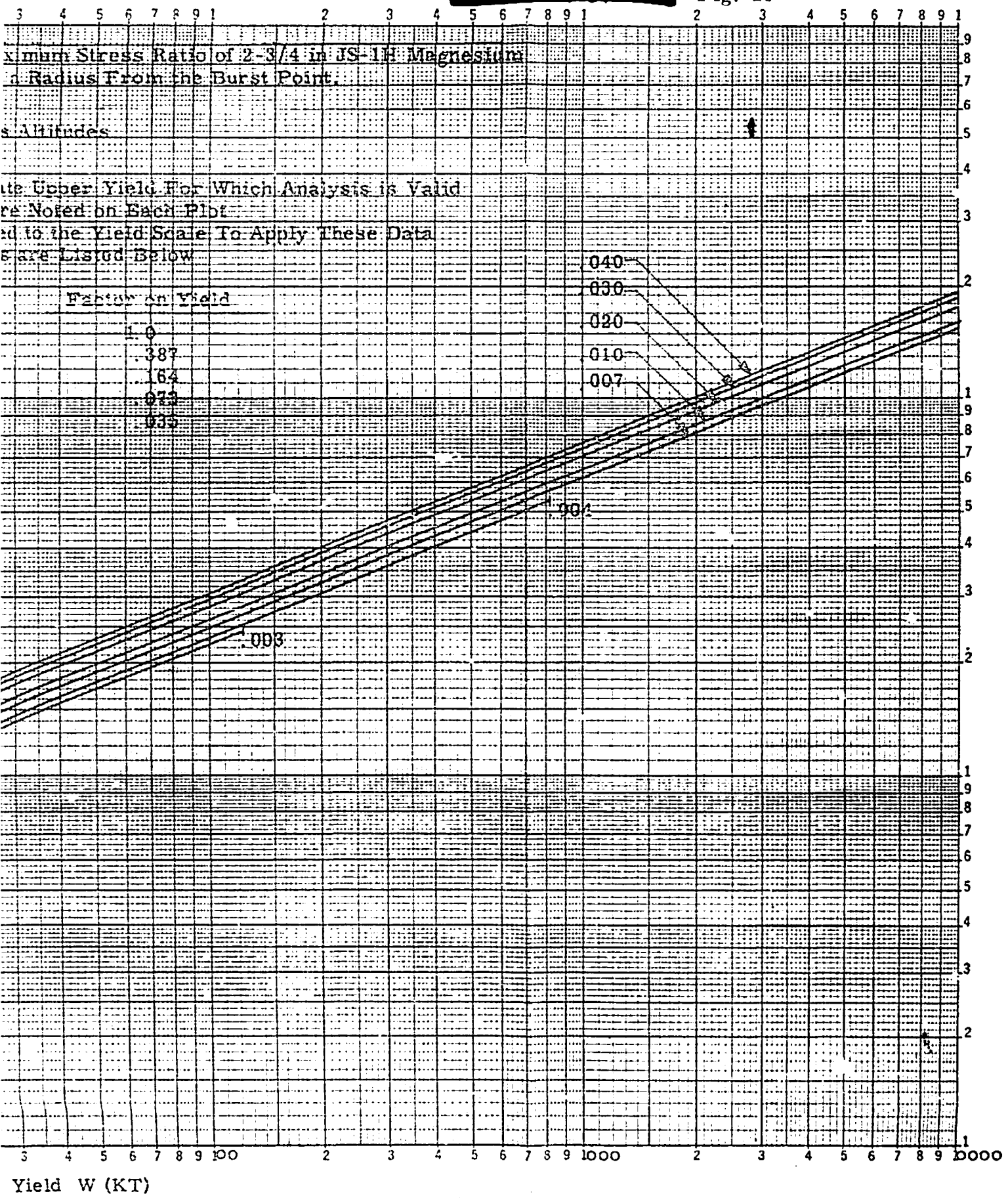

UNCLASSIFIED

[redacted]

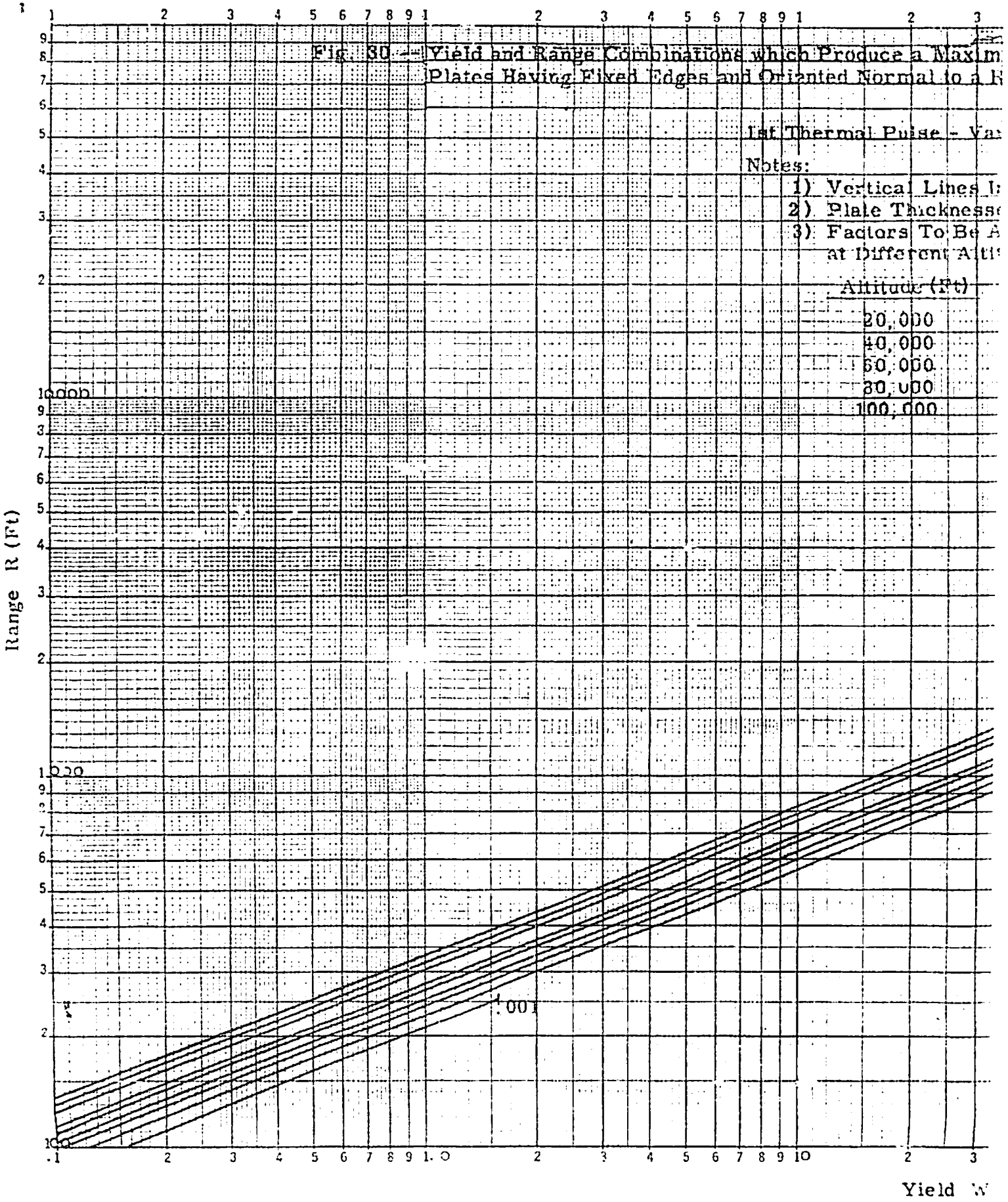

UNCLASSIFIED

[redacted]

UNCLASSIFIED

[redacted]) Fig. 30

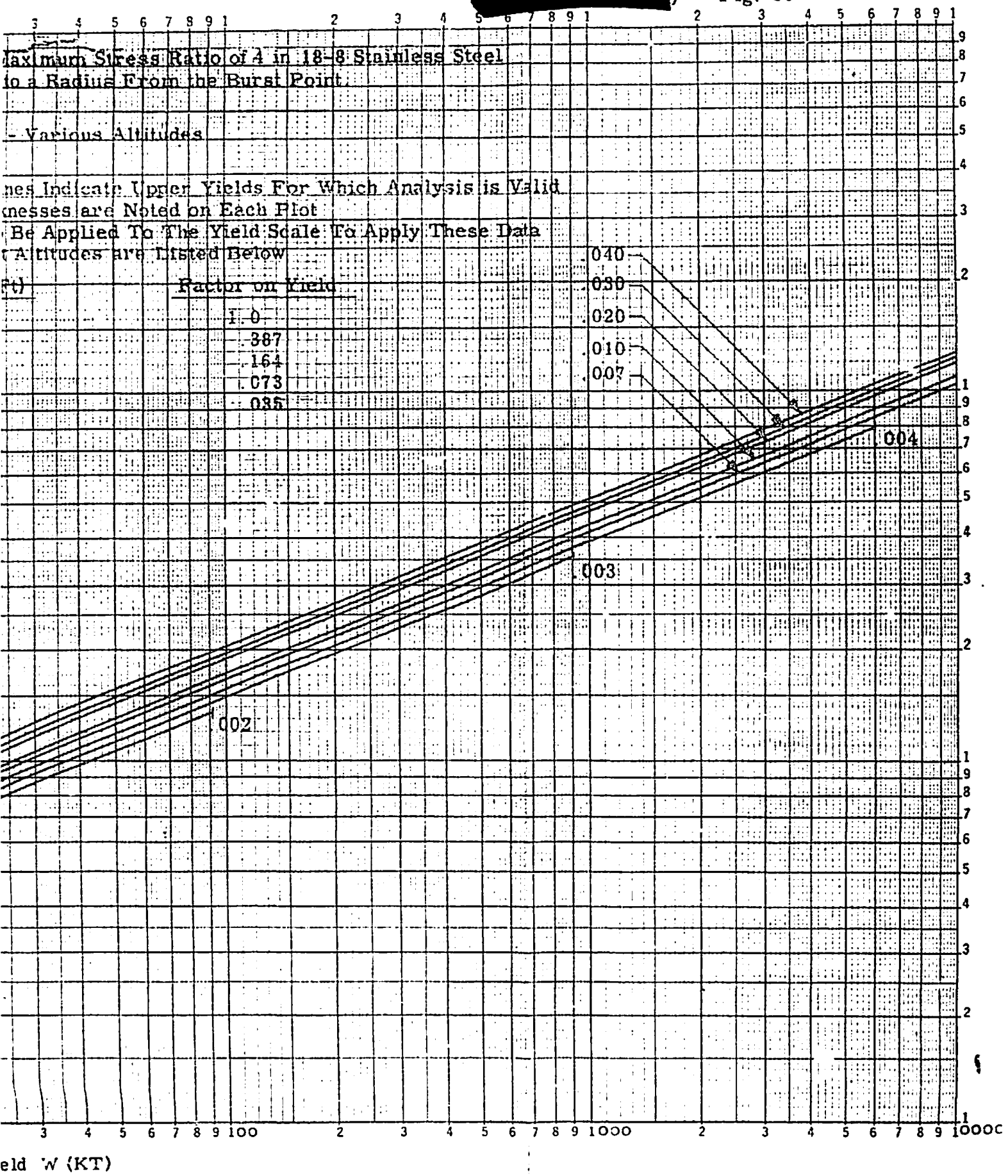

UNCLASSIFIED

[redacted]

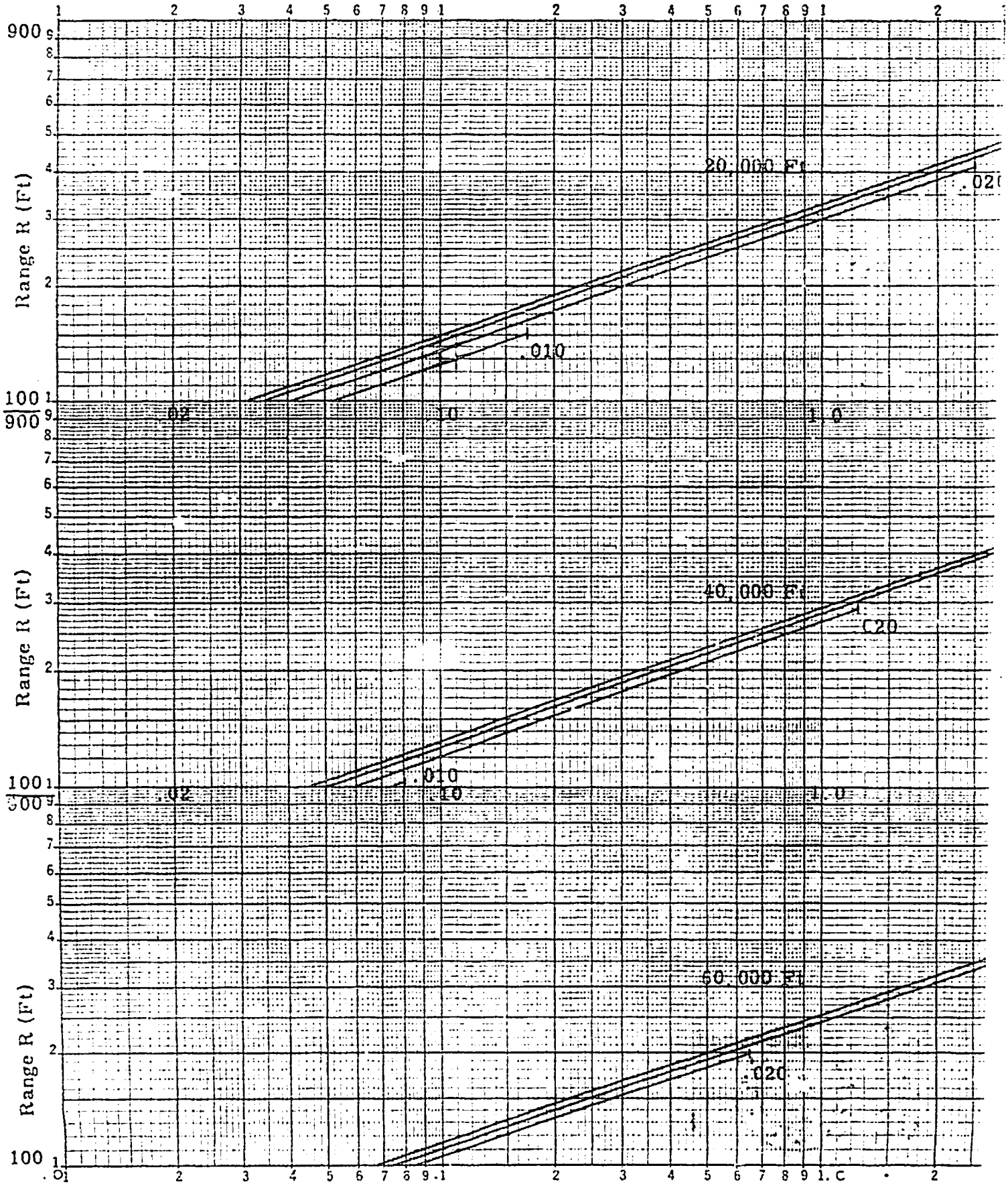

Yield W (

Fig. 31

[redacted]

UNCLASSIFIED

[redacted] Fig. 31

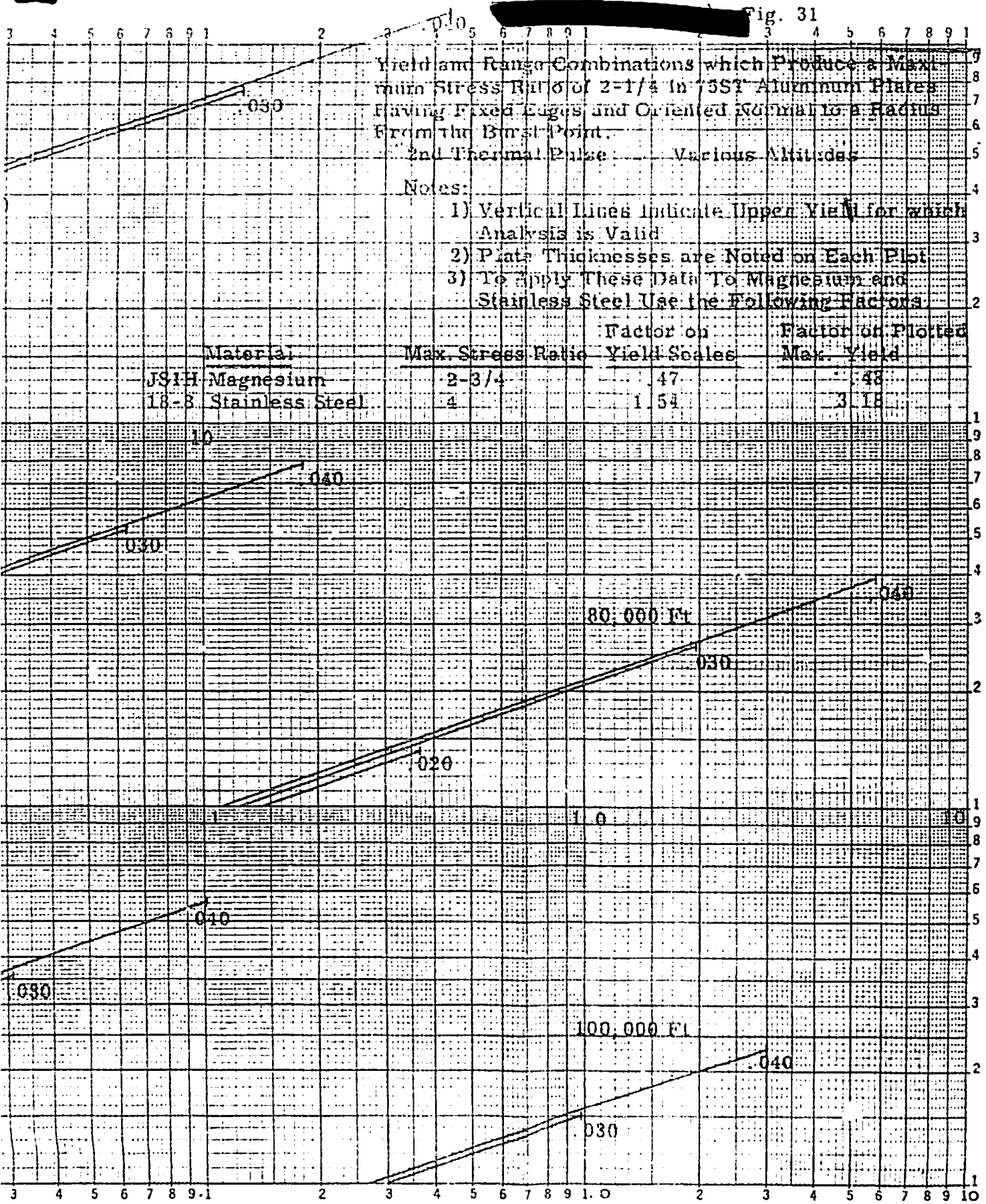

Yield and Range Combinations which Produce a Maximum Stress Ratio of 2-1/4 in 75ST Aluminum Plates Having Fixed Edges and Oriented Normal to a Radius From the Burst Point.

2nd Thermal Pulse — Various Altitudes

Notes:

1) Vertical Lines Indicate Upper Yield for which Analysis is Valid
2) Plate Thicknesses are Noted on Each Plot
3) To Apply These Data To Magnesium and Stainless Steel Use the Following Factors

Material	Max. Stress Ratio	Factor on Yield Scales	Factor on Plotted Max. Yield
JS1H Magnesium	2-3/4	.47	.48
18-8 Stainless Steel	4	1.54	3.18

(T)

UNCLASSIFIED